Preparation of Structure Lipid Containing Nervonic Acid via Enzymatic Acidolysis and Its Entrapment in Nanostructure Lipid Carriers

Yuan Zhou

ID 984470196

A thesis submitted in fulfilment of the requirements for the Degree of

Master of Science (Food Science)

The University of Auckland, New Zealand

August 2022

Abstract

This research aimed to incorporate nervonic acid (NA) into soybean oil via lipase-catalyzed acidolysis. The Lipozyme TL IM immobead 150 was selected as the lipase to catalyze the reaction in the *sn*-1,3 positions, and the critical reaction parameters were optimized to produce structured lipids with maximum nervonic acid incorporation. The optimal conditions were as follows: temperature of 60 ℃, substrate molar ratio (soybean oil:NA) of 1:4, the reaction time of 4 h, and enzyme load of 10 w/w%. Under these conditions, the incorporation of NA was 65.57 ± 0.99 w/w%. The modified NA-TAG oil was produced, and the fatty acid composition was analyzed by gas chromatography-flame ionization detector (GC-FID). The total saturated fatty acid was 9.58 w/w%, and the monounsaturated fatty acid and polyunsaturated fatty acid were 72.69 w/w% and 17.73 w/w%, respectively. Subsequently, purification of the NA-TAG oil mixture was carried out by silica gel column chromatography to remove the free fatty acids.

The encapsulation of lipophilic compounds in a nanocarrier system greatly enhances their biological efficiency and controlled delivery. The study further focused on producing the optimized nanostructured lipid carriers (NLCs) that entrapped the purified NA-TAG oil. The optimized NLCs was successfully prepared by hot high-shear homogenization, followed by sonication and recrystallization. The NLCs contained 3% Tween 80, soybean oil as liquid lipid, glyceryl monostearate (GMS) as solid lipid, NA-TAG concentration of 1%, and lipid phase to aqueous phase ratio of 10:90. Results showed that the nanoparticles have a mean size 82.11 ± 0.14 nm, polydispersity index of 0.26, the zeta potential of -50.47 ± 0.40 mV and achieve the highest entrapment efficiency of 99.82 ± 0.01%. The optimized NLCs with NA-TAG oil entrapped were lyophilized by the freeze-drying method, followed by analyzing via Differential scanning calorimetry (DSC) and Fourier transform infrared (FT-IR) spectroscopy. The DSC results showed a less-ordered crystalline structure in NLCs. FT-IR indicated no chemical interaction between the NA-TAG oil and the other NLC components. Short-term storage trials revealed good physical and chemical stabilities of the lyophilized NLC at 4 and 25 °C for 42

days. The storage stability test showed that significant aggregation of lyophilized NLCs was observed at 45 °C after the storage time. Lipid oxidation enhanced significantly with storage time and temperature.

The *in vitro* digestion was performed to investigate the behaviours of lyophilized NLCs during transient in the gastrointestinal tract (GIT), i.e., mouth, stomach, and small intestine. Extensive droplet flocculation was observed in the gastric phase, which would restrict lipase access to lipid droplet surfaces. The electrical charge of the droplets changed in different phases. The potential gastrointestinal fate of oil-in-water emulsions containing NA-TAG oil was characterized by the free fatty acid released profile versus time, generated by the pH-stat method. 46% of free fatty acid was released from NA-TAG-loaded NLC. The results enhance the understanding of the physicochemical changes of emulsified droplets containing NA within the gastrointestinal tract and provide information concerning the bio-accessibility of NA-TAG-loaded NLCs.

This research has provided scientific data for a comprehensive understanding of the synthesis of NA-TAG structured lipid using the immobilized lipase Lipozyme TL IM immobead 150 as the biocatalyst and the entrapment of the NA-TAG oil into nanostructured lipid carriers (NLCs).

Acknowledgement

Foremost, I would like to express my sincere gratitude to my supervisor, Professor Siew-Young Quek, for giving me an opportunity to study and research in this laboratory. I received excellent guidance and helpful comments about my research throughout my one-year Master of Science study. I have been blessed to have her benevolence, dynamism, and vision, which truly inspired me during my research project. Her encouragement and patience have helped me tremendously during the whole progress of my thesis. The sincerest thanks to her insights, making herself available to this thesis, and her time and efforts on the revision.

I am also thankful to many researchers and technicians in the Chemical Sciences for their technical support and assistance, especially Ms Sreeni Pathirana and Dr Peter Swedlund. I also wish to thank the PhD seniors, Pattarasuda Rawiwan (Noo), Xuan Dong, Yaoyao Peng, for selflessly sharing their insightful knowledge with me. A special thank you to Geoff Ang, for the consultative assistance, suggestions, and encouragement he offered to this research.

Next, I would like to extend my thanks to my friends. To Yuan Wen and Yijun Liu, for their constant companionship, support, and formatting skills for this thesis. To Bohan Zhang and Binyi Chen for their countless encouragement and emotional support during my study.

Finally, I am obliged to express my deepest love and sincere gratitude to my family, especially my mother (Han Zhou) and my grandma (Jinlian Tian), who have given me unconditional love and mental support to go through everything during this study. I love you two from the earth to the moon and back and cannot do this without you.

Last but not least, thank you to me for making this research available - for my perseverance and effort on the challenging days and nights to make the perception a reality.

Table of Content

List of Figures

List of Tables

List of Abbreviations

1,3-dioleinoyl-2-palmitoyl-sn-glycerol	OPO
2-monoacyl-sn-glycerols	2-MAG
2-monothioglycerol	2-MO
2-thiobarbituric acid	2-TBA
Anisidine value	AV
Diacyglycerols	DAG
Differential scanning calorimetry	DSC
Flame ionization detector	FID
Fatty acid ethyl ester	FAEt
Fatty Acid Methyl Esters	FAME
Fourier transform infrared spectroscopy	FT-IR
Free fatty acids	FFA
Gas chromatography	GC
Gas chromatography-flame ionization detector	GC-FID
Gastrointestinal tract	GIT
Generally Recognized as Safe	GRAS
Glycerol-3-phosphate	G3P
Glyceryl monostearate	GMS
High-Performance Liquid Chromatography	HPLC
Human milk fat substitute	HMFS
Immobead 150 *thermomyces lanuginosus* lipase	ImmTLL
Linoleic acid	LA

Lipid nanoparticles	LN
Long chain fatty acids	LCFA
Long-chain triacylglycerol	LCT
Low-Calorie structured lipids	LCSL
Malonaldehydes	MDA
Medium chain fatty acids	MCFAs
Medium-chain triacylglycerol	MCT
Medium-Long chain triacylglycerols	MLCT
Methyl tert-butyl ether	MTBE
Monoacyglycerols	MAG
Monounsaturated fatty acid	MUFA
Nano-sized particles	NPs
Nanostructured lipid carriers	NLCs
Nervonic Acid	NA
Novozymes 435	N435
Nuclear magnetic resonance spectroscopy	NMR
Palmitic acid	PA
Particle size	PS
Photon correlation spectroscopy	PCS
Poly unsaturated fatty acids	PUFAs
Polydispersity index	PDI
Rhizopus oryzae	rROL
Saturated fatty acids	SFA
Scanning electron microscopy	SEM
Self Nanoemulsifying Drug Delivery Systems	SNeDDS
Stearic acid	SA
Structured Lipids	SL
Structured Triacylglycerols	STAG
The compound annual growth rate	CAGR
Thermomyces lanuginosus lipase	TLL

Thin Layer Chromatography	TLC
Thiobarbituric reactive substances	TBARs
Transmission electron microscopy	TEM
Triacylglycerols	TAGs
Trioleoylglycerol	OOO
Ultrafiltration	UF
Unsaturated fatty acids	USFA
Very long chain fatty acids	VLCFA
Zeta potential	ZP

Chapter One

Introduction

1.1. Research Background

Nervonic acid (NA) is a long-chain monounsaturated fatty acid (24:1, n9) that plays a crucial role in the treatment of psychotic disorders and neurological development and has attracted increasing research interest (Fan et al., 2018). The inclusion of NA in the diet helps with the synthesis of myelin membrane outside the myelinated nerve fibres, binds to transcription factors and influences gene expression as well as lipid and energy metabolism (Zheng et al., 2006; Van Meer et al., 2008).

Although more studies are focusing on the biological effects of NA, the understanding of NA is still limited because systematic and reliable studies on the role of NA in the general population are still lacking.

NA is produced mainly by plants and microalgae. In particular, seed oils from *Lunaria biennis* or *Lunaria annua* constitute a significant source of NA, at about 20% in the lipid content. *Cardamine gracea*, *Heliophila longifola*, and *Malania oleifera* all contain nervonic acid (Taylor et al., 2009; Li et al., 2019). In all these species, NA is naturally incorporated into the *sn*-1 and *sn*-3 positions instead of the *sn*-2 position on the glycerol backbone of triacyglycerols (TAGs)

(Taylor et al., 2015). As NA is absent from the primary cultivated vegetable oil crops such as soybean, rapeseed, and sunflower, a low NA content in natural oilseeds prevents its mass production (Taylor et al., 2009; Li et al., 2019). Thus, NA incorporation into vegetable oil can be a competitive way to produce bioactive lipid supplements for advancing human and animal health (Taylor et al., 2015).

Fats and oils are essential food components. The nutritional and sensory value and its physical properties are greatly influenced by factors such as the position of fatty acids in the glycerol backbone, chain length, and degree of unsaturation. Lipases allow the modification of lipid properties by moving fatty acid chains in glycerides and replacing one or more fatty acids with new ones. As a result, a relatively inexpensive and less desirable lipid can be modified by lipase-catalysed transesterification to obtain a high-fat value (Sharma et al., 2001). Structured lipids (SLs) are generally referred to as fats or oils modified to be more nutritious and have specific functional and physical features that make them more suited for food or pharmaceutical applications (Houde, 2004). SLs are also defined as TAGs which have been chemically or enzymatically modified to change the fatty acids composition and/or positional distribution in the glycerol backbone, which can decrease the risk of cardiovascular diseases, arteriosclerosis, or neoplasms, and even high blood pressure (Adamczak, 2004; Shuang et al., 2009). For the highest production of SLs, acidolysis between TAGs and fatty acids might be preferable compared to interesterification between TAGs (Zhou et al., 2001). Moreover, lipase immobilization approaches would enhance productivity and market profitability while providing environmental benefits (Chandra et al., 2020).

Soybean oil is one of the most popular edible oils in the global production of oilseeds. The oil contains low saturated fat (15%) and relatively high unsaturated fat (61% polyunsaturated, 24% monounsaturated), including two essential fatty acids, linoleic (53.9%) and linolenic (7.1%). The production of SLs with soybean oil by incorporating a functional fatty acid into the TAG via either chemical or enzymatic methods can reduce the risk of metabolic diseases (Shuang et al., 2009). A recent study synthesized structured lipid using soybean oil, caprylic acid and an immobilized enzyme from *Rhizomucor miehei* (IM 60) via transesterification at 55˚C for 24 h. (Lichtenstein, 2013). Moreover, the food industry has applied modification of soybean oils by

chemical interesterification or hydrogenation to produce margarine (Bornscheuer et al., 2012). The fully hydrogenated soybean oil obtained from transesterification has improved oxidative stability (Kavadia et al., 2012).

Nanostructured lipid carriers (NLCs) derived from oil-in-water (O/W) emulsions have great potential to serve as a carrier system for bioactive compounds of foods or pharmaceuticals. Possessing small particle size, high entrapment efficiency and higher zeta potential of physical stability have made them very promising to the food industry (Zhu et al., 2015). NLCs are composed of solid and liquid lipids, active agents, surfactants and distilled water as major ingredients, in which a liquid lipid core is surrounded by a solid lipid matrix (Müller et al., 2002; Karimi et al., 2018). Compared to other particulate systems, lipid nanoparticles have many benefits, such as ease of large-scale production, biocompatibility and biodegradability of the materials, low toxicity, the potential for controlled and modified drug release, and increased drug solubility, and suitable for both hydrophilic and lipophilic drug incorporation (Hashemi et al., 2020).

NLCs were initially intended for pharmaceutical and cosmetic applications. However, they may improve the bioavailability and nutritional value of bioactive, increase their functionality (consumer acceptability, shelf life, stability, and safety of foods), and offer controlled release of the entrapped nutrients (Khan et al., 2019). This study aimed to produce, characterize, and optimize a food-grade NLC formulation.

Since NLCs contain a continuous aqueous phase, they have several drawbacks, including the possibility of microbial contamination, hydrolysis-related degradation, physicochemical instability, and loss of pharmacological activity of the drug or encapsulated core material (Morais et al., 2016). Freeze-drying, also known as lyophilization, has been applied to resolve these disadvantages. The conversion of liquid form into a dry powder form is necessary for incorporating nanocarriers into solid foods. Many pharmaceutical and food companies use the freeze-drying process to obtain dry products (Najjar & Stubenrauch, 2009). NLCs have been lyophilized to ensure the created nanocarriers were suitable for use in solid foods. Lyophilized products are stable, transportable, and storable. Characterization methods for lyophilized systems

are available, and literature has reported the freeze-drying of emulsions, microemulsions, and nanoemulsions. Drying techniques have been applied to emulsions mainly to increase their shelf life (Morais et al., 2016).

1.2. Research Objectives

Nervonic acid can regulate the function of brain cell membranes and have a neuroprotective effect as an energy supplement (Taylor et al., 2015). Hence, NA incorporation into TAGs as a bioactive lipid supplement could be a good choice for nutritional purposes. Up-to-date, there is a lack of research on nervonic acid (NA) incorporation by the enzymatic acidolysis process for the production of structure lipids. Therefore, this study was conducted to fill the knowledge gaps in the area.

The objectives of this research were: 1) to study the synthesis of structure lipid containing nervonic acid by modification of soybean oil using lipases as the enzymes, and 2) to evaluate the suitability of incorporating the structure lipid produced above into the nanostructured lipid carriers (NLCs) derived from oil-in-water (O/W) emulsions.

The following specific objectives were set to achieve the main objectives:

- To investigate the synthesis of structured lipid containing nervonic acid through lipase-catalyzed acidolysis reaction by exploring the optimized reaction conditions for obtaining the highest incorporation of NA in the modified oil through studying the effects of enzyme type, enzyme loading, substrate ratio, reaction time and reaction temperature. Optimisation was performed with an L9 (3^3) orthogonal design to determine the significant effects of the operating variables on nervonic acid incorporation to find the optimum parameter conditions.
- To identify the structure lipid and the oil mixture by thin-layer chromatography and to develop a reliable method for separating the purified structured lipid (NA-TAG oil).
- To compare the fatty acid profiles of the initial soybean oil and the purified structure lipid (NA-TAG oil).

- To study the entrapment of the NA-TAG oil into nanostructured lipid carriers (NLCs). Lipid screening experiments and orthogonal design were used to optimise the NLCs, and the physicochemical properties of NLCs were analysed.
- To carry out the freeze-drying process to obtain the lyophilized NLCs, followed by characterisation.
- To understand the stability of the lyophilized NLCs by conducting a storage stability test.
- To study the release properties of the lyophilized NLCs using an *in vitro* digestion model system to simulate the stomach and the upper small intestine in a fasting state.

1.3. Research Scope and Thesis Structure

1.3.1 Research Scope

The scope of the research conducted for this thesis is outlined in **Figure 1** below.

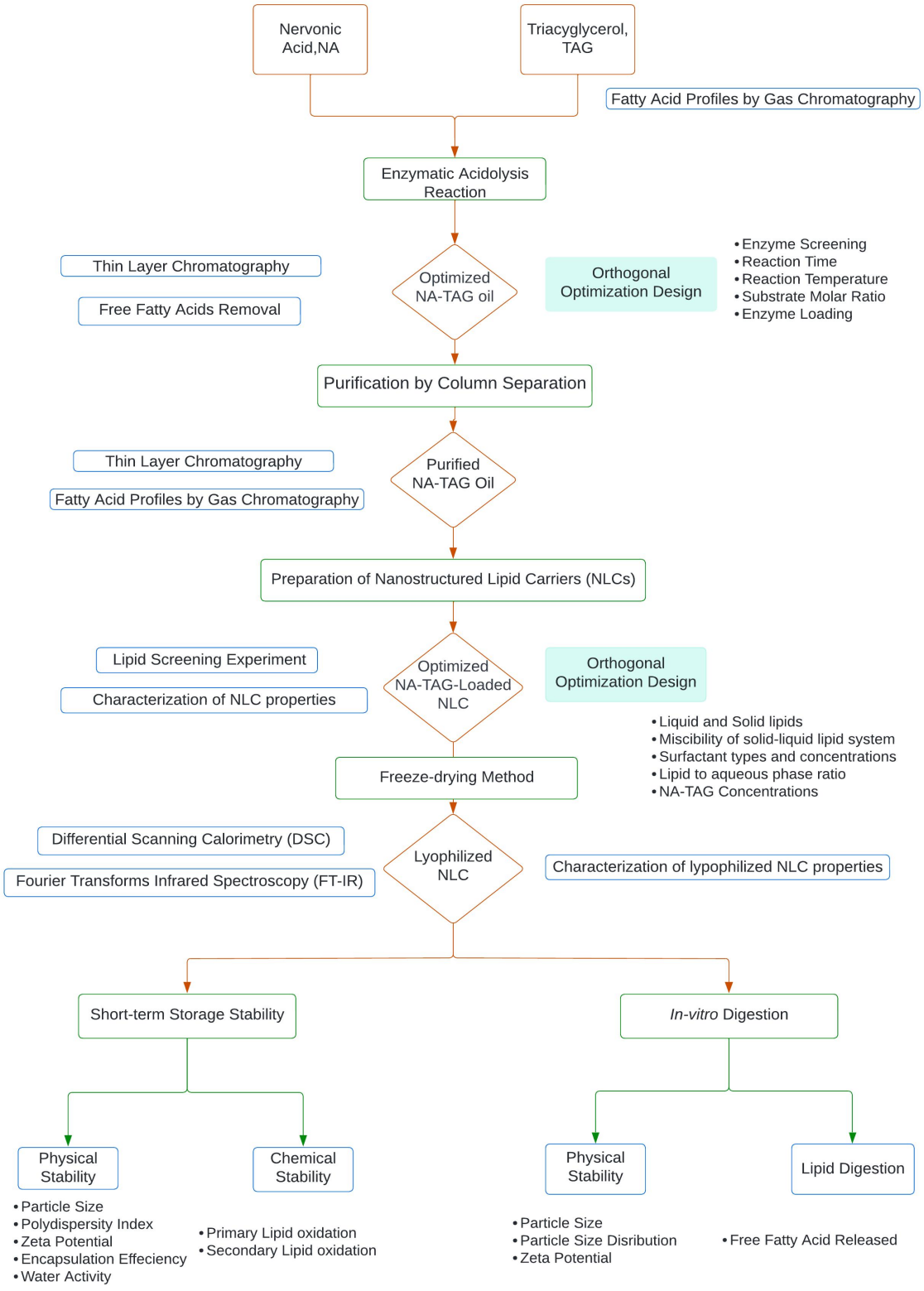

Figure 1. Research Scope.

1.3.2 Thesis Structure

This thesis consists of five chapters as outlined below:

- **Chapter 1 Introduction** introduces the research background, objectives, and research scope of the Thesis.
- **Chapter 2 Literature Review** provides a systematic review of structured lipids and nanostructured lipid carriers.
- **Chapter 3 Materials and Methods** describes the materials, chemicals and all the methods applied in this research.
- **Chapter 4 Results and Discussion** presents the data obtained from the experiments, interprets, and discusses the results referring to relevant literature study.
- **Chapter 5 Summary, Conclusion, and Future work** summarizes the important outcomes of the study, provides a conclusion and proposes potential future works.

Chapter Two

Literature Review

2.1. Nervonic Acid

2.1.1 Sources and Structure

Nervonic acid (24:1 15, cis-15-tetracosenoic acid, NA) is a long-chain fatty acid containing a double bond in its fatty acid chain (**Fig. 2**). It is prevalent in the white matter of animal brains and in peripheral nervous tissue, where nervonic sphingolipids are enriched in nerve fibre myelin sheaths (Taylor et al., 2015; Li et al., 2019).

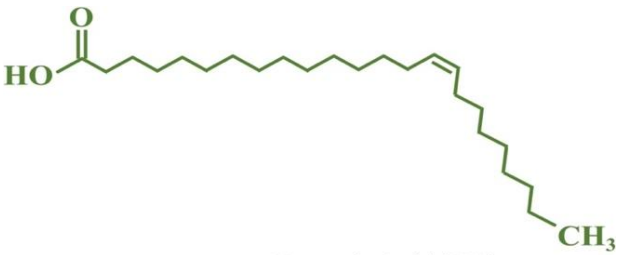

Name:	Nervonic Acid (NA); 24:1 Δ15; 24:1 ω-9; *Cis*-15-tetracosenic acid; Shark oil acid; Selacholeic Acid
Molecular formula:	$C_{24}H_{46}O_2$
Molecular weight:	366.6
Classification:	ω-9 very-long-chain monounsaturated fatty acid

Figure 2. The structure of nervonic acid (Liu et al., 2021).

Nervonic Acid (NA) is produced mainly by plants and microalgae. It is found in large quantities in plant seed oil. In particular, seed oils from the *Lunaria* species (*Lunaria biennis* or *Lunaria annua*) constitute a significant source of this long-chain fatty acid, at about 20%. *Cardamine gracea*, *Heliophila longifola*, and *Malania oleifera* all contain nervonic acid (Taylor et al., 2009; Li et al., 2019). In all these species, NA is naturally incorporated into the *sn*-1 or *sn*-3 positions instead of the *sn*-2 position of TAGs on the glycerol backbone (Taylor et al., 2015).

2.1.2 Functions and Applications

NA can be produced in the human body through a series of biochemical reactions that involve the conversion of other fatty acids. Dietary therapy using nervonic acid-containing lipids has been explored to see if the function can still be used as an intermediate in myelin production (Liu et al., 2021). Several studies on the benefits of nervonic acid have been conducted. Because of its excellent biological functions, NA is essential when used as a precursor in the pharmaceutical industry and nutraceutical applications. For example, NA supplements effectively treat neurological diseases, including demyelinating disorders (Li et al., 2019). NA is primarily acylated to sphingolipids, including ceramides, which are selectively reduced in an obesity mouse model (Keppley et al., 2020). Furthermore, the monounsaturated omega-9 fatty acid is required for the biosynthesis of myelin in the brain and can be used to predict brain maturation (Li et al., 2019). Trans-free fats rich in NA can be obtained through a physical-chemical or enzymatic interesterification process, which may have a high potential for use in margarine (Hu et al., 2017).

Interest in dietary therapy with nervonic acid-containing fats and oils developed when a hypothesis was put forward that dietary nervonic acid could support the normal synthesis and functionality of myelin in brain and nerve tissues. Dietary supplementation with nervonic acid might be beneficial for neurological development/function in the following groups of people: (i) individuals with genetic disorders of lipid metabolism associated explicitly with peroxisomes (adrenoleukodystrophy, Zellweger's syndrome, others); (ii) individuals with multiple sclerosis and other nervous disorders such as Parkinson's disease; and (iii) infants, mainly prematurely

born infants, receiving formula as a source of nutrition (Taylor et al., 2009; Liu et al., 2021). Increasing dietary NA has also been used improving energy metabolism, which may have the potential to be an effective strategy for the treatment of obesity and obesity-related complications (Taylor et al., 2009).

NA is not present in the primary cultivated vegetable oil crops such as soybean, rapeseed and sunflower, and its low proportion in natural oilseeds limits its production (Taylor et al., 2009; Li et al., 2019). Thereby, incorporating NA into seed oils as a bioactive lipid supplement for promoting human and animal health could be a way forward (Taylor et al., 2015).

2.2. Lipid Modification for Production of Structure Lipids (SLs)

The growing interest in the modification of fats and oils has initiated the development of lipid modification for certain functionality or nutritional attributes (Lichtenstein, 2013). Modifying or replacing fatty acids from TAG at specific positions significantly improves desired physicochemical, nutritional, and functional properties. Natural fats and oils contain saturated fatty acids, which are not beneficial to human health when overconsumed, so altering their fatty acid composition and stereochemical structure can improve their properties and nutritional value (Bornscheuer et al., 2012). Therefore, there is an increasing demand for various modification methods to produce structure lipids (SLs) that meet the requirements for a functional lipid. The modification has mainly been performed using triacylglycerols (TAG) as the substrate oils, but there are also limited attempts on some specific uses using other lipids. In this thesis, the scope of the literature is focused on the structured lipid produced from TAG and the abbreviation SLs refers to structure TAG in general.

A triacylglycerol (TAG) molecule composed of three identical or different types of fatty acids esterified into a single glycerol molecule (**Fig. 3**). About 90% of the molecular weight of triacylglycerol is made up of fatty acids (Seifi & Sadrameli, 2016). Changes in the molecular structure of triacylglycerol affect the metabolic fate of its component fatty acids (Iwasaki &

Yamane, 2000). For example, the stereospecific position of the long-chain polyunsaturated fatty acid on the glycerol backbone was investigated in human colostrum and mature milk TAG. Various diacylglycerol species were created based on the chemical or enzymatic degradation of human milk TAG. In mature milk and colostrum, the TAG structure was highly specific. Oleic acid has a special preference for the *sn*-1 position, palmitic acid for the *sn*-2 position, and linoleic acid for the *sn*-3 position. Linoleic and α-linolenic acids were found equally distributed in the *sn*-3 (50%) and *sn*-1 (30%) positions. Docosahexaenoic acid was found in the *sn*-2 and *sn*-3 positions (Martin et al., 1993).

On the other hand, the physical properties of the TAG are determined by specific fatty acids esterified to the glycerol moiety and the positional distribution of the fatty acid. Each of the three carbons that make up the glycerol molecule provides a stereo chemically different fatty acid bond position: *sn*-1, *sn*-2, and *sn*-3 in the TAG molecule (Lichtenstein, 2013). Most natural fats and oils contain unsaturated fatty acids at the *sn*-2 position and saturated or monounsaturated fatty acids at the *sn*-1,3 position of the TAG molecules (Lee and Lee, 2006). This is because the carboxylic acid head of fatty acids is more stable than the hydrocarbon chain, allowing carboxyl groups to distribute among all cuts of organic liquid products of the procedure. Thus, the second bound cleavage step along the hydrocarbon chain has occurred, and many fatty acid tails of triglycerides are released as free fatty acids. Furthermore, unsaturated fatty acids bound to the *sn*-2 position are more resistant to oxidizing agents due to their lower availability in the middle position of the glycerol backbone, when compared to those esterified at the *sn*-1 and *sn*-2 positions (Toorani et al., 2019).

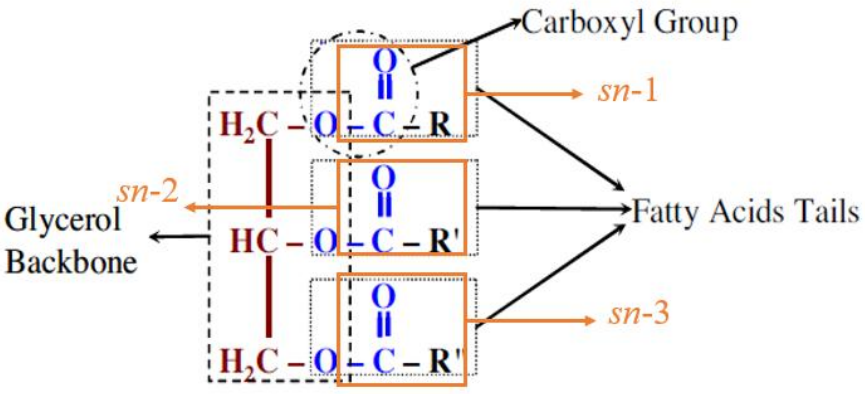

Figure 3. Molecular Structure of Triglycerides (Seifi & Sadrameli, 2016).

2.2.1 Lipid Modification Methods

Structured lipids (SL) are synthesized by either chemical or enzymatic methods, depending on what products are intended. At the same time, the regiospecific positions of fatty acids in the TAG molecules are essential for the metabolic and physical properties of SLs (Wang et al., 2012). Polyunsaturated fatty acids (PUFAs) are applied as pharmaceuticals, nutraceuticals, and food additives (Sharma et al., 2001). The presence of PUFA in the human body plays an essential role in preventing various diseases and disorders, such as cardiovascular disease, inflammation, allergy, cancer, immune response, diabetes, hypertension, and renal disorders (Utama et al., 2019). In chemical processing, the production of SLs is with medium-chain (6-12 carbon atoms) and saturated fatty acids(M) in the *sn*-1 and *sn*-3 position and with long-chain (14-24 carbon atoms) saturated or unsaturated fatty acids (L) in the *sn*-2 position can improve the unique nutritional purposes (Arifin et al., 2010). Selective lipase produces pure Structured Triacylglycerol (STAG), making them more favourable than chemical catalysts and chemical synthesis, which generate a mixture of TAG. The chemical process is also non-specific, resulting in TAGs containing a combination of fatty acids, including short-, medium-, and long-chain fatty acids esterified to the glycerol moiety. Chemical processing is often carried out at a higher temperature than the enzymatic technique. According to Ray and Bhattacharyya (1993), chemical interesterification was carried out at 90°C in a nitrogen environment using 0.2 % sodium methoxide as a catalyst. While the lipase-catalysed interesterified lipids performed at 60°C, the fatty acid distribution at the *sn*-2 position differed.

TAG synthesis starts with exporting free FAs of plastids and the subsequent acylation of those into glycerol-3-phosphate (G3P) *sn*-1, *sn*-2, and *sn*-3 positions (Kennedy, 1961; Lacey & Hills, 1996). Because the synthesis of structure lipids uses a large number of fatty acids, better functionality and properties are required to reap the greatest benefits from the production of SLs (Kim & Akoh, 2006). SL lipids can be synthesized using chemical or enzymatic methods such as direct esterification, acidolysis, alcoholysis, or interesterification, which require modifying specific fatty acid positions on the glycerol backbone of lipids (Iwasaki & Yamane, 2000). The

process by which acyl groups exchange distribution within the same glycerol backbone or other glycerol molecules among TAGs is known as interesterification (Lichtenstein, 2013). The fatty acids randomly attack in this process, resulting in the cleavage bone between the fatty acids and the glycerol backbone. The released fatty acid is then mixed with a free fatty acid, and the empty position of the glycerol backbone is randomly replaced by another FFA (Seifi & Sadrameli, 2016).

2.2.1.1 Chemical Synthesis

Chemical synthesis through transesterification results in desired randomized TAG molecule species, consisting of one or two medium-chain fatty acids (MCFAs), small quantities of unreacted medium-chain triacylglycerol (MCTs) and long-chain triacylglycerol (LCTs), and some unwanted by-products. However, removing unwanted products that require extensive post-processing steps is difficult. Under high temperature and anhydrous conditions, this chemical interesterification is catalysed by alkali metals or alkali metal alkylates. Due to the random nature of the chemical synthesis, the metal alkoxides are incapable of being modified in specific positions (Kim & Akoh, 2006). Because chemical transesterification is not apply the positional specificity of fatty acids as an essential factor in the metabolism of SL.

2.2.1.2 Enzymatic Synthesis

Due to their positional specificity modification of lipids, *sn*-1,3-specific lipases, and phospholipases are more attractive as enzymes, in the enzymatic production of TAGs. Specific lipases can hydrolyse fatty acids in the *sn*-1 and *sn*-3 locations without affecting the fatty acids in the *sn*-2 position. The synthesis of SLs can be accomplished in two steps. Lipases catalyse TAG hydrolysis and transesterification reactions with fatty acids (acidolysis), as well as the direct and rapid esterification of FFAs with glycerol (Muo et al., 2012). The capacity of lipases to undertake regiospecific change on the glycerol backbone of TAG to produce specific end products allows for the synthesis of designer TAGs. The addition of new fatty acids changes the position or content of lipids' fatty acids. Enzymatic production has also been examined on a

small and big scale to determine the best circumstances for creating TAGs, bringing valuable results for TAG manufacturing to the industries (Muo et al., 2012).

2.2.1.3 One-step Synthesis

According to **Fig. 4** which shows that in the one-step method, two triacylglycerols containing the desired fatty acids are interesterified with *sn*-1,3-regiospecific lipase and acidolysis with two equivalents of its ester, which are placed at the *sn*-1 and *sn*-3 positions of the final STAG.

Alteration of the positional distribution of fatty acids has changed the physical properties of individual fats and oils (Willis & Marangoni, 2006). The required acyl group may incorporate into a specific position of TAG because of enzymatic transesterification, and therefore lipase-catalysed transesterification can offer regio- or stereo-specific structural lipids for the development of nutritional, medicinal, and food applications (Lee & Akoh, 1998).

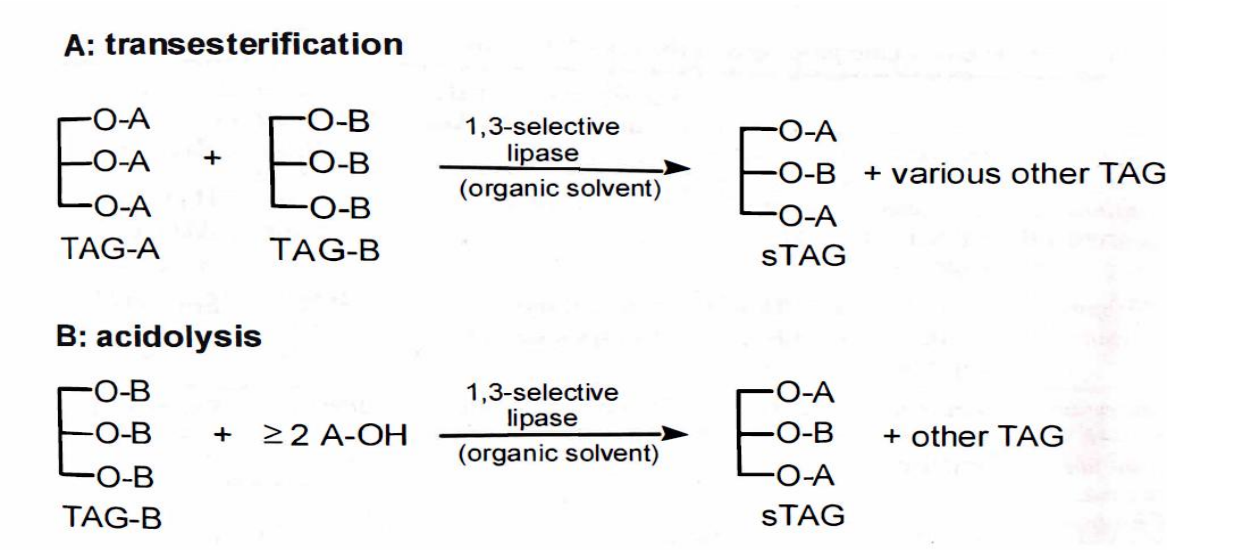

Figure 4. Reaction scheme indicating one-step synthesis to obtain the structured triacylglycerol (STAG) ABA catalyzed by a 1,3-selective lipase: (A), lipid-catalyzed transesterification between two triacylglycerols (TAG-A and TAB-B); (B), lipase-catalyzed acidolysis reaction between a triacylglycerol (TAG-B) and at least 2 equivalent of fatty acid A (A-OH). A and B represent different acyl chains (Kim & Akoh, 2006).

Acidolysis is the reaction in which the acyl moiety of acylglycerol exchanges with a free carboxylic acid. Acidolysis of triacylglycerol with fatty acids can theoretically produce a purer STAG because fewer by-products are generated. The main disadvantage of this method is that the STAG obtained are difficult to distinguish from the other TAGs. Because of the lower number of by-products, acidolysis of triacylglycerols with fatty acids yields STAG with a greater yield (Bornscheuer et al., 2012; Adamczak, 2004). When making structured TAGs, the literature suggests that parameters including enzyme screening, substrate ratio, reaction duration, temperature, and enzyme load must be considered (Kim & Akoh, 2006) These variables are crucial for small-scale experimentation and large-scale production (Xu et al., 2000; Kawashima et al., 2002). TAG is converted to free fatty acids and acylglycerol mixes (mono, di, and triacylglycerols) during acidolysis and purification (Esteban et al., 2011). Lipase-catalysed acidolysis has altered the fatty acid composition, TAG structure, minor components content and other physicochemical properties (e.g., viscosity, hydrophobicity) of the original substrate oils. (e.g., canola oil, soybean oil, palm oil, olive oil, fish oil, sunflower oil) (Kim & Akoh, 2006).

2.2.1.4 Two-Step Synthesis

As shown in **Fig. 5**, the first part of the two-step procedure, a pure triacylglycerol or natural fat/oil is alcoholised using a 1,3-regiospecific lipase, yielding 2-monoacyl-sn-glycerols (2-MAG). Pure 2-MAG should be extracted as easily and quickly as feasible from the reaction mixture. It is subsequently esterified with two fatty acid equivalents, giving the required high yield and purity STAG. The finding that high yields of 2-MAG may be generated by alcoholises of triacylglycerols in aprotic solvents such as methyl tert-butyl ether (MTBE) + ethanol at a regulated water activity was one of the key advantages of the two-step synthesis of STAG (Bornscheuer et al., 2012).

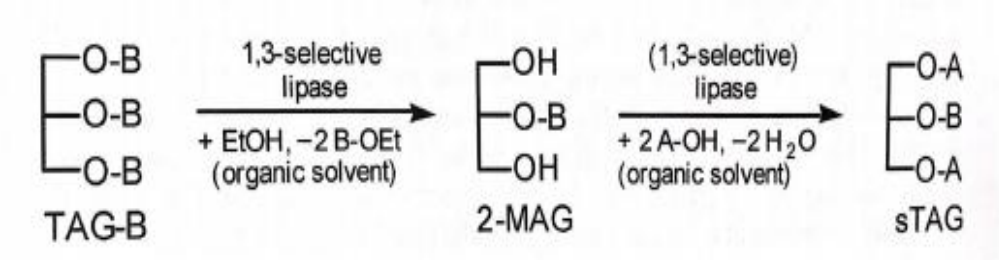

Figure 5. Reaction scheme indicating two-step synthesis of STAG by alcoholysis followed by esterification. A and B represent different acyl chains. EtOH, ethanol, 2-MAG, 2-monoacylglycerol (Kim & Akoh, 2006).

The advancement of synthetic techniques can have an impact on TAG yield, purity, and cost. Iwasaki and Yamane (2000) As a result, the synthesis of structured lipids can be used to improve and modify the physical and/or chemical properties of TAG (Lee & Akoh, 1998). The manufacture of STAG has resulted in the creation of several procedures that use a diverse variety of natural starting materials to produce value-added products with highly desirable nutritional and medicinal qualities.

2.2.1.5 Comparisons between Enzymatic and Chemical synthesis

In comparison with chemical production, the enzymatic method has some advantages. Only enzymatic lipase procedures may make MLM-types of SLs (medium-chain FAs at sn-1 and sn-3 positions, whereas long-chain FAs at sn-2 position) (Shuang et al., 2009).

Chemical modification of TAGs does not possess the selective modification of the regiospecificity position of TAG due to its random nature of the reaction that formulated few or no by-products. This method modifies the TAG using high temperature, pressure, and harsh pH conditions, which can cause environmental pollution due to the use of chemicals and solvents. . In contrast, the enzymatic method can create several advantages compared with chemical processing, resulting in the specific placement of the fatty acids on the glycerol backbone. Desirable fatty acids are available to incorporate at specific positions of TAGs. The selectivity or specificity of lipases is determined by the enzyme's molecular properties, the substrate's structure, and factors affecting the enzyme's binding to the substrate (Jensen, DeJong & Clark, 1983). Also, the enzymatic approach has few or no unfavourable side effects or products. The temperature,

pH, and reaction product thermal degradation conditions are mild, resulting in less loss of temperature-sensitive structured lipids. Thus, by reducing energy and preventing harmful reagents, the enzymatic approach provides a more environmentally friendly and safer alternative to ease product recovery (Kim & Akoh, 2015). Furthermore, the immobilized enzyme can be reused many times, which lowers production costs. Because the refining procedures are easier, the cost is also reduced (Moreira et al., 2020).

In general, modified TAG can be synthesized through enzymatic or chemical methods. In the last decade, intense research efforts have resulted in numerous processes that use a diverse range of natural starting materials to produce value-added products with essential and highly desirable nutritional and medical properties. These accomplishments are expected to lead to the commercialization of lipase-catalysed reactions to produce structured triacylglycerols (Bornscheuer et al., 2012; Adamczak, 2004). Hence, enzymatic lipase is preferable to chemical catalysts for modifying fats and oils because it is more environmentally friendly, specific, and selectively with mild reaction conditions, consumes less energy, and produces fewer byproducts (Lee et al., 2012). Lipid modification is essential for fatty acid and positional specificities (Shimada, 2006). In addition, an immobilized enzyme efficiently catalyses transesterification in a water-free mixture (Shimada, 2006). Furthermore, modifying the novel lipases has a high potential to improve TAG properties, particularly in enzymatic transesterification, which can provide regio- or stereo-specific structure lipids for nutritional, medical, and food applications (Lee & Akoh, 1998).

2.2.2 Immobilized Lipases

Lipases (triacylglycerol acyl hydrolases, EC 3.1.1.3) are ubiquitous enzymes of considerable physiological significance and industrial potential. And lipases catalyse the hydrolysis of TAG to glycerol and free fatty acids (Sharma et al., 2001). One of the main uses of lipases is in the modification and production of new oils and fats, to produce healthier foods (Fernandez-Lafuente, 2010).

According to **Fig.6**, lipases are versatile enzymes because they catalyze different reactions such as hydrolysis, esterification interesterification, acidolysis, alcoholises, and aminolysis activity for various applications (Chandra et al., 2020). Lipases can be classified as non-specific and specific lipases based on their mode of action. A non-specific lipase reacts randomly and produces a similar mixture of products to a chemical interesterification. In contrast, the specific lipase acts uniquely towards producing a specific product type and can be subclassified based on positional, substrate or stereospecificity (Utama et al., 2019). Furthermore, most regioselective lipases preferentially operate on ester bonds in the *sn*-1 and *sn*-3 positions in the triglyceride structure, with only a few lipases active in the *sn*-2 position (Houde et al., 2004). Both native and immobilized lipases are available commercially. However, industrial applications remain limited due to the expensive cost of some lipases. Hence lipases are immobilized to be reused.

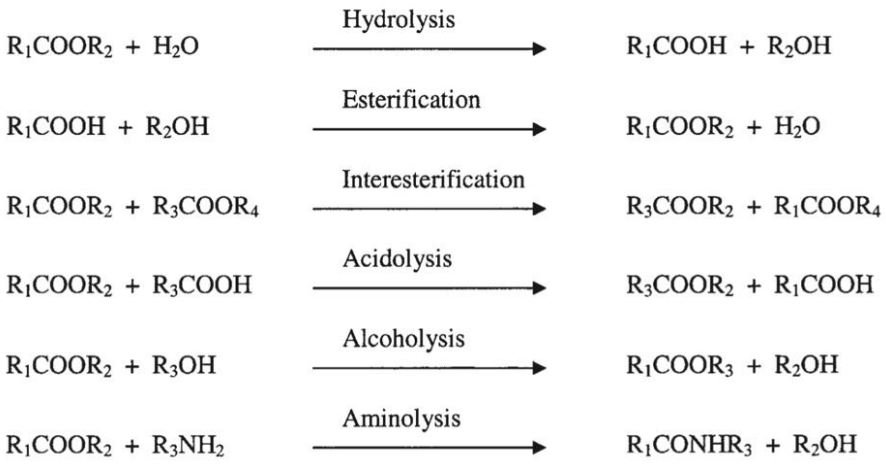

Figure 6. Lipase catalyzed different reactions (Houde et al., 2004).

Using isolated enzymes such as wild-type or protein-engineered enzymes or microorganisms in fats and oils can modify fats and oils derived from renewable resources (Bornscheuer, 2014). However, the cost of enzymes is always a major concern during the production of STAGs, so developing novel lipases with alternative synthesis to cost-effectiveness is more prevalent. For example, ABA-type SL output can be aided by *sn*-2-specific lipases (Iwasaki & Yamane, 2000). Immobilized lipases have been studied in both aqueous and organic media for hydrolytic,

synthetic, and inter-/transesterification reactions (Weete et al., 2006). According to a recent study, immobilized lipases would aid in enzymes' continuous operation or recycling. As a result, the main advantages of the immobilization process improve recyclability or reusability, greater enzyme stability in extreme pHs, including good chemical, mechanical, and thermal resistance, and low cost due to improved activity of costly lipase. Furthermore, the procedure can easily control the process of enzymatic reaction purity of the products and its reusability (Chandra et al., 2020). Immobilized lipases can metabolize the distinguishing of different fatty acids from geometric and positional isomers, which can have negative biological effects (Lichtenstein, 2013). As a result of the increasing demand for fat and oil production, there is an excellent opportunity for the application of immobilised lipases as versatile enzymes in the oleochemical industry (Filho et al., 2019).

Lipase immobilization methods would increase productivity and market profitability while decreasing logistical liability and providing environmental benefits (Chandra et al., 2020). The high enzyme cost would reduce the economic viability of the biosynthetic process on an industrial scale. Thus, the reusability of lipase, such as immobilized lipase, would significantly improve cost efficiency. According to Sellami et al. (2012), there is no significant decrease in immobilized lipase enzyme activity after four use cycles. Furthermore, the novel enzymes can improve their stability by using enzyme screening and mutagenesis techniques. Immobilized lipases can improve thermal and ionic stability, increasing their effectiveness. Immobilized lipase allows for more precise control of reaction parameters such as flow rate and substrate convenience (Chandra et al., 2020).

Many methods have been used to immobilize lipases and physical or chemical procedures can be used for production. The interactions between enzymes and support are strengthened in the physical method by weaker bonds such as hydrogen bonds and Van der Waals exchanges, which adjust these interactions. Physical absorption methods are modest, low-cost, and mild conditions that do not affect its catalytic activity because there is a low chance of conformational changes of the enzymatic structure at a lower cost. Mechanical stability has been effectively and significantly increased for improved usability and flexibility. In chemical methods, the interface

between the enzyme and the support is more critical due to the covalent bonds created by the procedure. It also has higher enzymatic stability, highly catalysed enzymatic activities, and a low cost of immobilization production and time (Chandra et al., 2020). Hence, the immobilization process has improved the recyclability, enzyme stability such as good chemical, mechanical and thermal stability, and activity of expensive lipases, which is low cost under slight conditions.

The main advantages of the use of immobilized lipases are the possibility of reuse, greater stability in extreme pHs, and thermal resistance (Filho et al., 2019). The selection of appropriate immobilization methods and carrier material, on the other hand, is critical for success. For instance, Novozymes A/S tested Lipozyme TL IM's reusability and 435 lipases. The two enzymes were reused five times under solvent-free conditions and then washed and dried after each reuse to characterise stearidonic acid soybean oil enriched with PA produced by solvent-free enzymatic interesterification (Teichert & Akoh, 2011). Thus, the form of enzymatic immobilization can make enzymatic catalysis even more efficient, diversified, and with lower costs to use lipase enzymes immobilized in many industrial processes (Filho et al., 2019).

2.2.2.1 Lipozyme TL IM and Lipozyme TL IM Immobead 150

Animals, plants, and microbes (fungi, yeast and bacteria) have been identified as sources of lipases (Utama et al., 2019). Different microorganisms have been modified the native lipases by developing genetic engineering techniques, which reduced the cost of lipases and facilitated economically affordable enzymatic reactions. Moreover, the microbial lipases have more benefits than plants or animals because of their higher catalytic activities available, rich yield production, safer stability, and their versatility for industrial application (Utama et al., 2019; Chandra et al., 2020). Between 2015 and 2020, the industrial market scope of lipase is expected to reach $590.5 Million by 2020 globally, at a CAGR of 6.5%. (Chandra et al., 2020). Several commercial immobilized lipases, including Lipozyme TL IM and immobead 150 (from *Thermomyces lanuginosus*), Heterologous lipase immobead 150 (from *Rhizopus oryzae*), Novozyme 435 and Lipozyme 435 have been widely used for investigations. **Table 1** shows different immobilized lipases for the synthesis of structured lipid in this research.

Table 1. Immobilized lipase for hydrolysis of triacylglycerols into glycerol and free fatty acids.

Enzyme	Microbial Sources	Specific/Non-specific	Immobilization Material	Reference
Lipozyme TL IM	*Thermomyces lanuginosus*	*sn*-1,3 specific	Silica gel	(Silroy et al., 2011)
Lipozyme TL IM immobead 150	*Thermomyces lanuginosus*	*sn*-1,3 specific	Silica gel	
Heterologous lipase immobead 150	*Rhizopus oryzae*	*sn*-1,3 specific	Amberlite^{TM}IRA 96	(Costa et al., 2017)
Novozyme 435	*Candida antartica*	*sn*-1,3 specific	Acrylic resin	(Willett & Akoh, 2018; Lu et al., 2017)
Lipozyme 435	Recombinant lipase from *Candida antartica*, expressed on *Aspergillus niger*	*sn*-1,3 specific	Macroporous hydrophobic resin	(Willett & Akoh, 2018)

Source: Utama et al., 2019.

Lipases are produced by several microorganisms and, as a consequence, exhibit different physical properties and specificities. The lipase from *Thermomyces laguginosus* (formerly *Humicola laguginosa*) (TLL) is a basophilic and noticeably thermostable enzyme, commercially available in both soluble and immobilized forms (Fernandez-Lafuente, 2010). TLL is a lipase preparation from the fungus *Thermomyces lanuginosus* produced in industrial scale using recombinant *Aspergillus oryzae* as the host microorganism and commercialized in soluble and immobilized forms by Novozymes. TLL is classified as 1,3-specific and has a high affinity for long-chain fatty acids (Filho et al., 2019). Although TLL was initially oriented toward the food industry, the enzyme has found applications in many different industrial areas, from biodiesel production to fine chemicals (mainly in enantio and regioselective or specific processes) (Fernandez-Lafuente, 2010).

Lipozyme TL IM is a versatile enzyme and has been widely used in industrial processes and laboratory tests, particularly in the interesterification of bulk fats and frying fats, because it was inexpensive and commercially available (Fu et al., 2014). For instance, Lipozyme TL IM has been successfully used in the interesterification of palm stearin and coconut oil to synthesize margarine (Bornscheuer et al., 2012). Also, Khodadadi et al. (2013) reported that Lipozyme TL

IM and Novozyme 435 were more effective in transesterification reaction between flaxseed oil and tricaprylin than Lipozyme RM IM and Amano DF. Moreover, Immobead 150 is new commercial support of methacrylate polymers with epoxy functions and an average particle size of 0.15–0.30 mm. Supports containing epoxy groups are characterized as having short spacer arms and being very stable at neutral pH. The modified supports might be suitable for the development of strategies of immobilization of TLL. Lipase from *T. lanuginosus* on Immobead 150 showed a half-life of 5.32 h at 70 °C, being approximately 30 times more stable than its soluble form; it showed high stability (Matte et al., 2014).

2.2.2.2 Heterologous Lipase Immobead 150

Novel non-commercial *sn*-1,3 regioselective lipases are used as an alternative to high-cost commercial enzymes, namely, the heterologous lipase from *Rhizopus oryzae* (rROL) immobilized in AmberliteTM IRA 96 and Carica papaya lipase (CPL) self-immobilized in papaya latex. The native microorganism only produces one form of extracellular lipase with high biotechnological potential as the enzymes for lipid enzymatic modifications, resulting from its high regioespecificity acting only at the *sn*-1 and *sn*-3 locations (Valero, 2012). Between the different *Rhizopus* species, lipase from R. *oryzae*, is used as a feasible noncommercial catalyst for the synthesis of TAG or SL production (Costa et al., 2017). The non-commercial *sn*-1,3 regioselective recombinant R. *oryzae* lipase can be obtained by acidolysis of grapeseed oil with caprylic or capric acid (Costa et al., 2017).

2.2.2.3 Novozymes 435

Lipozyme RM IM and Novozymes 435 are the most popular and widely used commercial immobilized lipases for STAG synthesis (Bornscheuer et al., 2012; Ortiz et al., 2019). Both enzymes perform admirably in the synthesis of STAG. Furthermore, the lipase from *Rhizomucor miehei* (sold as ‘Lipozyme RM IM' from Novozymes, Denmark) and lipase B from *Candida antarctica* (sold as ‘Novozymes SP435' as the catalysts are highly active and stable at temperatures ranging from 60 to 80°C (Bornscheuer et al., 2012).

While Novozymes 435 (N435) is a commercially available immobilized lipase produced by Novozymes, it is based on immobilization through interfacial activation of lipase B from

Candida antarctica on a resin. N435 is perhaps the most widely used commercial biocatalyst in both academy and industry. However, the mechanical fragility, moderate hydrophilicity that permits the accumulation of hydrophilic compounds (e.g., water or glycerine), and the most critical one, support dissolution in some organic media, can be specific problems. Even with these problems, N435 may continue in the coming future due to its excellent properties if some simpler alternative enzymes are not developed (Ortiz et al., 2019).

2.2.2.4 Lipozyme 435 C

Novozym 435 and Lipozyme 435 are CALB immobilized on Lewatit VP OC 1600, a polymethacrylic acid cross-linked with divinylbenzene. Differently modified Lipozyme 435 (L435) (immobilized lipase B from *Candida antarctica*) preparations were used as enzymes in the esterification reaction (Gonçalves et al., 2021). The ethanolysis of fish oil can be catalyzed by the immobilized commercial lipase Lipozyme 435 (*Candida Antarctica*) (Bucio et al., 2015). Also, the limited repeatability and stability of Lipozyme 435 are crucial factors for cost reduction in large-scale production (Gonçalves et al., 2021).

2.2.3 Types of Triacylglycerols (TAGs)

The synthesis of structured lipids with high purity influences the structure of TAGs. From **Fig.7**, the structured lipids are categorized into several types, including monoacid, diacid, and triacid TGs, with the synthetic strategies for each type based on their structures. While the monoacid TAG was AAA type with only one kind of fatty acid species. This type as the simplest TAGs structure can be synthesized chemically or enzymatically from fatty acids and glycerol. In contrast, most of the AAA types of TGs can be produced by chemical methods. Consequently, the diacid TAGs have positional isomers of ABA and AAB-type SLs. The ABA-type SLs can be synthesized by two methods. Firstly, it can employ a two-step reaction for the synthesis by sn-1,3-position-specific lipases catalysed, and then interesterification of two different TGs. For instance, in the synthetic route for the pure 1,3-di-capryloyl-2-oleoylglycerol (COC) through 2-monothioglycerol(2-MO). The pure trioleoylglycerol (OOO) was deacylated by sn-1,3-position-specific lipase to yield 2-MO. Then the 2-MO has enzymatic esterification with caprylic acid,

resulting in COC formation. Secondly, the lipase-catalysed esterification has the acyl exchange of TG with fatty acids or ethyl acid (FAEt). On the other hand, the AAB-type SLs are synthesized by *sn*-1,3-specific lipase-catalysed acylation of glycerol with fatty acid to give symmetric 1,3-diacyl-sn-glycerol, and then chemical acylation at the *sn*-2 position. Triacid TGs as ABC type are much more complicated among the classes described above (Iwasaki & Yamane, 2000).

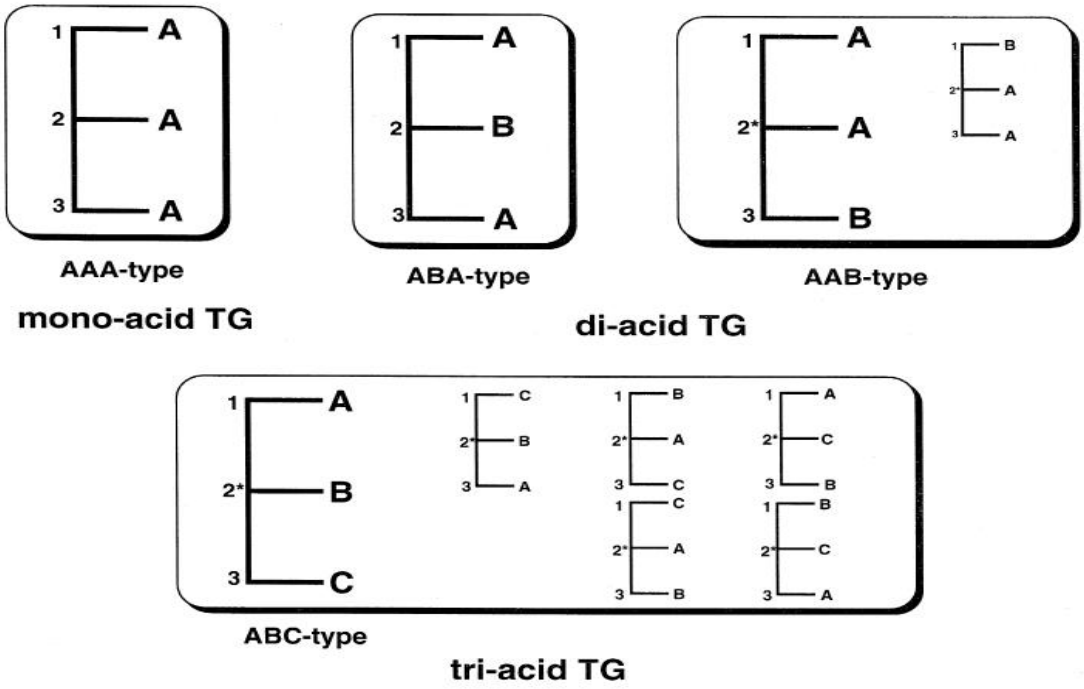

Figure 7. Classification of TGs according to their structure. Structure of TAGs is schematically represented. “A”, “B”, and “C” denote any acyl groups, but they are not identical. TAGs are classified into mono-, di- and triacid TGs. The di-acid TGs are further categorized into ABA and AAB types. AAB- and ABC- type TGs have chiral centres at the sn-2 carbons (Iwasaki & Yamane, 2004).

2.2.4 Food Applications of Modified TAGs

The development of measures to improve fats and oils' nutritional and functional qualities is always of significant interest to the food industries (Willis & Marangoni, 2006). As the synthesis of STAGs can increase or modify each fatty acid's physical and/or chemical properties, such as

melting behaviour, digestion, absorption, improving stability, and metabolism, to facilitate positive nutritional and metabolic qualities for nutraceutical and medicinal applications. Furthermore, it is utilized in the production of shortenings, margarine, and spreads to improve their textural qualities (Willis & Marangoni, 2006). As a result, modified TAGs are referred to as nutraceuticals and functional foods that can be customized to meet clients' needs. Structured TAGs were applied to produce cocoa butter substitutes, human milk fat replacers, low-calorie fats & oils, and nutraceuticals.

2.2.4.1 Cocoa Butter Substitute

Firstly, the best-known application of a one-step process is synthesising a cocoa butter equivalent, predominantly modified fat as 1,3-stearoyl-2-oleoyl-glycerol, where palmitic, stearic, and oleic acids account for more than 95% of the total fatty acids. Cocoa butter is a mixture of oil and fat composed of TAG possessing palmitic acid, stearic acid, and oleic acid as the major components (Houde et al., 2004). Palmitic and stearic acids at the 1,3-positions and oleic acid at the 2-position (Shimada, 2006). Transesterification of cocoa butter using non-specific lipase to enhance the plasticity in diethyl ether provides a convenient analytical methodology for determining fatty acid distribution with triglycerides (Goh, Yeong & Wang, 1993). Currently, the food companies use *sn*-1,3-selective lipases for replacing palmitic acid with stearic acid in the *sn*-1 and *sn*-3 position of TAGs. This process proceeds through transesterification or acidolysis of cheap oils and tristearin or stearic acid as a donor of acyl groups. However, the availability of cocoa butter has limited and results in high cost. Thereby, alternative replacements for cocoa butter were obtained through the structural modification of low-cost vegetable oils. Cocoa butter substitutes were produced with a cooling, melting sensation characteristic of chocolate and similar physical properties at a lower cost. Transesterification has been used to improve the textural properties of fat and rapeseed oil mixtures, and the development of cocoa butter equivalents is an example of structured lipids with a similar TAG composition. A new process utilizing a fixed-bed bioreactor packed with immobilized 1,3-specific lipase significantly influenced subsequent oil processing with lipases.

Additionally, MLCT showed potential to be used as a substitute for canola oil in making cold spreadable butter. The synthesis of structured TAGs based on Canarium oil can be exploited as starting material for functional food applications (Willis & Marangoni, 2006; Bornscheuer et al., 2012; Kim and Akoh, 2006; Adamczak, 2004; Shimada, 2006; Houde et al., 2004). In addition, Newlase, an immobilized lipase from *Rhizopus niveus*, incorporates stearic acid, particularly at the *sn*-1 and *sn*-3 sites of triglycerides in safflower oil or sunflower oil. Since 1993, Fuji Oil has used this technique to create a cocoa butter substitute (Houde et al., 2004).

2.2.4.2 Human Milk-Fat Substitute

Infant formula is a viable replacement for breast milk and, ideally, mimics human milk as closely as possible. Milk fat is the primary energy source in human milk and provides the lipids needed to construct cell membrane structures. Another possible application of SLs could be their use in infant formula as a human milk fat (HMF) analogue. The two-step STAG synthesis method was also used to synthesise 1,3-dioleinoyl-2-palmitoyl-sn-glycerol (OPO) as a human milk-fat substitute, which could be applied for the nutrition of infants because the infants require proper nutrition for growth through mimicking the fat like palmitic acid (PA) found in breast milk. Human milk fat contains 20-25% palmitic acid, and about 70% of the fatty acid is esterified to the *sn*-2 position of TAGs. Also, the second major TAG component of human milk is palmitic acid found in acylglycerols, mainly esterified in the *sn*-2 position, which helps improve the absorption of fat and calcium in infants (Teichert & Akoh, 2011; Adamczak, 2004). Hence, human fat substitutes by enzymatic acidolysis are STAG rich in palmitic acid at the *sn*-2 position and oleic acid at sn-1,3 positions (Shimada, 2006). Lipase modification of the triglyceride to increase the proportion of palmitic acid at the *sn*-2 position results in fat with better absorption in newborns (Houde et al., 2004). For the first commercial product of an HMF analogue, the STAG is produced by acidolysis of tripalmitin and oleic acid with the use of a 1,3-specific lipase from *Rhizomucor miehei* (Lipozyme RM IM) and is sold under the commercial name "Betapol^{TM}" (Akoh & Xu, 2002). The simple one-step transesterification has been frequently used in literature as documented in numerous publications, but a major limitation is that various TAG species are produced and not the desired one (Bornscheuer, 2014). The achieved product of "Betapol^{TM}"

contains as little as only 65% of palmitic acid in the *sn*-2 position, causing undesired side effects in infants due to the formation of calcium soaps from palmitic acid in the *sn*-1- or *sn*-3- position (Esteban et al., 2011; Adamczak, 2004).

2.2.4.3 Beverages or Margarine

Furthermore, the sensory and nutritional properties of SLs could be comparable or superior to original oil when SLs were applied to beverages or margarine (Lee & Lee, 2006). Canola oil is often used to prepare beverages, which is beneficial for individuals who need a quick energy source rich in important fatty acids. It is critical to use canola oil-based structured lipid so that the producer does not have to adjust the formulation when substituting canola oil with canola oil-structured lipid.

As the food industry strives to substitute trans-fat in its products with functionally similar and economically viable formulations, enzymatic transesterification may be a technological solution for producing trans-free fat for commercial uses in an environmentally responsible manner. According to the rheological profile, margarine made with the transesterified blend had superior spreadability than control margarine made with non-transesterified fats. Thus, lipase-catalysed interesterification converts hydrogenated fats to trans acid-free alternatives to make shortening and margarine. Also, because palm oil and palm products are naturally viscoelastic semi-solid food products that can be further modified by fractionation, interesterification, hydrogenation, and blending for food product formulations or preparation, palm oil and palm products have become essential raw materials in the application of shortenings and margarine. Furthermore, the health benefits of MLCT from enzymatic procedures are important for food industry applications. MLCT with C6-C12 carbon chain length is more rapidly metabolized than LCFA and it can be produced via the lipase-catalysed acidolysis, esterification, or interesterification reactions. MLCT can also be used to make shortening and margarine by combining a hard stock (fully hydrogenated soybean oil) with a soft oil (rice bran oil, coconut oil), which gives the newly created oil the plasticity required to be converted into margarine and shortening. Because of the

health consequences, the oils and fats sector expects to commercialize zero- or low-trans products (Nor Aini & Miskandar, 2007; Sellami et al., 2012; Sitompul et al., 2018).

2.2.4.4 Low-Calorie Fats

Consumers are becoming more conscious of food's nutritional quality, energy content, and long-term health effects. Although fats have a high-calorie intake, their pleasant flavour and smoothness make them difficult to avoid. Calorie-reduced and fat-substituted products are now available. These low-calorie and dietetic SLs can be used to manage obesity and other metabolic issues using enzymatic or chemical approaches. Chemical interesterification completely randomizes the position of acyl groups in triacylglycerols. Despite their lack of selectivity, sodium methoxide and sodium alkoxides act as catalysts in manufacturing commercial goods with the necessary nutritional function. Because medium-chain fatty acids at the *sn*-1 and *sn*-3 positions are easily digested by pancreatic lipase, taken into the intestines, and quickly transported into the liver where the immediate energy source can be digested (Lee and Lee, 2006). From a nutritional standpoint, fatty acids that are positioned at *sn*-2 are easily digested and absorbed *in vivo* (Hu et al., 2017). Triacylglycerols containing palmitic acid in the *sn*-2 position and short-chain fatty acids in the *sn*-1,3 position are low-calorie STAG. Low-Calorie structured lipids (LCSL) could be efficiently synthesized by lipase-catalysed transesterification of triacetin with stearic acid in a solvent-free system. Also, the commercially available STAG can apply to many products, among them low-calorie structured fats, ‘Salatrim’ and ‘Caprenin’, which are widely applied to achieve a particular functional or nutritional purpose in food products. One of the advantages of this STAG is to provide the physical properties of fat with approximately half of the calories of typical edible oils. SALATRIM (short and long acyl triglyceride molecule) fats as the most familiar low-calorie structured lipids (LCSL) are defined as TAG mixtures and catalysed by alkali metal chemical interesterification of hydrogenated vegetable oils with short-chain TAG. Thus, the removal of the toxic materials after reaction and subsequent purification steps are needed to obtain. Although lipase-catalysed esterification offers some benefits under mild conditions, there has been no enzymatic production of LCSL commercially currently.

While ‘Salatrim’ is a mixture of short-chain (2-4) and long-chain (16-22) triacylglycerols produced by a random interesterification, the properties of the ‘Salatrim’ depend on the chain length and positional distribution of acyl moieties on the TAG backbone. As a low-calorie fat (5 kcal/g), it is intended for use in oven-baked French fries, baked and dairy products, dressings, dips, sauces, cocoa butter substitute, and chocolate-flavoured coating.

The enzymatic synthesis can also produce products similar to ‘Salatrim’ as ‘Caprenin’ which contains caprylic (8:0), capric (10:0) and behenic (22:0) acids has been produced by both enzymatic and chemical processes. This GRAS product is synthesized by interesterification between coconut, palm kernel, and rapeseed oils and has the application of low-calorie fat (5 kcal/g), ingredient of soft candies, candy bars, and confectionery coatings for nuts, cookies, etc. (Bornscheuer et al., 2012; Yang et al., 2001). Thus, SLs as ‘Salatrim’ and ‘Caprenin’ can be used in various food applications from cocoa butter, human milk fat analogue, margarine, shortenings, cookies and salad dressings, and Low-Calorie structured lipids.

2.2.4.5 Structured Lipids and Human Health

Structured lipids (SLs) can be used as constituents of functional foods for maintaining good health and nutritive or therapeutic purposes, including prevention and/or the treatment of certain diseases. The SL might deliver desired fatty acids targeting specific diseases and metabolic conditions (Lee & Akoh, 1998) when structured lipids are produced with edible oils, which have beneficial properties with their specific fatty acids.

Fats and oils give palatability to food products and cannot be entirely eliminated from our diet, but the high consumption of dietary fats can be detrimental to health. Therefore, the production of medium-long-chain triacylglycerol (MLCT) has the speciality of structured lipids that can be metabolized differently compared to conventional fats and oils, which can result in reducing fat accumulation in the body. Also, the application of MLCT in food industries can be used for obesity management as it contains nutritional properties that can be used to treat metabolic

problems. The advantage of MLCT oil on humans is that it can act as functional oil that prevents fat accumulation in our body, thereby reducing body fat and weight. MCT does not accumulate in the fatty tissue and does not form a reserve fat as the human body rapidly metabolizes it. Thus, MCTs can be applied to infants and in the clinical nutrition of patients with digestion or nutrient absorption disorders (Lee et al., 2012; Adamczak, 2004).

2.3. Bioactive Delivery via Encapsulation Technology

2.3.1 Overview of Encapsulation

Encapsulation is a process that entraps the bioactive ingredients such as food ingredients, enzymes, cells, or other substances within another, which protects bioactive material and prevents the loss of its beneficial effects (Karimi et al., 2015). Encapsulation technology can enhance nutraceuticals' stability, water solubility, and bioavailability, which has become one of the most helpful research areas in the food and drug industries (Moghimi et al., 2016; Karimi et al., 2018). Scientists were able to manufacture numerous lipid-based carriers such as nano and microemulsions, liposome, and lipid nanocarriers, after gaining a fundamental knowledge of the increased chemistry and physicochemical properties of amphiphilic capabilities of lipids (Eh Suk et al., 2020). These self-assembled colloidal lipid systems are the most diverse possibilities for the topical delivery of drugs (Elsayed et al., 2007).

During the last 20 years, there has only been one revolutionary carrier system that can be called a significant innovative contribution in the dermal area: liposomes, which Dior initially presented to the cosmetic market in 1986. Due to their composition, variability and structural properties, liposomes are incredibly versatile, leading to many applications, including pharmaceutical, cosmetics and food industrial fields. Generally, it is believed that liposomes are suitable delivery systems for nutraceuticals and can be applied in the food industry (Karimi et al., 2015).

The presence of biological lipids that are highly biodegradable and biocompatible has drawn scientific attention to lipid nanoparticles. At the beginning of the 1990s, the advantages of solid

particles, emulsions and liposomes were combined by developing solid lipid nanoparticles (SLNs) (Müller et al., 2002). However, the conventional liposomes and emulsions suffered from certain disadvantages, including physical and chemical instability, the requirement of time-consuming multistep processes, and non-reproducible release of the drug and toxicity due to organic solvent residues based on the preparation technique (Uner M, 2006). Generally, encapsulation is typically applied for several reasons, including i) delivering the bioactive components at the appropriate gastrointestinal target with controlled release; ii) ensuring the stability of the compounds in the gastrointestinal system and functional food systems; iii) advancing the absorption of nutraceuticals at the intestinal site; and iv) hiding the unpleasant characteristics of the core material in food products (Karimi et al., 2018).

Selecting encapsulation methods is essential to developing micro or nano-structured encapsulated systems. The coating of different substances within another material at nanoscale sizes is known as nanoencapsulation. Microencapsulation is comparable to nanoencapsulation, except that it uses larger particles and has a longer application history (Suganya & Anuradha, 2017). Lipid nanoparticles (LNs) have a good potential for developing new biocompatible carrier systems, improving controlled release, and enabling precision targeting the bioactive compounds rather than microencapsulation (Lacatusu et al., 2011; Suganya & Anuradha, 2017).

2.3.2 Lipid Nanoparticles (LNs)

Over the past decades, great improvements have been made in developing bioactive materials delivery systems for plant actives and extracts. Encapsulation is advantageous for various delivery and food processing systems. However, many challenges are still associated with these nanoformulations, including process complexity, lack of stability, higher manufacturing costs, and toxicity in the case of polymeric nanoparticles. Recently, lipid nanoparticles (LNs) have become increasingly of interest to scientists due to their potential to overcome topical drug delivery challenges using solid lipid nanoparticles (SLNs) and nanostructured lipid carriers (NLCs) as significant lipid-based nanoparticles (Müller et al., 2002; Puglia et al., 2014). For SLNs and NLCs, the technologies used to create the final topical formulation have been

explained, particularly the manufacture of highly concentrated lipid nanoparticle dispersions with lipid content of >30–80%. Clinical batch production, large-scale manufacturing, and regulatory issues are likewise production issues (e. g., status of excipients or proof of physical stability) (Müller et al., 2002). The encapsulation of fatty acids in nanocarrier systems is an alternative carrier as an effective technique for enhancing their biological efficiency and controlled delivery (Hashemi et al., 2020).

Lipid nanoparticles (LNs) are colloidal carrier systems because they are composed of a biocompatible/biodegradable lipid matrix. The use of LNs in pharmaceutical technology has been reported for several years. LNs protects the loaded bioactive compounds from chemical and enzymatic degradation and gradually releases drug molecules from the lipid matrix into the blood, resulting in improved therapeutic profiles compared to the free drugs (Severino et al., 2012). Nano-sized drug carriers formulated from various materials offer a versatile platform to carry an array of therapeutic agents in a targeted manner (Alavizadeh et al., 2015). The main advantages of LNs over conventional drug carriers as they are formulated with high biocompatibility, good physical stability, the possibility of controlled release of drugs and active substances, ease of large-scale production, and low raw material costs (Puglia et al., 2014; Müller et al., 2002; Eh Suk et al., 2020; Hashemi et al., 2020). LNs protects bioactive compounds, such as vitamins, antioxidants, proteins, and lipids, which enhances functionality and stability (Karimi et al., 2015).

In recent years, using LNs for food fortification has been a positive approach, as they can be effective in the delivery and stability of hydrophobic compounds. The entrapped bioactive components in food and feed products are expected to improve additive stability and extend the shelf life (Holser, 2011). LNs increase bioavailability during digestion and prevent the food's development of off-flavours and off-colours (Hashemi et al., 2020). For example, lipids and lipid nanoparticles are extensively employed as oral-delivery systems for drugs and other active ingredients (Severino et al., 2012).

Furthermore, SLNs and NLCs have been developed to improve solubility and enhance the permeability of lipophilic drugs by providing a large surface area and hydrophilic surfactant layer at its outer side and lipid matrix at its inner core (Rai et al., 2021). SLNs have an application in the drug delivery system, enhancing drug release at the desired tumour site (Rai et al., 2021). Also, pharmaceutical applications included oral, parenteral, and topical drug delivery for solid lipid particles. However, drug loading capacity and reports of drug expulsion and storability have been limited to SLNs (Holser, 2011). Hence, NLCs as second-generation lipid nanoparticles were developed to improve drug loading as detailed in the following section.

2.4. Nanostructured Lipid Carriers (NLCs)

Nanostructured lipid carrier (NLC) is the second generation of lipid-based nanocarriers formed from a mixture of solid and liquid lipids, which developed a distinct structure and unique advantages in comparison to traditional lipid carriers, such as high encapsulation efficiency (EE), physicochemical stability, bioavailability, long shelf life and low release rate of functional hydrophobic ingredients in food products (Karimi et al., 2018; Hashemi et al., 2020; Eh Suk et al., 2020). Recounting NLC based formulations have been increasingly provoked to develop safe and valuable delivery systems. The lipid system is composed of well-tolerated and physiological lipids and acts as a physical barrier that may prevent the encapsulated bioactive components from unpleasant factors in the aqueous phase (Lacatusu et al., 2011; Karimi et al., 2018). As NLC are the binary system containing both solid lipids and liquid lipids as a core matrix, which are characterised by a less organised structure called lipidic core and allows for higher loading capacity and more active ingredients stability during the storage (Elmowafy & Al-Sanea, 2021; Müller et al., 2002; Eh Suk et al., 2020). They are also stabilized with the addition of blends of surfactants at an appropriate concentration.

2.4.1 Comparison NLCs and SLNs

The encapsulation of structurally sensitive chemicals in a solid lipid matrix act as a barrier to prooxidant substances, thereby limiting oxidative destruction and preserving the bioactivity of

labile structures (Holser, 2011). On the capability of a lipid-based drug delivery system, Müller and Gasco firstly developed and nominated solid lipid nanoparticles (SLNs) in the 1990s as an alternative carrier system such as emulsions, liposomes, and for the sake of avoiding the use of organic solvents in the preparation of polymeric nanoparticles (Müller et al., 2002; Muller et al., 2011; BHATT et al., 2021). The advantages of SLNs are physiological lipids, the avoidance of organic solvents, and the applicability of large-scale production (Fang et al., 2013). However, SLNs show some disadvantages as drug carriers, including unpredictable gelation tendency, polymorphic transition, and low incorporation due to the crystalline structure of solid lipids, drug loading and expulsion that might occur during the storage (Fang et al., 2013; Azmi et al., 2020).

These liquid lipid-containing nanoparticles, as a novel type of lipid nanoparticles in the delivery system, were further named nanostructured lipid carriers (NLC), composed of biocompatible and biodegradable natural materials, including a liquid lipid blended with a solid lipid to form special nanostructures in the matrix. Liquid lipid in NLC is employed to change the formation of SLN and resolve the problems raised by SLN. This structure intensifies the drug loading and improves the incorporation of the drugs during storage (BHATT et al., 2021; Hashemi et al., 2020; Azmi et al., 2020).

The formation of a perfect crystal that can be compared to a dense ‘brick wall’ is a potential disadvantage in SLN and leads to drug expulsion (**Fig. 8).** Drug loading in SLN has been limited due to the lipid crystal. In contrast, the NLC can control the transformation process that can be used to trigger the release of drugs. Drug loading is a significant disadvantage of SLN. The SLN has the drug expulsion during the storage, while NLC improve drug entrapment with the lowest leakage. Incorporating a liquid lipid in the preparation of nanoparticles helps incorporate more drugs into the nanoparticle and enhances the physical stability of the nanocarrier

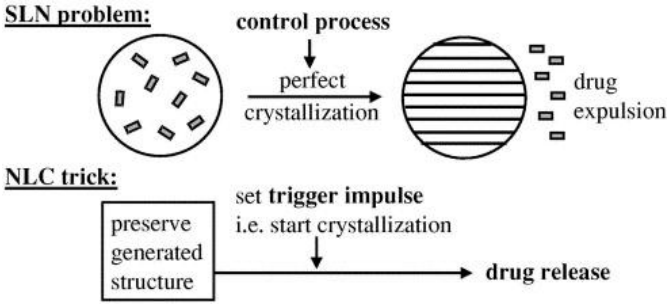

Figure 8. Triggered release of active compounds by controlling the transform (Müller et al., 2002).

Compared to the less highly ordered matrix of SLN, the increase in ordered structure was nicely shown in the three different types of NLC productions: imperfect, amorphous, and multiple types. Thus, NLC has superior drug loading capacity due to a less ordered solid lipid matrix than the SLN. The payloads of SLN for many drugs were insufficient. The payload for active compounds of NLC has been enhanced, and compound expulsion during storage should be avoided by giving the lipid matrix an individual nanostructure. Furthermore, the NLC has low toxic side effects potential when compared to polymeric nanoparticles (Naseri et al., 2015). Furthermore, NLC can control drug release and contain fewer amounts of surfactant and cosurfactant when compared to emulsions. Also, the most lipid reported as an excipient in the production of NLC, which are generally considered safe (GRAS) and biodegradable (Elmowafy & Al-Sanea, 2021; Müller et al., 2002; Ghate et al., 2016; BHATT et al., 2021; Hashemi et al., 2020; Naseri et al., 2015). Therefore, NLC represents the second generation of lipid nanoparticles that overcome the limitations of conventional SLN. The incorporation of bioactive materials into NLC enhances their stability and bioavailability.

2.4.2 Materials for NLCs Preparation

The essential ingredients for NLCs are composed of the lipid phase, aqueous phase, and surfactants. These ingredients and their concentrations in NLCs significantly impact the final behaviour of the fabricated NLCs and drug release profiles of the nanoparticles. The stability of NLC solutions is influenced by lipid properties such as melting temperature, viscosity,

crystalline shape, and hydrophilicity (Babazadeh et al., 2017). **Table 2** shows the common ingredients for composing nanostructured lipid carriers.

Table 2. The excipients for composing nanostructured lipid carriers (NLCs).

Ingredients	Material
Liquid lipids	Medium chain triglycerides, paraffin oil, 2-octyl dodecanol, oleic acid, squalene, isopropyl myristate, vitamin E, Miglyol® 812, Transcutol® HP, Labrafil Lipofile® WL 1349, Labrafac® PG, Lauroglycol® FCC, Capryol® 90
Solid lipids	Tristearin, stearic acid, cetyl palmitate, cholesterol, Precirol® ATO 5, Compritol® 888 ATO, Dynasan®116, Dynasan® 118, Softisan® 154, Cutina® CP, Imwitor® 900 P, Geleol®, Gelot® 64, Emulcire® 61
Hydrophilic surfactants	Pluronic® F68 (poloxamer 188), Pluronic® F127 (poloxamer 407), Tween 20, Tween 40, Tween 80, polyvinyl alcohol, Solutol® HS15, trehalose, sodium deoxycholate, sodium glycocholate, sodium oleate, polyglycerol methyl glucose distearate
Lipophilic surfactants	Myverol® 18-04K, Span 20, Span 40, Span 60
Amphiphilic surfactants	Egg lecithin, soya lecithin, phosphatidylcholines, phosphatidylethanolamines, Gelucire® 50/13

Source: Fang et al., 2013.

2.4.2.1 Liquid Lipids

Various types of lipids could be utilised in this formation of NLC. Both solid and liquid lipids are included in NLC for constructing the inner cores (Fang et al., 2013; Sakellari et al., 2021). Liquid lipids typically used for NLC consist of digestible oils from natural sources. The commonly used liquid oils are often utilized as the constituents of liquid lipids because of their similar structures such as soybean oil (Pardeike et al., 2011) and olive oil (Huguet-Casquero et

al., 2020). Alternatively, fatty acids, such as oleic acid (Elmowafy et al., 2018b), are included in NLC for their value as having oily components and being penetration enhancers of topical delivery. Most lipids have already been given the "generally recognised as safe (GRAS)" status by the European and American regulatory authorities for clinical purposes. Novel and biocompatible oils that may be applied without irritation, are affordable, and can be sterilized are needed (Fang et al., 2013). For example, the lipids are biodegradable and, thus, are less toxic to the skin application (Ghate et al., 2016). Incorporating a liquid lipid in the nanoparticle preparation helps incorporate more drugs into the nanoparticle and improves the physical stability of nanocarriers.

2.4.2.2 Solid Lipids

The common solid lipids for the preparation of NLCs can be Compritol 888 ATO (Khan et al., 2019; Pradhan et al., 2015), Precirol ATO 5 (Mohammed Elmowafy et al., 2019) or Stearic acid (Elmowafy et al., 2018a) (Ghate et al. 2016), and glyceryl monostearate (GMS) for loaded NLCs (Rai et al., 2021). These lipids are in a solid state at room temperature. They would melt at higher temperatures (e.g. > 80 °C) during the preparation of NLCs (Fang et al., 2013). For instance, high melting point glyceryl monostearate (GMS) for Docetaxel-loaded SLNs is based on the idea that high melting triglycerides are excellent excipients for Docetaxel (Rai et al., 2021).

Moreover, the solid lipid core should have structural imperfections to improve drug incorporation into the system. NLCs are novel drug delivery systems for delivering actives with high solubility, stability, powerful skin penetration, and low skin discomfort. Because of its physiological lipid composition and occlusive affect properties, the system has been demonstrated to be an effective system for increasing skin hydration as the small size of NLCs ensures close contact with the stratum corneum and can improve the amount of active compound penetration the skin (Azmi et al., 2020).

2.4.2.3 Emulsifiers / Surfactants

Although NLCs comprises a combination of solid and liquid lipids dispersed in the aqueous phase, the particles tend to agglomerate and are less stable in NLCs formulation. The surfactants used to stabilize lipid dispersions in the formation and characterization of NLCs. **Table 2** summarizes the detailed information on the different types of surfactants for NLCs. The most widely used aqueous phase consisting of hydrophilic surfactants are Poloxamer 188 (Khan et al., 2019), Poloxamer 407 (Hashemi et al., 2020), Tween 80 (Khan et al., 2019; Pradhan et al., 2015). Lipophilic or amphiphilic surfactants such as Span 80 and lecithin (Khan et al., 2016) are employed to fabricate NLCs if necessary. The surfactants can improve the electrostatic interactions between droplets and incorporation into the lipid phase, enhance the stability of the emulsions via lowering the Ostwald ripening rate and significantly increase the high-temperature stability (Tian et al., 2015). In addition, it has been discovered that combining various surfactants can more effectively prevent particle aggregation (Fang et al., 2013). A mixture of (hydrophilic and lipophilic) surfactants can improve the systems' developed physical stability and functional properties (Elmowafy & Al-Sanea, 2021).

Moreover, suitable surfactants reduce interface tension and facilitate droplet dispersion during homogenization (Babazadeh et al., 2017). Non-ionic surfactants such as polysorbates and poloxamers are alternatives for stabilizing the NLCs dispersion in this study. For different surfactant types, the solubility and miscibility of NLCs could be enhanced. The emulsions stabilized by other surfactants showed relatively different structures at the interface, while various forms and sizes of free surfactants were presented in the solution.

Polysorbates (Tweens) are primarily common hydrophilic emulsifiers and powerful steric stabilisers permitted in foods (Babazadeh et al., 2017). Tweens were effectively incorporated into a lipid nanocarrier as a surfactant for dispersing hydrophobic particles in aqueous solutions, which has the potential to be developed as a carrier for a variety of active components, including nutrients, extracts, and medicines (Kerwin, 2008). The incorporation of Tween caused crystallization, which improved self-assembly properties and decreased the agglomeration of

NLCs, resulting in more single NLCs particles being detected. The effects of polysorbate nonionic surfactants, namely Tween 20 and 80, on the NLCs formulation were investigated. Tween 20 and 80 are biocompatible surfactants in food, biotechnical, and pharmaceutical applications. They are both miscible in water and yield a clear, yellow solution. However, despite their similar functions, there are still differences between the two types of tweens, especially in types of applications. For biochemical applications, Tween 20, known as Polysorbate 20, is attached to 20 repeat units of polyethene glycol and spread throughout four chains with a hydrophobic dodecanoic tail. Tween 20 is more hydrophilic (Eh Suk et al., 2020). In contrast, Tween 80 is a polyethylene sorbitol ester, known as Polysorbate 80 or polyoxyethylene sorbitan monooleate. Thus, Tween 80 has a longer aliphatic tail and, therefore more lipophilic (Eh Suk et al., 2020). Tween 80 has been extensively used in the formulation of drugs, skin care products, and foods as a solubilizer, emulsifier, and stabilizer. It is a direct food additive, which allows for some special foods by FDA (21CFR172.840) (Babazadeh et al., 2017). The average particle size for formulation incorporated with Tween 80 reduced the most in comparing Tween 20, 40, 60 and 80. This could be due to the blend and kink at the double bond of monooleate in Tween 80, which enhances the curvature of the NLCs particles (Eh Suk et al., 2020).

Different poloxamer excipients have been extensively used in pharmaceutical industries as water-soluble emulsifiers, solubilizers for hydrophobic drugs, and suspension stabilizers. Poloxamer 407, in combination with a liposome, remarkably improved liposome formulation stability by increasing half-life, preventing aggregation, and fusion of phosphatidylcholine multilamellar vesicles (Pezeshki et al., 2014; Hashemi et al., 2020). This study chose three non-ionic surfactant types, poloxamer 407, Tween 20 and Tween 80, to prepare NLCs. Non-ionic surfactants have lower toxicity than ionic ones (Babazadeh et al., 2017).

On the one hand, the concentration of the surfactant also mainly affects the particle size of loaded NLCs. The surfactant type and concentration have proved to play a critical role in stabilizing the formulation of NLCs and preventing particle agglomeration (Severino et al., 2012; Wei et al., 2020).

Sufficient emulsifiers are present to hold freshly formed smaller particles produced during homogenization. At higher surfactant concentration, the oil has an inverse effect observed in the particle size, which is consistent with serval studies. Hence, it prevents particle coalescence, increasing stability (Anarjan et al., 2011). The plausible reason for this increase is the higher viscosity of NA-TAG oil which makes the disruption of droplets more difficult during homogenization. (Mehmood, 2015). Generally, the higher the surfactant co-homogenisation, the smaller the particle sizes (Elmowafy & Al-Sanea, 2021). In addition, a high surfactant concentration results in a high burst release (Müller et al., 2002). Aggregation accelerated at lower surfactant concentrations where the coated fraction of particle surface area remained small (Azmi et al., 2020; Pezeshki et al., 2019).

Therefore, surfactant type and concentration play a critical role in stabilizing the formulation of NLCs (Wei et al., 2020) because different types of surfactants stabilize NLCs by efficiently adsorbing onto particle surfaces and lowering interfacial tension (Elmowafy & Al-Sanea, 2021).

2.4.3 Types of NLCs

NLCs are composed of solid and liquid lipids, surface active agents and water, in which a liquid lipid core is surrounded by a solid lipid matrix (Karimi et al., 2018). NLCs is produced by mixing spatially significantly different lipid molecules, i.e., blending solid lipids with liquid lipids (oils). Other types of NLCs are obtained depending on the production method and lipid blend composition (Müller et al., 2002). According to the lipidic structure of prepared NLCs in **Fig.9**, there are three different types of NLCs based on the composition of the lipid mixture and the method used to produce them for their preparations. The structures of NLCs can be imperfect, amorphous, and of multiple types (Elmowafy & Al-Sanea, 2021).

The NLCs type 1 (**Fig. 9A**) shows a structure with imperfection. This lipid matrix has imperfections due to lipids with various chemical properties, such as carbon chain length and saturation level. Such lipid mixtures affect crystallization and cause disorder in the crystal lattice

(Elmowafy & Al-Sanea, 2021). Consequently, the lipid matrix can accommodate a higher amount of drugs, and thereby it will be less likely to be expelled during storage than using single lipid (Müller et al., 2002).

The second type of NLCs (**Fig. 9B**) is the solid lipid matrix but not crystalline in an amorphous state. This amorphous type can avoid an ongoing crystallization process to a perfect crystal by mixing some special lipids. In this type, obtaining a structureless solid amorphous matrix results in a high drug payload as the lipid matrix will crystallize in a less ordered amorphous state. Nuclear magnetic resonance (NMR) and differential scanning calorimetry confirm lipid solid state and transition temperature, respectively (Elmowafy & Al-Sanea, 2021).

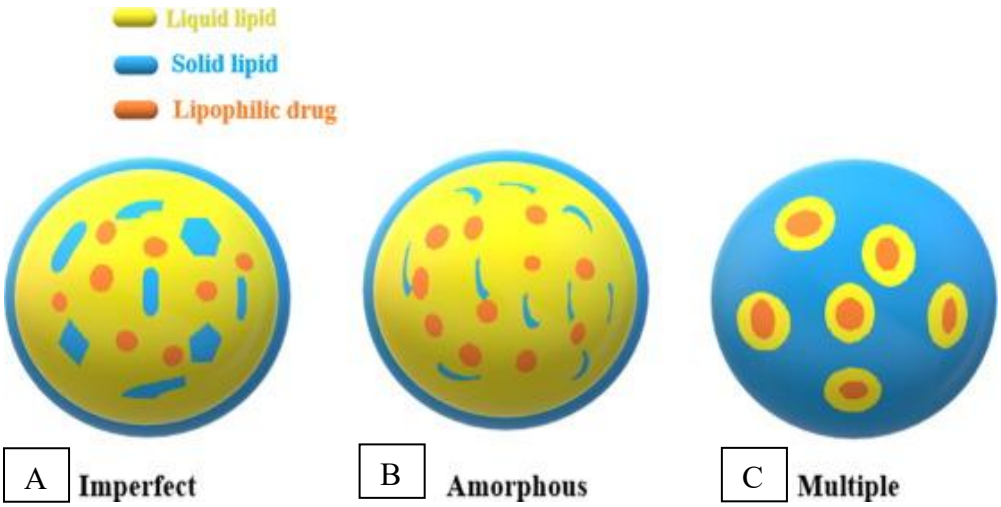

Figure 9. Types of NLCs (Elmowafy & Al-Sanea, 2021).

A multiple (**Fig. 9C**) is the third type of NLCs produced by mixing solid lipid with higher liquid oil. While in this study, it is an oil-in-solid lipid-in-water dispersion. This NLCs type takes advantage of the fact that many drugs have a higher solubility in oils than in solid lipids. The oil molecules are dispersed inside the solid lipid matrix at a lower oil solubility, and there are no oily nano compartments. When the oil concentration is increased, the solid lipid's solubility of the oil molecules is exceeded, phase separation occurs, and oily nano compartments form. This happens during the cooling process after the particles have been produced using the hot homogenization method. Retinol is multiple classic examples. The oil nano compartments are

incorporated into the solid matrix; they contain a larger concentration of the active substances, but the solid lipid barrier around them still regulates their release. Thus, a concentration of 5% retinol could be incorporated and firmly preserved during long-term storage (Elmowafy & Al-Sanea, 2021; Müller et al., 2002).

2.4.4 Preparation Methods for NLCs

As reported in the literature, various techniques have been employed to fabricate NLCs. According to energy consumption, these methods can be categorized into three types: high energy required methods such as high-pressure homogenization and high shear homogenization/sonication; low energy required forms such as microemulsion and double emulsion; and lastly, the very low or no energy required methods such as emulsification solvent evaporation, emulsification solvent diffusion and solvent injection (Elmowafy & Al-Sanea,2021). The most widely used method for NLCs preparation is high-pressure homogenisation (HPH) and high shear homogenization or sonication, due to the ease in preparation and short production period with the aim for future scaling up (Eh Suk et al., 2020). NLCs is formulated from the mixture of solid and liquid lipids dispersed in the aqueous phase. HPH produces highly stable particles and requires no organic solvent addition as the result of no solvents being added during the preparation of NLCs. It is a powerful technique for large-scale production (Elmowafy & Al-Sanea, 2021; Khan et al., 2019). At first, the lipid phase and aqueous phase are prepared separately. The lipid phase consists of solid and liquid lipids and lipophilic emulsifiers, while the aqueous phase consists of double-distilled water and hydrophilic emulsifiers. Both phases are heated separately to a high temperature for a determined time. The aqueous phase is added to the lipid phase and mixed. A high-shear homogenizer can homogenize the mixture. In some cases, the mixture can be further treated using a water-bath or probe-type sonicator to obtain a smaller and more-regular size distribution (Fang et al., 2013).

The instruments and processing steps such as high shear homogenizer and lyophilized used in preparing stable NLCs formulations can be easily employed in the pharmaceutical industry for

large-scale production (Khan et al., 2019). Moreover, the bioavailability of drug loaded NLCs can be improved by design and optimization.

2.4.5 Physiochemical Characterization of NLCs

The physicochemical characterization of NLCs is essential in confirming quality control and stability. Both physical and chemical properties can be determined for NLCs (Fang et al., 2013). NLCs constituents mainly affect the physicochemical properties and effectiveness of the final loaded NLCs product (Elmowafy & Al-Sanea, 2021). One of the main purposes was to attempt to produce nanostructured lipid carriers were done using the hot high shear homogenization/ sonication method. The successfully obtained formulation was further characterized using several essential parameters such as the particle size, polydispersity index, zeta potential of NLCs systems, physical and chemical stability, and transmission electron microscopy. In addition, the lipid nanoparticles are characterized by differential-scanning calorimetry (DSC), X-ray, nuclear magnetic resonance (NMR), and Fourier transforms infrared spectroscopy (FT-IR). As the drug is incorporated into NLCs, the encapsulation efficiency and drug-release behaviour provide essential information to judge the feasibility of NLCs as drug delivery systems (Fang et al., 2013).

2.4.5.1 Particle Size and Polydispersity Index

The most frequent parameters for determining NLC are particle size and zeta potential. Photon correlation spectroscopy (PCS) and laser diffraction are the most powerful methods for routine particle size measurement. PCS is also known as dynamic light scattering. It measures the fluctuation of the scattered light intensity produced by particle movement (Fang et al., 2013). The particle size is the most critical characteristic of an NLC formulation (Azmi et al., 2020). The types and ratios of lipid and surfactants used in NLC greatly affect the particle size. For instance, in the penetration of the skin, the small size of nanoparticles ensures close contact of the extract with the stratum corneum, making it easier for the extract to penetrate. Because of the small size of NLC, the system has a large surface area and low interfacial tension of the droplets, allowing for easy penetration through the skin (Azmi et al., 2020).

Furthermore, the narrow PDI also shows the stability of nanoparticle dispersion. As reported by Mitri et al. (2011), the polydispersity index (PDI) parameter provides important indications concerning sample homogeneity, as values below 0.25 reflect relatively homogeneous nanoparticles with a minimum predisposition to aggregation (Mitri et al., 2011). The narrow polydispersity index ranges from 0.01 to 0.7, indicating a monophasic system.

2.4.5.2 Zeta Potential

Zeta potential is an essential measurement that controls electrostatic interactions in particle dispersions and predicts the physical stability of colloidal dispersions in the application. All measurements reported in this paper were made at a temperature of 25℃ on a Zetasizer Nano ZS (Malvern Instruments Ltd, Malvern, UK) fitted with a high-concentration zeta potential cell. It can optimize the formulation of suspensions and emulsions and help predict short-term or long-term stability. Most colloidal dispersions in the aqueous phase have an electric charge, and the development of this charge at the particle surface influences the ion distribution in the surrounding interfacial region (Kaszuba et al., 2010). They will repel each other and thus stabilizing the suspension. As a result of the electrostatic repulsion between particles with the same electrical charge, particle aggregation phenomena are less likely to occur for charged particles with a high zeta potential (>|30| mV) (Gonzalez-Mira et al., 2010; Lu et al., 2018; Azmi et al., 2020).

2.4.5.3 Electron Microscopy

The particulate radius and size distribution of NLCs can also be measured by scanning electron microscopy (SEM) and transmission electron microscopy (TEM). Scanning electron microscopy (SEM) uses electrons to image in the same way that a light microscope does, with the main differences being the greater depth of field and higher magnification (>100,000). SEM generates various signals at the surface of solid samples by using a focused beam of high-energy electrons. The incident electron beam is scanned across the surface of the sample in a raster pattern, and the electrons emitted are detected by an electron detector for each position in the scanned area

(Hashemi et al., 2020). In addition, electron microscopy is beneficial in observing the shape and morphology of the particles (Fang et al., 2013).

TEM was used to determine the shape and size of the particles. A TEM is similar to a standard microscope. However, it uses electrons instead of photons to achieve higher magnification and a clearer image. The wavelengths of electrons are shorter than the wavelengths of light (Azmi et al., 2020). TEM allows the visualization of nanoparticles after freeze-drying or freeze-thawing (Fang et al., 2013).

2.4.5.4 Encapsulation Efficiency

Determination of encapsulation efficiency is essential for NLCs since it affects the release characteristics. The encapsulation percentage of the drugs in NLCs is based on separating the internal and external phases (Fang et al., 2013). Encapsulation efficiency (EE%) estimates the quantity of encapsulated drugs per unit weight of nanoparticles (Azmi et al., 2020). Different techniques such as ultrafiltration, ultracentrifugation, gel filtration by Sephadex, and dialysis are commonly used to separate the dispersions. To obtain EE%, the amount of free NA-TAG was separated from encapsulated NA-TAG using the ultrafiltration method (Amicon Ultra centrifugal filter - nominal cut-off of 30,000Da) with centrifugation according to the size exclusion concept. Nano-sized particles (NPs) have evolved into important systems for bioimaging, biosensing, targeted drug delivery, and controlled release therapeutic agents. Efficient collection and preparation of nanoparticles are critical in nanomaterial manufacturing. Ultrafiltration (UF) has been widely used in the preparation and purification of nanoparticles after synthesis. Also, the separation and concentration of molecules during ultrafiltration are based on size exclusion. The particle size of NLCs systems and physical stability of the NLCs systems was evaluated over a storage period, and the encapsulation efficiency (EE %) (Hashemi et al., 2020).

2.4.5.5 Lipid Oxidation

Lipid oxidative stability is one of the major characteristics in determining the loss of quality of food products and affecting the colour and nutritional value of foods. As oxidation of lipids is an important quality indicator of fats, meat, and meat products because oxidized lipids not only change the colour, aroma, flavour, texture (sensory properties), and even the nutritive value of foods, but they also have several negative biological effects on human health (Reitznerová et al., 2017). This process by which oxygen reacts with unsaturated lipids present in the foodstuff. Oxygen acts on lipids in forming lipid hydroperoxides, which then react to produce low molecular weight volatile components such as aldehydes and ketones. An unpleasant organoleptic experience might appear, described as rancidity (Irwin & Hedges, 2004). Oxidation and hydrolysis are the main reactions resulting in oil and fats rancidity (Talbot, 2016). Analytical methods can detect rancidity or the precursors to rancidity at an earlier stage. For example, shorter shelf-life experiments for oxidative stability testing would be reliable in detecting significant oxidation lipid products early. Although monitoring the oxidative damage would not enhance the product stability, it would help identify potential risks in the supply chain and ultimately result in improved product quality. Thus, measurement of lipid oxidation can be carried out by a wide range of methods such as peroxide value (PV) and thiobarbituric acids reacting substances (TBARs).

Peroxide Value (PV)

The most common approach used to determine the primary oxidation products of lipids are peroxide value (PV), which can be achieved by titration or spectrophotometric method (Liu & Kong, 2021). PV is a straightforward test frequently used to investigate shelf-life or the antioxidant properties of various additives. As hydroperoxides are produced in the early stages of the lipid oxidation process, determining PV can provide an early indication of rancidity (Irwin & Hedges, 2004). For instance, in the investigation of the frying oil and packaging used for potato chip manufacture, PV was used in conjunction with FFA and sensory data to demonstrate that a shelf-life of 90 days could be obtained with sunflower oil and aluminium foil packaging (Sandhu et al., 2002). In a study of cooking comminuted herring flesh, chitosans were found to reduce PV, TBARs (thiobarbituric acid reactive substances) and volatile aldehyde levels (Kamil et al., 2002). However, because hydroperoxides can degrade during storage as propagation reactions take off,

PV cannot be relied on to provide a complete picture of the oxidative status (Murthi et al., 1987). However, due to the complex nature of lipids, it is still debatable to conclude on each specific method or oxidized compound produced during lipid oxidation. It was found that the primary oxidation products are further oxidized to form secondary and tertiary oxidation products. These products include a high amount of aldehydes with small to large chain structures. The aldehydes and other reactive substances are one of the leading causes of rancidity in foods during preparation and storage (Zeb & Ullah, 2016).

Thiobarbituric Acid (TBA) test

The thiobarbituric acid–reactive substances (TBARs) test is a common indicator for investigating secondary oxidative products, particularly those found in polyunsaturated fatty acids like malonaldehydes (MDA, a secondary lipid oxidation product). TBA test can be used to determine the number of aldehydes in the oil; however, unlike the anisidine value (AV), it can be conducted on foods without extracting the oil (Talbot, 2016). Malondialdehyde (MDA) is one of the most abundant aldehydes generated during secondary lipid oxidation. It is probably the most commonly used biomarker for enzymatic degradation and lipid peroxidation of polyunsaturated fatty acids (Zelzer et al., 2013). The most widely used method for the determination of MDA is the spectrophotometric determination of pink fluorescent MDA-thiobarbituric acid (MDA-TBA) complex produced after reaction with 2-thiobarbituric acid (TBA) (Reitznerová et al., 2017). MDA, as the primary marker in lipid peroxidation, reacts with thiobarbituric acid to produce a colourimetrically detectable red pigment at 540 nm by a spectrophotometer due to the oxidation of fatty acids with three or more double bonds (Bai et al., 2022). TBARs are generated as a by-product of lipid oxidative damage (i.e., as degradation products of lipids) and can be detected using the TBARs assay (which uses TBA as a reagent) (Dorsey & Jones, 2017). TBARs is commonly used as an indicator of lipid oxidation in rancidity, particularly in meat and fish products (Irwin & Hedges, 2004). This simple and highly sensitive spectrophotometric method was developed to determine TBARs as a marker for lipid peroxidation in most fried fast foods. The method can successfully be used to determine TBARs in other food matrices, especially in the quality control of food industries (Zeb & Ullah, 2016).

2.4.6 Application of NLCs

NLCs is a colloidal system that has the potential to be used in food fortification (Hashemi et al., 2020). Most applications of NLCs were introduced in pharmaceutical sciences, and few types of research on food compatible NLCs (Babazadeh et al., 2017). They can also be utilized efficiently in various applications, including oral, cutaneous, ophthalmic, and pulmonary (Elmowafy & Al-Sanea, 2021). Applying NLCs as a potential encapsulation system in food products is one of the innovative sights of food science that could be achieved using food-grade components (Babazadeh et al., 2017). Food-grade delivery systems can increase the bioavailability, functionality, and physical and chemical stability of lipophilic nutraceuticals in aqueous-based foods during processing and storage.

On the other hand, these types of NLCs could also be extensively used in the pharmaceutical and biomedical fields. The selection of vehicles is also essential for drug delivery to enhance the maximum activity and inhibit adverse effects. Because NLCs have a higher drug loading capacity than other colloidal carriers, the capability to target specific sites by surface modification and increased knowledge of the fundamental mechanisms of transport via various routes of administration (Elmowafy & Al-Sanea, 2021). Hence, the researchers have more attention to NLCs and discovered different applications as they can enhance drug loading capacity, drug targeting, physical and chemical long-term stability, trigger the release and potentially supersaturated topical formulations (BHATT et al., 2021). NLCs have a remarkable range of properties that make them useful for drug delivery via parenteral, dermal, pulmonary, and topical pathways. These products were developed to reduce the toxic side effects of the highly potent drugs that were incorporated while also increasing the efficacy of the treatment (Naseri et al., 2015; Hashemi et al., 2020). For instance, owing to reduced particle degradation and extended simulated gastrointestinal (GIT) residence times after oral administration, NLCs represent supreme contenders for enhancing rug bioavailability, treating inflammatory bowel diseases, and alleviating drug-induced toxicity (Elmowafy & Al-Sanea, 2021). Poorly soluble medicines such as vinpocetine, fenofibrate, and camptothecin can improve their solubilization. Nanoparticles have been proposed as insulin carriers to make possible the administration of the

peptide via friendlier pathways without the need for injection, i.e., via oral or nasal routes (Souto et al., 2019). Improving transmucosal transport and defense against GIT degradation would be the key benefit of adding insulin (Severino et al., 2012). NLCs could improve oral bioavailability by enhancing the solubility of drugs in the gastrointestinal tract (Liu & Wu, 2010).

Regarding cutaneous applications, NLCs are a practical drug delivery vehicle because they can eventually hydrate skin and combine with skin lipids. NLCs provide favorable aerosolization properties and practical stability for pulmonary use. Additionally, they can get past local defenses and gather in the lung. They provide prolonged residence duration when administered to the eye, boosting the actives' ocular bioavailability with no or minimal adverse effects. Even though a strong barrier protects the brain, NLCs can enter the brain by decorating its surface, passing the blood-brain barrier (BBB) through receptor-mediated transcytosis (Elmowafy & Al-Sanea, 2021).

As both food and pharmaceutical staff deal with human health, the safety standards considered in food science are as crucial and inclusive as those in the pharmaceutical standards even more seriously due to the long-term use of foods rather than drugs. Drugs are consumed in an acute and particular period, while foods are consumed for chronic and longer times. Thus, the health and safety standards used in food science could certainly be applied to pharmaceutical sciences (Babazadeh et al., 2017). Despite the advantages, formulating with NLCs has been suffering some drawbacks. Most potential drugs rarely move to clinical trials (Fang et al., 2013). Due to pH changes, ionic strength, drug release upon enzymatic degradation, and other factors, the stability of particles must be carefully examined (Severino et al., 2012). Cosmetic products are the most used NLCs on the market (Ghate et al., 2016).

2.5. Digestion and Absorption of Lipids

Lipids play an important role in the human diet, providing energy, essential nutrients, and bioactive components. The importance of digestible lipids in the human diet has led to significant advances in understanding the mechanisms of lipid digestion and absorption. In modern processed food, fat may also be incorporated within the food matrix in the form of

emulsions as the emulsion is protein-stabilized and provides a layer of complexity to the digestion of these lipid-containing products (Singh et al., 2009; Zhang et al., 2015). This review focuses on the numerous physicochemical properties of lipid emulsions throughout the gastrointestinal tract in dietary lipid digestion and absorption.

2.5.1 Formation and Stability of Food Emulsions

The common practice to describe an emulsion as being oil-in-water (O/W) or water-in-oil (W/O), where the first phase is the dispersed phase and the second phase mentioned is the continuous phase (Singh et al., 2009). In this section, only O/W emulsions are investigated. In the food industry, although the O/W emulsions will disrupt the droplets by a combination of turbulence and intense shear flow when they are prepared by high-pressure homogenization, a stabilizing layer is created at the droplet surface by the surfactants being absorbed in the oil-water interface. Since surfactants often have a higher solubility in one phase than the other, they tend to partition between the oil and water phases following those solubilities (Singh et al., 2009).

Emulsions are thermodynamically unstable at the time they are produced. After a given time, become thermodynamically unstable and break into individual phases. Thus, the kinetic stability of the emulsion is essential. Several kinds of physical and chemical processes can cause unstable emulsions. Creaming, flocculation, and coalescence are the main physical processes. In contrast, chemical instability involves altering the composition of emulsion droplets through lipid oxidation and hydrolysis or the interfacial layer. The creaming rate can be decreased by lowering the droplet size, enhancing the continuous phase viscosity, or reducing the difference in density between two phases. The flocculation occurs when droplets collide and associate because of the unbalanced attractive and repulsive forces. The aggregation generally gives rise to higher surface coverage and thicker absorbed layers (Singh et al., 2009).

2.5.2 Physicochemical Changes in Emulsions During Processing in the Gastrointestinal Tract

The influence of food structure, particularly emulsion properties, is essential in lipid digestion and absorption. Lipid digestion can be viewed as consisting of at least three sequential steps. The first step consists of the dispersion of the dietary lipid into finely divided emulsion particles, which take place in the stomach. Establishing a lipid-water interface enables water-soluble lipases to interact with their insoluble substrate. The second step involves the enzymatic hydrolysis of TAGs by specific lipases at the emulsion. Human gastric lipase has a pH optimum ranging from 3.0 to 6.0 (Singh et al., 2009). Lipid digestion depends on the complex physicochemical and enzymatic processes, as shown in **Fig.10**, indicating the possible emulsion changes as they pass through the gastrointestinal tract.

2.5.2.1 Lipid Digestion

In the mouth, the ingested food is mixed with saliva and experiences temperature, ionic strength, and pH changes. The emulsion interacts with numerous salivary enzymes, which are subjected to mechanical forces that alter the lipid phase's structural organization, physical state, and interfacial properties (Singh et al., 2009; Sagalowicz & Leser, 2010; Zhang et al., 2015). Although liquid emulsions stay in the mouth for a very short period, the flocculation and coalescence of the emulsion may be induced by saliva and mucin in the oral system (Singh et al., 2009).

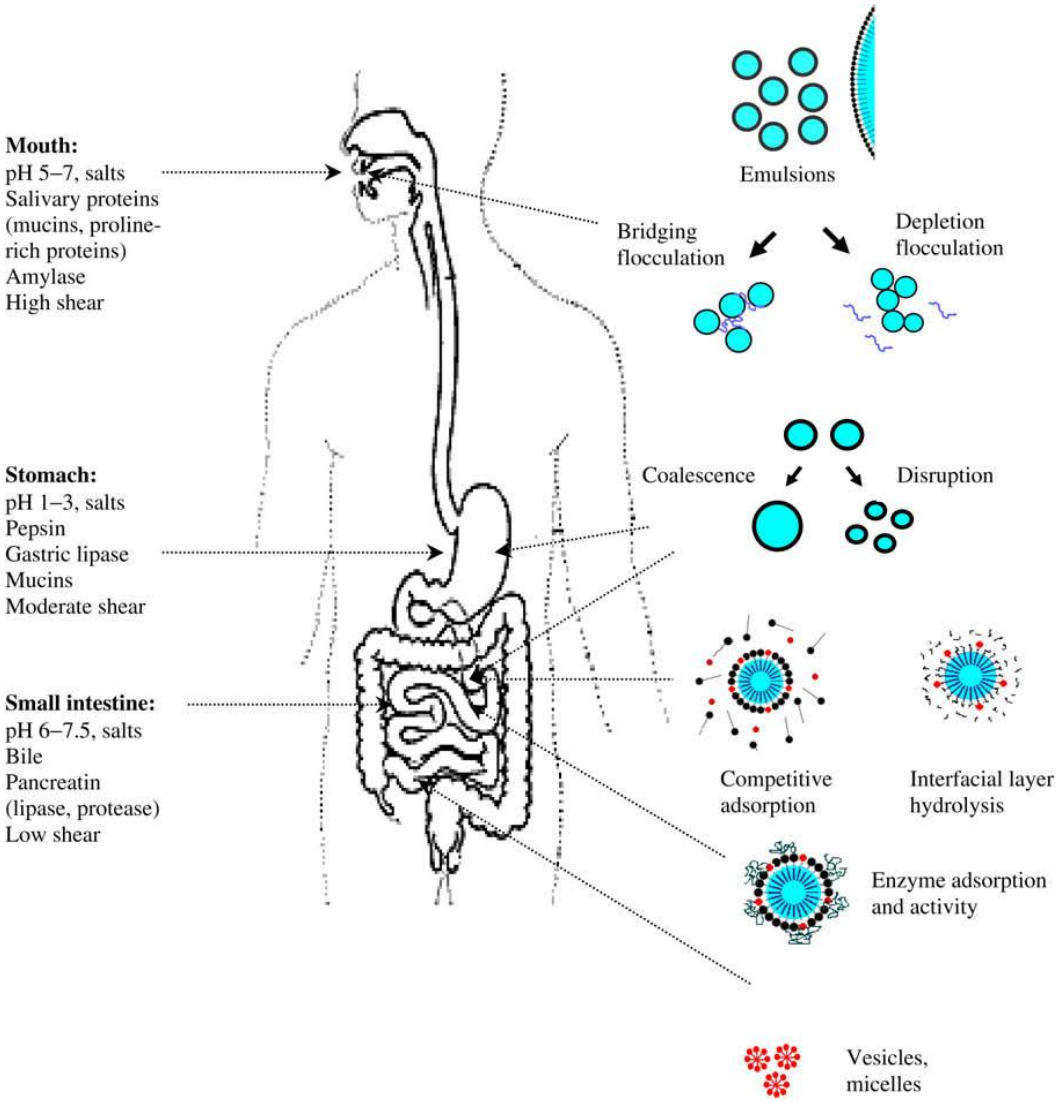

Figure 10. Schematic representation of the possible changes in emulsions as they pass through the gastrointestinal tract (Singh et al., 2009).

2.5.2.2 Lipid Digestion in the Stomach

After spending a few seconds in the mouth, the emulsions are swallowed. Swallowing involves integrated movements of the tongue, pharynx, oesophagus and stomach. Once the emulsion passes through the oesophagus into the stomach, it is subjected to extremely low pH (pH 1–3 in the human stomach) and mechanical agitation as a result of the peristaltic movements of the stomach stage (Singh et al., 2009). The lipids are mixed with highly acidic gastric fluids that contain minerals, biopolymers, surface-active lipids, and enzymes (Zhang et al., 2015).

The emulsion droplet size changes in the stomach due to several complicated reasons. Suppose the smaller droplets contained some adsorbed protein. In that case, droplet fragmentation or aggregation in the stomach is possible due to proteolysis, also leading to an increase in droplet size and changes in the nature and composition of the lipid-water interface. However, looking at particular aspects of the digestion process was challenging to achieve a smaller droplet size range (Singh et al., 2009; Zhang et al., 2015). More directed studies on *in vitro* digestion models would be more effective.

Moreover, the nature of adsorbed layer will dictate the stability when exposed to the stomach acidic environment. A protein-stabilized emulsion would shift into a cationic form as the pH range dropped from neutral, along with changes in the structure of the proteins adsorbed. There is a chance of some aggregation around their isoelectric points (pH 4.5-5.2) and an incomplete reversal of aggregation at lower pH levels. The proteolytic effect of pepsin on the adsorbed protein would also remove steric repulsion barriers and lower droplet charge, causing the emulsion droplets to aggregate further and possibly consolidate (Singh et al., 2009).

2.5.2.3 Lipid Digestion in the Small Intestine

The modified emulsions move from the stomach into the small intestine and experience higher pH (neutral) and high ionic strength (Singh et al., 2009). Higher levels of surface-active agents, such as bile salts and pancreatic lipase, can either partly or fully displace the adsorbed materials from droplets arriving from the stomach. The progress of the lipolysis reaction depends on surface-active materials derived from gastric secretions (e.g. mucins, enzymes) or other partly digested food (proteins, phospholipids, enzymes) that could alter the composition of adsorbed layers through competitive adsorption effects and could influence the droplet stability. The droplet sizes in the small intestine typically range from 1 to 50 μm (Singh et al., 2009).
Bile salts can adsorb the surfaces of the lipid droplets, encourage lipase binding to the interfacial layer, and accelerate the breakdown of lipids. Diacylglycerols, monoacylglycerols, and free fatty acids are among the additional surface-active compounds that are produced during the hydrolysis of the droplet core by pancreatic lipases (Singh et al., 2009). There are noticeable changes in the

physical, chemical, and nutritional properties due to differences in their chain length and unsaturation (Zhang et al., 2015). Functional foods with decreased fatty acid availability would suit populations with high blood lipid levels and at an increased risk of cardiovascular disease and obesity (Singh et al., 2009). These lipid digestion products are then mixed with bile salts and phospholipids to form the mixed micelle phase.

However, the bioavailability of nutrients for absorption in the intestine is relatively complex and varies for a given food depending on processing situations and interactions with other compounds, the chemical status of the nutrient, release from the food matrix, suppressors or cofactors present in the food composition, formation of stable complexes that are gradually metabolized, and other factors (Parada & Aguilera, 2007).

2.5.3 *In vitro* Digestion Model

There is growing interest in understanding and controlling the digestibility of emulsified lipids as they pass through the human gastrointestinal (GI) tract (Li & McClements, 2010). The bioavailability and bio-accessibility of nutrients and bioactive compounds can be determined by various procedures such as *in vitro* methodologies (simulated gastrointestinal digestion, ex vivo methodologies (gastrointestinal organs under controlled laboratory conditions), and *in vivo* methodologies (human and animal studies) (Carbonell-Capella et al., 2014). *In vitro* digestion was one of the most frequently used methodologies. *In vitro* digestion models are commonly used to determine the bio-accessibility of bioactive compounds. Lipid digestion models are increasingly used to facilitate improved *in vitro* evaluation of lipid-based drug delivery systems (Porter et al., 2007). The standardized protocol presented in *in-vitro* is based on an international consensus developed by COST INFOGEST network. The static digestion method is designed to be used with standard laboratory equipment and encourage a wide range of researchers to adopt it (Brodkorb et al., 2019). The method are inexpensive, rapid, economical, and reproducible methods to investigate structural modifications in clinical trials. *In vitro* models simulate the gastrointestinal system by the initial digestion with pepsin-HCl (gastric digestion), followed by digestion with pancreatin with bile salts (small intestine conditions), and ending with dialysis

(absorption process) (Santos et al., 2019; Jones et al., 2019). The properties of the optimized NLCs such as particle size, zeta potential, stability and *in vitro* drug release were investigated. The advantage of colloidal drug carriers is that they are generally linked to their size in the submicron range. Thus, the preservation of particle size of the colloidal carrier is a crucial point. However, the gastric environment (ionic strength, low pH) may destabilize the system and lead to aggregation. In addition, the relationship between *in vitro* digestion and enzymatic activity has been studied. It has been defined that the *in vitro* technique can use enzymes specifically chosen to obtain maximum digestibility values or determine the initial rate of hydrolysis.

Moreover, the pH-stat method is commonly used to characterize the *in vitro* digestibility of lipids under simulated small intestine conditions. This method measures the fraction of free fatty acids (FFA) released from lipids over time. This model provides a valuable means of quantifying the influence of specific parameters on lipid digestion using the pH-stat method. The lipid-containing sample to be analyzed is placed within a temperature-controlled reaction chamber that contains simulated small intestinal fluid (SSIF). The SSIF typically includes appropriate concentrations of the major digestive components that influence lipid digestion, such as lipase, colipase, bile salts, phospholipids, and mineral ions. The pH-stat method facilitates the comparison of various lipid formulations under comparable experimental settings and is, in theory, relatively quick and straightforward to execute. Therefore, this method can be utilized to quickly screen the effects of various physicochemical parameters that are anticipated to affect lipid digestion (Li & McClements, 2010).

There are two main methodological digestions: *in vitro* and *in vivo*, assessing the bio-accessibility through analysis and comparison. Compared to the *in vivo* study, the *in vitro* digestion study can rapidly determine the bioavailability of various foods and provide direct results. *In vivo* studies are limited by some analytical and ethical constraints, are time demanding, and require many experimental control resources. However, *in vivo* studies should be used to validate *in vitro* methodologies (Cardoso et al., 2015; Santos et al., 2019). Therefore, *in vitro* digestion has lower cost, time and energy-saving properties, and independence from physiological factors than *in vivo* methods.

Due to its simplicity, low cost, and high reproducibility, bio-accessibility is the most frequently used food research method. The bio-accessibility or bioavailability assessment considers the advantages and disadvantages of each methodology. Although the *in vitro* digestion methodologies are normally used to determine the bio-accessibility of bioactive compounds and nutrients, it has some limitations: unpredict the number of specific substances that humans can consume; poor simulation of complex mechanical forces and gastric emptying; low level of integration into an overall digestive process; excessive attachment to healthy and average digestion conditions (Guerra et al., 2012; Santos et al., 2019; Jones et al., 2019).

A wide range of Gastric and small intestinal (GSI) models has been developed and applied in many nutrition and health studies (Guerra et al., 2012). Applications of this method for the bio-accessibility or bioavailability of certain bioactive compounds are also reviewed, taking into account research on the bioavailability of carotenoids, polyphenolic compounds, glucosinolates, vitamin E, and phytosterols (Sagalowicz & Leser, 2010; Carbonell-Capella et al., 2014; Mehmood, 2015; Hashemi et al., 2020;).

Chapter Three

Materials and Methods

3.1. Materials

Pure Soybean oil (100% Malaysia) was purchased from a NJK Asian Supermarket in Auckland, New Zealand. Nervonic acid (98% purity) was purchased from Shenzhen Dieckmann Tech Co.,Ltd, Shenzhen, China. Five commercially immobilised lipases were obtained as below: Lipozyme TL IM from *Thermomyces lanuginosus* (TLL) and Novozyme 435 from *Candida antarctica* were purchased by Novozymes A/S (Bagsvaerds, Denmark); Lipase, immobilised on Immobead 150 from *Thermomyces lanuginosus,* was purchased from Sigma Aldrich Co. (St.Louis, USA); Lipozyme® RM IM from *Rhizomucor miehei* lipase immobilised on a resin carrier, and Lipozyme® 435 as recombinant lipase from *Candida antarctica*, expressed on Aspergillus niger, and immobilised on a macroporous hydrophobic resin were obtained from Novozymes North America, Inc. (Franklinton, NC).

Chromatographic grade n-hexane, diethyl ether and acetic acid were obtained from ECP limited, New Zealand. TLC plates (silica gel 60 F_{254}) were purchased from Merck Ltd., Germany. While Silica gel 60 was 230-400 size in mesh (for flash chromatography 0.04 -0.06mm) and purchased from Chem-Supply Pty Ltd., Australia. Stearic acid, GMS, Tween 20 (polyoxyethylene sorbitan monolaurate), Tween 80 (polyoxyethylene sorbitan monoleate), and poloxamer 407 (1,1,3,3-tetra ethoxy propane) were provided from Sigma Aldrich (Auckland, New Zealand). Thiobarbituric acid (TBA) 99% purifity, chloroform, methanol, ammonium thiocyanate, Iron (II) and cumene hydroperoxide were purchased from Merck (New Zealand). Pepsin from porcine gastric mucosa and lipase were purchased from Sigma- Aldrich (Sigma Chemical Co., Auckland, New Zealand)

and as reported by the manufacturer their activity was 250 units/mg. Pancreatin (Pancreatin porcine pancreas, Product # P8096, 1 USP specifications), porcine bile extract, sodium chloride (99.5%), calcium chloride (96%) monobasic sodium phosphate and dibasic sodium phosphate were obtained from Sigma-Aldrich (Sigma Chemical Co., Auckland, New Zealand).

All solvents and reagents used were of analytical grade. Double distilled water from a water purification system was used for the preparation of all solutions. All tested chemicals were analytical grade and obtained from Merck Chemical Co.

3.2. Enzymatic Acidolysis

3.2.1 Procedure for Enzymatic Acidolysis

Acidolysis reaction with soybean oil and nervonic acid (NA) was set up in a 100 mL conical flask with a stoppered cap, according to Kavadia et al. (2012). The intended substrate molar ratio (soybean oil to NA ratio) was chosen and added to the flask. Selected enzyme type and enzyme loading was then added. The mixture was placed in a water bath and stirred continuously at 100 rpm using a hotplate magnetic stirrer. The reaction was performed at the chosen temperature and time (**Section 3.2.2**). Sampling (50μL) was conducted at certain intervals. After the reaction, the lipases were removed from the mixture by centrifugation (Thermo Scientific™ Sorvall™ LYNX 4000 superspeed centrifuge, Fisher Scientific, USA) at 7000 rpm for 3 min. The upper lipid fraction was transferred into a new centrifuge tube and stored at -20℃ for further analysis. All experiments were performed in triplicates.

3.2.2 Optimization of Acidolysis Reaction

Single-factor experiments were conducted to investigate the effect of different enzyme types, substrate ratio, enzyme loading, and reaction temperature as the preliminary study before optimising the acidolysis reaction.

From the single-factor experiments, we selected three lipase enzymes (Lipozyme TL IM, Heterologous Immobead 150 and Lipozyme TL IM Immobead 150), three substrate molar ratio levels of soybean oil to NA (1:4, 1:5, and 1:6), three enzyme loading levels (5, 10 and 15% w/w) based on the highest incorporation of NA (C24:1) into the soybean oil or TAG. An L9 (3^3) orthogonal design was used to optimize the acidolysis reaction as shown in **Table 3.** Acidolysis experiments using factors (each with three levels) were conducted as described in **Section 3.2.1**.

Table 3. The L9 orthogonal array design for optimization of acidolysis.

Experimental run number	Immobilised lipase Type	Enzyme Loading (w/w %)	Substrate molar ratio (TAG/NA)
1	Lipozyme TL IM	5	1:4
2		10	1:5
3		15	1:6
4	Heterologous Immobead 150	5	1:5
5		10	1:6
6		15	1:4
7	Lipozyme TL IM Immobead 150	5	1:6
8		10	1:4
9		15	1:5

For all experiments, the reaction time of 4 h and reaction temperature of 60 ℃ were kept constant. TAG, Triacylglycerol; NA, Nervonic acid.

3.3. Analysis of Lipid Mixture by Thin Layer Chromatography (TLC)

Thin Layer Chromatography (TLC) is a conventional method for separating and enriching fatty acid classes. The lipid mixtures from the acidolysis experiments were separated on TLC plates consisting of silica gel (60G F_{254} glass plates 20x20cm, Sigma-Aldrich, New Zealand) and developed with the TLC solvents, i.e. n-hexane/diethyl ether/acetic acid (70:30:1.5, v/v/v) according to the method of Yadav et al. (2014) and Arifin et al. (2010).

A one-dimensional TLC was applied. TLC solvents were added into the chamber and covered with aluminium foil for 5 mins to saturate the chamber. Each sample was spotted on the silica gel plates and placed vertically inside the saturated TLC chamber. Samples were spotted 1 cm from the lateral border. The samples were left to develop, and after the brands developed, 0.2% dichlorofluorescein in methanol was sprayed on the TLC plate.

For Fatty acid determination, the bands that appeared on the TLC were scraped off from the plate and transferred into a test tube for FAME preparation.

3.4. Fatty Acid Composition

The FA composition of the soybean oil and the purified NA-TAG oil samples were determined according to the modified method of Caballero et al. (2014).

3.4.1 Fatty Acid Methyl Esters (FAME) Preparation

Fatty acid methyl esters were prepared by adding 1000 µL 0.25M sodium methoxide and 50µL 10 mg/mL IS (internal standards) as the catalyst to each sample. The catalysts and mixture were stirred for 5 min at 45℃ using a magnetic hot plate stirrer. After 5 mins, 2000µL hexane was added, followed by 3000µL sodium chloride (0.9%, w/w). The mixture shakes vigorously and

allowed to settle for phase separation. The upper phase containing fatty acid methyl esters (FAMEs) was transferred to a 1.5 ml GC vial for analysis using Gas chromatography (GC).

3.4.2 Determination of Fatty Acid Composition by Gas Chromatography

After methylation, the methyl esters were injected into a Gas chromatography (Agilent Technologies, Palo Alto, CA, U.S.A). The GC is equipped with an auto-injector, and a flame-ionization detector (FID, Agilent Technologies). A 6890-capillary column (Dimensions: 30 m length x 0.25 mm internal diameter x 0.25 μm thickness, Agilent Technologies) was used (DKSH, New Zealand Ltd.). The oven temperature was programmed with an initial temperature of 150 °C, and held for 7 min. Afterwards, the oven temperature was increased to 210 ℃ at the rate of 10 ℃/min, then to 230 ℃ at the rate of 20 ℃/min. The injector and detector temperatures were set at 260 ℃ and 300 ℃, respectively. The fatty acid composition was determined by comparing the peak retention times with the respective retention times of the fatty acid standard mixture (Moreira et al., 2020).

3.5. Separation and Purification of NA-TAG oil from Optimization Study

After the optimised acidolysis reaction, separation and purification of the NA-TAG oil were conducted using column chromatography. A glass column with a 250 mL reservoir with an internal diameter of 20.0 mm and a length of 305 mm was used. The stationary phase used was Silica gel 60, purchased from Chem-Supply Pty Ltd. (Australia) and had the following specifications: 230 to 400 mesh size, pore diameter-Å was 55-60 Å, and the surface area was 450-650 m^2/g. The TLC solvents were used as the mobile phase for the column chromatography.

The column was placed in a ring stand at a vertical position. It was rinsed by pipetting the solvent down the inside edge. Silica gel 60 (120 g) was weighed and mixed in 500 mL of TLC solvent with agitation. The mixture was poured gently into the column to set the gel and drain the

solvent. The solvent should always cover the Silica gel 60 adsorbent before loading of sample into the column to avoid any crack formation in the silica gel column. After the column was appropriately set up, a 4 mL sample (NA-TAG oil from the optimisation study) was loaded into the silica gel column, and 250 mL of solvent was added to elute the column. The fractions eluted from the column chromatography were collected using 1.5 mL centrifuge tubes and flushed with nitrogen, followingly analyzed by TLC (as described in **Section 3.3**) to confirm the separation of purified NA-TAG oil from the free fatty acids.

The TLC analysis found that the NA-TAG fractions would appear after 30 minutes of elution and lasted for 7 minutes. Based on this finding, the column chromatography was repeated multiple times to collect the purified NA-TAG fractions from 30 to 37 minutes of column elution. The fractions were pooled, and the solvent evaporated using a rotary evaporator (with the water bath set at 50 °C). The purified NA-TAG sample was then transferred into an amber vial, flushed with nitrogen gas, and stored at - 20℃ until further experiments (fatty acid composition and encapsulation in NLCs).

3.6. Screening of Materials for NLCs Preparation

Screening of materials for NLCs preparation was carried out to determine the suitability of selected lipids and surfactants for incorporating the NA-TAG in the NLCs. The selection of the components and ratios can particularly affect the final behaviour of the developed formulation. Different concentrations of solid lipids (stearic acid and GMS), liquid lipid (soybean oil, olive oil), and surfactants (Poloxamer 407, Tween 80, and Tween 20) prepared the hot high-shear homogenization followed by hot melt probe sonication (Li et al., 2017; Khan et al., 2019).

The preparation involved two phases: the lipid phase and the aqueous phase. The lipid phase consisted of selected solid lipid, liquid lipid, and core lipids (purified NA-TAG oil) content. The NLCs were produced with the total lipid phase (solid-lipid, liquid-lipid, and NA-TAG) from the total formulation and the aqueous phase (surfactant & distilled water). The special weight ratio describe as below of solid-lipid to liquid-lipid in the aqueous bath were heated to 70 ℃. The

aqueous phase consists of surfactants with distilled water prepared at the same temperature as the melting point of lipids. Then, the aqueous phase was added dropwise to the lipid phase and allowed the mixture with constant stirring by a high-speed stirrer. The mixture of the lipid and aqueous phases was mixed and further homogenised at 12,000 rpm for 10 min in a hot water bath using an IKA®, T 18 digital Ultra-Turrax® homogenizer (Staufen, Germany) to get a smaller particle size. Then, the dispersion was sonicated with a probe ultrasonic homogenizer (Sonic Ruptor 250, Omni International, USA), with the power set at an amplitude of 100% with 70% pulse for 5 min to get uniform size distribution. The emulsion was sealed and effectively cooled down to recrystallise the lipid phase in an ice bath for 30 minutes, under stirring at 400 rpm, to homogenous NLCs dispersion. The preparation was then left to cool at room temperature (25 ◦C ± 2 ◦C) and stored at 5 ◦C before further characterisation and lyophilization. Triplicate experiments were performed.

3.6.1 Selection of Liquid and Solid lipids

The choice of the liquid lipid used for the NLCs dispersion was based on their solubility. Adding an increasing amount of NA-TAG oil in 1 g of each liquid lipid (soybean oil and olive oil) thermostatic at 85°C and with continuous stirring to simulate the process followed for the preparation of the lipid particle dispersions (BHATT et al., 2021; Sakellari et al., 2021).

A similar method described above was used for the selection of solid lipids. The solid lipid was selected based on the solubility studies of the NA-TAG in stearic acid and glyceryl monostearate (GMS). It was cooled to room temperature and was examined for precipitation by visual observation. Solid lipids that did not show any precipitation by observation, i.e. GMS, was selected for further studies.

3.6.2 Miscibility of the Solid and Liquid Lipid System

The selection of liquid and solid lipid was performed to evaluate the solubility of liquid lipid and the selection of solid lipid in a variety of ratios between solid and liquid lipids, a parameter of

critical importance in the formulation development process. The miscibility between GMS and soybean oil was initially evaluated by preparation of solid lipid nanoparticles (SLNs) in different w/w ratios: 90:10, 80:20 and 70:30, and 90:10 to establish the miscibility of the two lipids.

The soybean oil and GMS with the best-solubilizing potential for NA-TAG were mixed in different ratios, 1:2, 1:1, 2:1, 3:2 and 2:3, in different glass vials to establish the miscibility of the two lipids while the aqueous phases were maintained constant. Investigated the selection of these two solid lipids on the minimised particle size (PS), polydispersity index (PDI) and the maximised zeta potential (ZP). It was allowed to attain room temperature, and the miscibility was assessed visually.

3.6.3 Selection of Surfactant Types and Concentrations

The surfactant type and concentration play an important role in designing NLCs. Generally, the higher the surfactant concentration, the smaller the particle sizes (Ghate et al., 2016; Elmowafy & Al-Sanea, 2021). GMS and soybean oil were kept unchanged; the surfactants studied in the aqueous phase included Poloxamer 407, Tween® 20, and Tween® 80 at 1: 89, 2: 88 and 3: 87 in distilled water (aqueous phase). However, when surfactant Poloxamer 407 was present, the phase stage of NLCs emulsion turned to a solid phase, and no further analysis of physicochemical properties could be performed. Thus, the NLCs formulation with poloxamer 407 was discarded. On the other hand, the formulation with Tween 20 led to a significantly higher PDI exceeding 0.6, which suggests the formation of a poorly uniform system and a great tendency to aggregation phenomena (Cirri et al., 2018). Finally, Tween 80 was selected for further analysis.

3.6.4 Selection of NA-TAG Concentrations

The aqueous phases of the Tween 80 and distilled water were maintained constant. The NA-TAG oil concentrations were increased from 10% to 50% in the liquid phase. When the NA-TAG oil accounts for more than 30%, the phase states were solid (by visual observation).

The formulations (with appropriate levels of solid lipid, liquid lipid, NA-TAG, and surfactants) that gave the minimum particle size (PS) and polydispersity index (PDI), and the highest values in zeta potential (ZP) would be used to serve as a reference for the further optimization experiments using the orthogonal design (**Section 3.7**).0

3.7. NA-TAG-Loaded NLC Preparation

3.7.1 Optimization of NLC Preparation

Based on the preliminary studies in **Section 3.6**, a L9 (3^3) orthogonal experimental design was used for optimization of NA-TAG NLC preparation. The level settings of individual factors as shown in **Table 4**. The effect of composition of lipid carriers, such as level of Tween 80 surfactant (1, 2, 3 w/w%) and NA-TAG concentrations (1, 2, 3 w/w%), lipid phase to aqueous phase ratio (10:90, 15:85, 20:80 w/w%) on particle size, polydispersity index, zeta potential and encapsulation efficiency of the NLCs in the optimisation experiments. The significant effect of 3 independent variables to find the optimum combination to produce the NLCs (Wu et al., 2012; Peng et al., 2019). Triplicate experiments were conducted, and the data was analyzed using analysis of variance (ANOVA).

Table 4. The L9 orthogonal experimental design for NA-TAG NLC preparation.

Formulation Code	NA-TAG Concentrations (w/w %)	Lipid phase to aqueous phase ratio (w/w %)	Aqueous Surfactant Concentrations (w/w %)
NLC 1	1	10:90	1
NLC 2	1	15:85	2
NLC 3	1	20:80	3
NLC 4	1.5	10:90	2
NLC 5	1.5	15:85	3

NLC 6	1.5	20:80	1
NLC 7	2	10:90	3
NLC 8	2	15:85	1
NLC 9	2	20:80	2

Array method to be applied with surfactant Tween 80 to all reactions in triplicate after selection of solid to lipid ratios and the preliminary experiments. TAG, Triacylglycerol; NA, Nervonic acid.

3.7.2 Method of NA-TAG-Loaded NLC Preparation

The lipid phase consisted of solid lipid GMS, liquid lipid (Soybean oil) and core lipids (purified NA-TAG oil) content. The NLCs were produced with 10 w/w% of the total lipid phase (solid-lipid, liquid-lipid, and NA-TAG oil) from the total formulation and 90 w/w% of the aqueous phase (Tween® 80 & distilled water). The special weight ratio of solid-lipid to liquid-lipid was 2:1 in the aqueous bath were heated to 70 ℃. The aqueous phase consists of Tween® 80 with distilled water prepared at the same temperature as the melting point of lipids. Briefly, GMS was melted at 50-55℃. So, the liquid flow was controlled to occur as fast as possible to reduce the solidification of the melted lipid phase. Then, the aqueous phase was added dropwise to the lipid phase and allowed the mixture with constant stirring by a high-speed stirrer.

NLCs incorporated with NA-TAG oil were prepared by the high-shear homogenization followed by melt probe sonication technique as described in **Section 3.6**. The emulsion was sealed and effectively cooled down to recrystallise the lipid phase in an ice bath for 30 minutes, under mild stirring (400 rpm), to form the homogenous NLCs dispersion. The preparation was then left to cool at room temperature (25 ◦C ± 2 ◦C) and stored at 5 ◦C before further characterization (**Section 3.8**) and lyophilization (**Section 3.9**). The data are reported as mean value ± standard deviation (SD, n=3).

3.8. Characterization of Optimized NA-TAG-Loaded NLCs

The optimised NLC were characterised in terms of particle size (PS), polydispersity index (PDI), zeta potential (ZP), laser diffusion (LD), and entrapment efficiency (% EE).

3.8.1 NLCs Properties

The average particle size (PS), zeta potential (ZP, mV) (surface charge) and polydispersity index (PDI) were measured by the Photon Correlation technique (Zetasizer Nano S, Malvern Instrument, Malvern, UK. To avoid multiple scattering effects and achieve an adequate scattering intensity prior to the measurement, all NLCs samples were first diluted and ultrasonicated using Mili Q water at a ratio of 1:100 to ensure the light scattering intensity was within the instrument's sensitivity range before the particle size measurement (Shahparast et al., 2019; Azmi et al., 2020). Then, the sample was placed on the disposable folded capillary cells cuvette for analysis at 25 ± 2 °C in triplicates. The particle size, polydispersity index was measured. Each measurement was conducted in triplicate and after overnight storage of samples. Refractive indices for particles were 1.54, and for water was 1.33.

The physical stability of optimized NA-TAG-loaded NLCs can be evaluated by measuring the electrophoretic mobility (zeta potential) using the same device by Zetasizer Nano Z (Malvern Instrument, Malvern, UK). Before the analysis, the samples were diluted with milli Q water, and all measurements were performed at 25 °C. Each reading was taken in triplicate. The refractive indices of particles and water used were 1.54 and 1.33, respectively (Azmi et al., 2020).

3.8.2 Encapsulation Efficiency

Encapsulation efficiency was measured through an indirect method by determining the un-entrapped NA-TAG in the supernatant after centrifugation. To obtain the entrapment efficiency (%EE), the amount of free NA-TAG was separated from encapsulated NA-TAG using the

ultrafiltration method (Amicon Ultra centrifugal filter units with nominal at 30,000 Da) followed by centrifugation. NLCs was regularly mixed with 50% w/w ethanol (in the ratio of 1:6), followed by centrifugation for 10 min at 2000 g to disrupt the lipid matrix of NLCs and release the free encapsulated NA-TAG. The total NA-TAG content in the NLCs dispersion was the sum of the encapsulated NA-TAG and the free NA-TAG. The filtrate was diluted with 50% w/w ethanol and determined by using an Ultraviolet-Visible Spectrophotometry UV-1800, Shimadze, Kyoto, Japan) at 22 ℃ at λ = 450 nm. The results were expressed in the standard curve with mg optimized NA-TAG-loaded NLC vs absorbances (nm) (**Appendix 1**). All experiments were repeated three times. The encapsulation efficiency was calculated using Equation (1) as modified from Babazadeh et al. (2017), Shahparast et al. (2019), Hashemi et al. (2020) and Azmi et al. (2020):

$$\text{EE (\%)} = \frac{W_i - W_u}{W} * 100 \qquad \text{Equation (1)}$$

where "W_i" is the mass of initially added NA-TAG oils in the formulation and "W_u" is the mass of unloaded free NA-TAG.

3.9. Freeze Drying of NLC and Their Properties

The optimized NLCs formulation was selected from the orthogonal method (**Section 3.7.1**) to prepare freeze-dried NLCs. After homogenisation, NLCs emulsions were cooled down to room temperature before being fed into the freeze dryer. The emulsions were then placed in a scintillation vial and immediately frozen at – 80 ºC. After 24 h, the frozen emulsion was dried for 48 h at – 51 ºC under the pressure of 0.120 millibars using a Free Zone 6 litre Freeze Dryer System (model 77585-30, LabConco Corporation, USA).

The physical properties of the lyophilized NLCs were analyzed by differential scanning calorimeter (DSC) and Fourier transforms infrared spectroscopy (FT-IR).

3.9.1 Differential Scanning Calorimetry (DSC)

Thermal analysis using a differential scanning calorimeter (DSC-7, Perkin Elmer, USA) was performed on the NA-TAG, lyophilized of NA-TAG-loaded NLC, lyophilized unloaded NLC and the solid lipid GMS. A 8 mg samples were accurately weighed and placed in an aluminium pan and then sealed using a crimper press (Perkin-Elmer; Beaconsfield, UK). A standard empty aluminium pan was used as a reference and the thermograms were recorded between 10 °C and 300 °C at a scan rate of 10 °C/min under nitrogen gas. All samples were analysed in triplicate.

3.9.2 Fourier-Transform Infrared (FT-IR) Spectroscopy

The NLCs samples that were used in the DSC scan were further analysed through the FT-IR. Interaction between the NA-TAG and NLCs components (solid lipid GMS, unloaded NLC, liquid lipid phase (i.e., soybean oil) was studied using a FTIR spectrometer (PerkinElmer Spectrum 400, FT-IR/FT-FIR spectrometer, USA). Samples were kept on the diamond surface with a consistent application of low pressure. The analysis was performed between 4400 and 500 cm^{-1} wavelength range. Background noise was corrected with a blank diamond. All samples were scanned in triplicate.

3.10. Storage Stability of lyophilized NA-TAG-Loaded NLC

A storage study of the freshly prepared lyophilized NA-TAG-loaded NLCs was carried out for six weeks to evaluate their stability. The lyophilized powder (200 mg) was accurately weighed and placed in a 20 mL glass scintillation vial, and the cap was tightly closed. The vial was then covered with aluminium foil completely. A total of 30 samples or vials were prepared as described above. These samples were placed in three desiccators containing silica gel at the bottom, with ten samples stored in each desiccator. The desiccators were all covered with aluminium foil and stored at three different temperatures: at 4 ± 2 °C (in a refrigerator), 25 ± 2 °C (in a cupboard in the lab), and 45 ± 2 °C (in a vacuum drying oven) for 6 weeks (42 days). Samples were removed from storage at a certain time interval for analyses (**Section 3.10.1 and**

3.10.2). Triplicate experiments were performed. Three freshly lyophilized samples were also analyzed to obtain data for Day 0 storage (according to **Section 3.10.1 and 3.10.2)**.

The properties of the NLCs samples, i.e., physical stability including particle size, polydispersity index, zeta potential, entrapment efficiency and water activity, were measured. The chemical stability in terms of primary and secondary lipid oxidation was estimated to indicate oxidative stability at certain storage intervals.

3.10.1 Physical Stability

The physical stability of NLCs samples during storage (refrideged temperature 4 ℃, room temperature 25 ℃ and high temperature 45 ℃), including the average droplet size, PDI and zeta potential of optimized NLCs, were determined using a dynamic light scattering analyzer (Zetasizer Nano ZS, Malvern Instruments Ltd., Worcestershire, UK) as described in **Section 3.8.1**.

The encapsulation efficiency (EE%) was determined according to **Section 3.8.2**. The results were expressed in the standard curve with lyophilized NLC vs absorbances (nm) (**Appendix 2**).

Water activity (a_w) of NLCs samples at room temperature (25 °C) were measured with a Novasina AW sprint Water Activity Meter (New Zealand). Measurements were performed in triplicate and the mean value was reported. After measurements, the samples were used to analyze other factors.

3.10.2 Chemical Stability

A rapid spectrophotometric method was applied and modified for the peroxide value measurement. The NLCs oxidative stability was expressed as the changes in peroxide value (PV) and the quantification of the thiobarbituric acid (TBA) reactive substances (TBARs) of the oil phase after the storage at a certain period. The degree of lipid oxidation was periodically

analyzed on the primary and secondary oxidant products on days 0, 1, 3, 5, 7, 10, 14, 21, 28, 35 and 42. The methods of peroxide value was modified from Tura et al. (2022).

3.10.2.1 Primary Lipid Oxidation

Calibration of Fe (III) — The 1000 µg/mL stock solution of Fe (III) was prepared by dissolving $FeCl_3$ in 1 % HCl. A working standard (10µg/mL) was obtained by 100 times dilutions with chloroform: acetic acid (2:3) from the stock solution. A set of different concentrations of Fe (III) solution (0, 0.5, 1.0, 2.5, 5.0, 7.5 and 10µg/mL) was prepared by a series dilution of the working standard. 2 mL of each standard was taken and reacted with 200 µL saturated ammonium thiocyanate solution. The absorbance was measured at 470 nm against a blank consisting of water (the spectrum baseline was corrected at 670 nm) after the mixture had reacted for 10 min. A reaction blank was also performed. The calibration curve was obtained by plotting the absorbance versus Fe (III) concentration (**Appendix 3)**.

Preparation of Fe (II) solution — The Fe (II) solution was prepared by mixing $BaCl_2$ solution (0.4 g $BaCl_2 \bullet 2H_2O$ in 50 mL Milli-Q water), and $FeSO_4$ solution (0.5 g of $FeSO_4 \bullet 7H_2O$ in 50 mL Milli-Q water), followed by adding 2000 µL concentrated HCl and stored undercover. This solution was prepared as freshly and discarded if a pale pink colour appeared with the addition of a few drops of thiocyanate solution.

Sample preparation — 10 mg sample was weighed into a 15 mL screw-capped test tube. 1000 µL of chloroform: acetic acid (2:3) was added to the test tube to dissolve the lipid sample, followed by a 200 µL Fe (II) solution. The mixture was mixed for 15 s by a vortex mixer and then left in the dark for 10 min. Milli-Q water (2000 µL) and n-hexane with hexane (4000 µL) were added to extract the oil. The organic phase was discarded, and the aqueous phase was flushed with nitrogen to remove the remaining n-hexane. 2000 µL of the aqueous phase was transferred into a test tube and mixed with 200 µL of saturated ammonium thiocyanate solution. After 10 min, the measurement was undertaken as to the standard. The peroxide value of the sample was calculated using the equation:

$$PV\ (mequiv\ peroxide/kg\ of\ sample) = \frac{A_{sm} - A_{b1}}{55.84 * 2 * m * W_{sm}}$$ Equation (2)

where A_{sm} is the absorbance of the sample at 470 nm; A_{b1} is the absorbance of the blank at 470 nm (both absorbances were corrected after subtracting the absorbance at 670 nm); m is the slope of the calibration curve; W_{sm} is the sample weight (g). The data were reported as mean ± standard deviation of triplicate measurements.

3.10.2.2 Secondary Lipid Oxidation

The secondary oxidation products, especially in polyunsaturated fatty acids such as malonaldehydes, were monitored by quantification of the thiobarbituric acid (TBA) reactive substances (TBARs) as described by Wang et al. (2015). Malonaldehyde (MDA) reacts with thiobarbituric acid to produce a colour compound that can be detected calorimetrically. The values of TBARS were expressed in mg of malondialdehyde (MDA) per kg of oil.

Preparation of MDA and Calibration Standards — The standard curve of 1,1,3,3-tetraethoxypropane (TEP) was used to determine the malondialdehyde (MDA) concentrations. MDA is not commercially available. MDA is an unstable compound and the only possibility to obtain it is by hydrolysis of its stable derivative. MDA standard was prepared by dissolving 25 µL 1,1,3,3-tetraethoxypropane (TEP) in 100 ml distilled water to give a 1 mM stock solution. The working standard was prepared by hydrolysis of 1 ml TEP stock solution in 50 ml 1 v/v% sulfuric acid and incubation for 2 h at ambient temperature. The resulting MDA standard of 20 nmol/ml was further diluted with 1 v/v% sulfuric acid to yield the final concentration of 10, 5, 2.5, 1.25 and 0.625 nmol/ml to get the standard curve for the estimation of total MDA concentration (Pilz et al., 2000). The final concentration of MDA in every standard solution was determined by measuring its absorbance at 532 nm. Each standard for the calibration was repeated (n = 3). The calibration curve was obtained by plotting the absorbance versus MDA concentrations (**Appendix 4**).

TBA solution — TBA solution was prepared by dissolving 15 g of trichloroacetic acid (15 w/v%) and 0.375 g of TBA (0.375 w/v%) in 100 mL of 0.25 mol L-1 HCl.

Sample preparation — 20 mg of the NLC dried samples were mixed with 1.8 mL of deionized water and 4.0 mL of TBA solution. The mixtures were heated in a boiling water bath for 15 minutes and then cooled to room temperature. Finally, the mixtures were centrifuged (2000 g for 15 min). After cooling, the solutions are read against the reagent blank and compared with standards prepared from 1,1,3,3 - tetraethoxypropane. The intensity of the colour created from the reaction between TBA with MDA, an essential by-product of lipid peroxidation, was measured at 532 nm using the UV-visible spectrophotometer model PharmaSpec 1700 (Shimadzu, Japan) (Shahparast et al., 2019; Irwin & Hedges, 2004).

3.11. *In vitro* Digestion of Lyophilized NLCs

3.11.1 Determination of Lipid Digestion

Initial phase

20.0 mL containing 2 wt% oil was placed into a glass beaker in an incubator shaker (Innova Incubator Shaker, Model 4080, New Brunswick Scientific, New Jersey, USA) at 37 °C.

Gastric/Stomach phase

Simulated gastric fluid (SGF) was prepared by placing 2 g NaCl, 7mL HCl, 3.2 g of pepsin (from porcine gastric mucosa) and adding double distilled water to 1 L. 20 mL of the “bolus” sample resulting from the initial emulsions as mixed with 20 mL of simulated gastric fluid preheated to 37 °C and then the pH was adjusted to 2.5 using 1.0 M HCl. This mixture was incubated in the incubator shaker for 2 h at 37 °C with an agitation speed of 100 rpm to mimic stomach digestion.

Small intestinal phase

30 g of "chyme" sample obtained from the simulated stomach phase was placed into a 100 mL glass beaker that was placed into a water bath at 37 °C and then adjusted to pH 7.00. 1.5 mL of simulated intestinal fluid (SIF) (containing 0.25 M CaCl2 and 3.75 M NaCl) was added to the reaction vessel, followed by 3.5 mL of bile salt solution (375 mg bile salts dissolved in 5 mM phosphate buffer, pH 7.0) with constant stirring. The pH of the reaction system was adjusted back to 7.00. The solution was prepared fresh immediately prior to each digestion experiment. 2.5 mL of freshly prepared pancreatic lipase (60 mg lipase powder (30000 U/g) dispersed in phosphate buffer at pH 7.0) solution was then added to the sample, and a pH-stat automatic titration unit (Metrohm, USA Inc.) was used to monitor the pH and maintain it at pH 7.0 by titrating 0.1 mM NaOH solution into the reaction vessel of digestion cell for 2 h at 37 °C. The volume of NaOH added to the emulsion was recorded and assumed to be related to the amount of free fatty acids (FFA) generated by lipolysis of the initial triacylglycerol.

The amount of free fatty acids released was calculated from the titration curves as described previously (Li & McClements, 2010). The percentage of free fatty acids released in the small intestine phase was calculated from the number of moles of NaOH required to neutralize the FFA using the following formula:

$$\%\text{FFA} = 100 * \frac{V_{NaOH} * m_{NaOH} * M_{Lipid}}{W_{Lipid} * 2} \qquad \text{Equation (3)}$$

Here V_{NaOH} is the volume of sodium hydroxide required to neutralize the FFAs produced (in mL), m_{NaOH} is the molarity of the sodium hydroxide solution (0.1M = 0.0001 mol/mL), W_{Lipid} is the total weight of lipid initially present in the reaction vessel (0.2 g), and M_{Lipid} is the molecular weight of the structure lipid, i.e. NA-TAG (g/mol).

3.11.2 Determination of Droplet Size (nm) and ζ-potential (mV)

The determination of droplet size and the electrical charge (ζ -potential) of the emulsion after each digestion step was measured according to **Section 3.8.1**.

3.12. Statistical Analysis

Experiments were performed in triplicate, and results were presented as mean ± SD. The statistical significance level was determined at a 95 % confidence limit ($p < 0.05$) was determined by a one-way analysis of variance (ANOVA, Tukey's HSD) using SPSS 22.0 (IBM Corp., Armonk, NY, USA). The Fisher test value (*F*-value) was obtained from the ANOVA test generated by the software.

Chapter Four

Results and Discussion

4.1. Enzymatic Acidolysis Reaction

Both enzymatic and chemical esterification methods can produce structured lipids with a defined fatty acids profile, but the enzyme-catalyzed synthesis gives some decisive advantages over chemical reactions. The enzymatically catalyzed reaction is more acceptable than the chemical approach in practical applications. The reaction has a higher specificity, can be performed under milder conditions, the enzyme is reusable, and the process is more environmentally friendly (Adamczak, 2004). The enzymatic modification method enables the incorporation of FA at

specific *sn* positions in the glycerol backbone if a specific enzyme is chosen. The nutritional value of a TAG product relies on the fatty acid composition and positional distribution of the acyl groups within the TAG molecules (Mu et al., 1998). Also, the compositions of positions *sn*-1 and *sn*-3 could obtain by complex "stereospecific analysis" procedures with many reactions involving degradation, synthesis, enzymatic hydrolysis, and chromatographic separation of the products (Karupaiah & Sundram, 2007). Through enzymatic reaction, the incorporated fatty acids can be placed at the *sn*-1,3 positions of the TAG products. In addition to the above benefits, the structure lipid produced from the enzymatic reaction can be easily seperated from the final reaction mixtures in the acidolysis reaction (Zhou et al., 2001).

This section investigated the enzymatic acidolysis reaction to incorporate nervonic acid (NA; C24:1) into soybean oil. Four critical parameters for the reaction, including reaction time, enzyme loading, factors of reaction temperature, and substrate molar ratio, were elucidated for the optimization.

4.1.1 Enzyme Screening

Various lipases have been investigated for the enzymatic modification of oils and fats. Among the microbial, plant and animal sources of lipases, microbial lipases are the most attractive commercial lipases (Yang et al., 2003). Immobilized lipases have a wide range of applications in lipid modification studies, and they provide advantages of higher catalytic activity and stability over other enzymes (Cui et al., 1997). The most vital factors of these immobilized enzymes are their recovery and reusability, which can enhance thermostability in industrial applications (Romero et al., 2005). However, choosing the right type of enzyme is essential when running an acidolysis reaction, as different enzymes may have different stereo configurations, thus resulting in different effects even in the same enzymatic acidolysis reaction under the same optimal parameters (Liu et al., 2015). **Fig.11** shows the ideal modified TAG with nervonic acid in *sn*-1, 3 position.

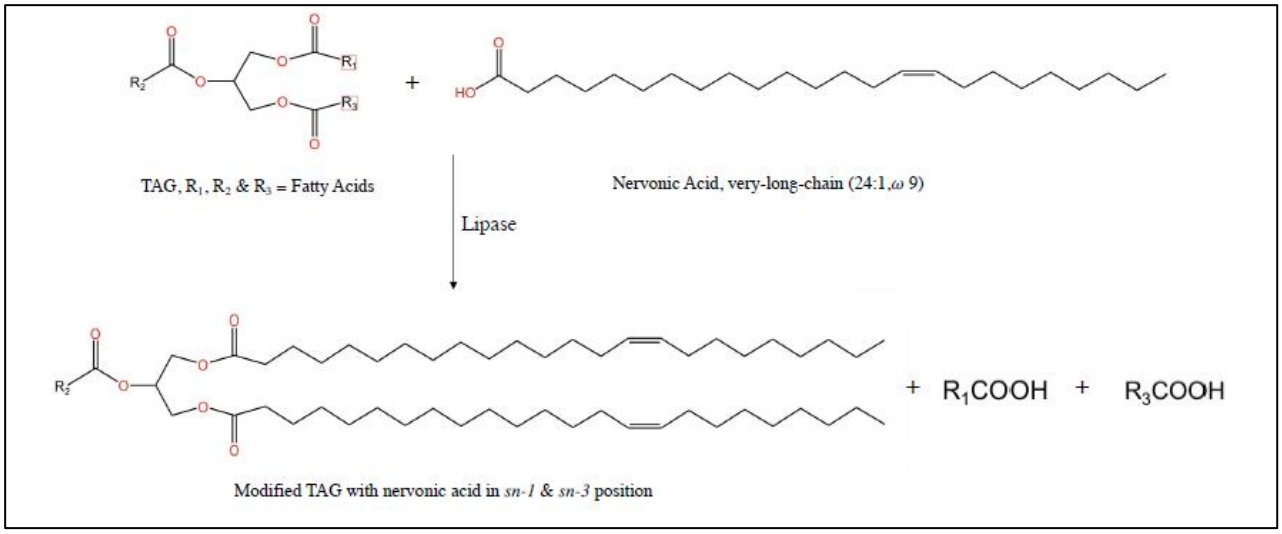

Figure 11. Lipase catalyzed acidolysis of TAG incorporated with nervonic acid. TAG, Triacylglycerol.

Ezymes were initially selected based on the literature data indicating that Lipozyme TL IM and Novozyme 435 effectively catalyze the structural modifications of natural triacylglycerols. Lipozyme TL IM was widely known as *sn*-1,3 specificity lipase, which hydrolysed the ester bond at *sn*-1 and *sn*-3 positions of TAG as a highly effective catalyst to carry out the position-specific replacement of fatty acids in TAG and can be attributed to acyl migration (Liu et al., 2016). In contrast, Novozyme 435 shows no regiospecificity to triacylglycerol (Yasuda & Yamamoto, 2020).

Enzyme screening is a method of determining which enzyme has the highest catalytic activity. It is crucial when performing an acidolysis reaction since different enzymes affect fatty acid incorporation and the yield of structure lipid (NA-TAG). **Fig. 12** shows the time course of incorporating NA into TAG by lipases. It can be observed that both lipases from *T. lanuginosus* immobilized (Lipozyme TL IM and Lipozyme TL IM immobead 150) produced the better incorporation level among all tested enzymes. Both enzymes exhibited the highest catalytic activity in enzymatic modification giving above 60% incorporation of NA into TAG fraction after 6 h of reaction.

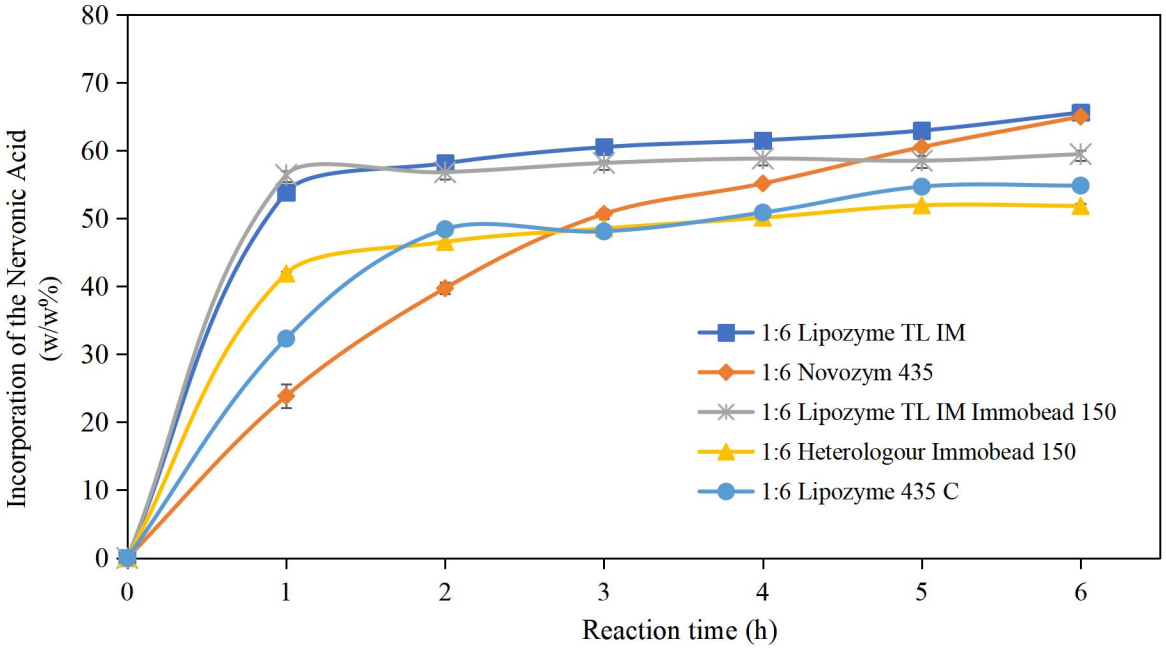

Figure 12. Enzyme screening for acidolysis of NA-TAG oil (reaction conditions: 1:6 TAG/NA substrate molar ratio, enzyme load 20 (w/w%), temperature (60 °C).

According to the results, Lipozyme TL IM was selected as a catalyst to evaluate the subsequent single factor experiments of acidolysis reaction. This lipase offers higher catalytic efficiency, specificity and selectivity in the *sn*-1,3 position. However, we retained our interest in the selection of lipases and liked to compare Lipozyme TL IM with Lipozyme TL IM immobead 150, and Heterologous immobead 150 for the acidolysis reaction, and this is further investigated in the optimization experiments later (**Section 4.2**).

4.2. Optimization of NA-TAG Structure Lipid Preparation

Before optimizing the NA-TAG structure lipid preparation, preliminary acidolysis experiments was performed to study the effect of reaction temperature and time. From the observation, the reaction temperature and time did not affect the incorporation of NA into TAG by enzymatic acidolysis. The reaction rate did not change when reaching 4 h reaction time. Thus, 4 h reaction time and temperature of 60 ℃ were adopted for the optimization study. Three factors, each with three levels, were included, i.e., the enzyme type, enzyme loading and the substrate molar ratio were optimized using an L9 (3^3) orthogonal experimental design. This experimental design significantly shortened the experimental process and reduced solvent and energy consumption (Shahavi et al., 2015). As shown in **Table 5**, nine experimental groups were carried out and evaluated by three response factors. The results of these experiments were used to find the optimum acidolysis conditions.

The optimal acidolysis conditions was determined according to the range analysis and ANOVA analysis of the results obtained from the nine orthogonal experimental groups (**Table 5**). From the range analysis, the optimization could be determined using the combination of the best level for each factor. An *F* value was calculated from the ANOVA analysis of each factor to ensure that the level selected from the range analysis was highly significant than the other levels. As shown in **Table 6**, the optimized acidolysis reaction to obtain the maximum incorporation of nervonic acid by range analysis was A3B2C1. The influence of the parameters on the incorporation of NA decreased in the order of A (Enzyme Types) > B (Enzyme Loading, w/w%) > C (Substrate Molar Ratio) according to the *F* values. The most significant parameter (at the 95% confidence level) was only factor A (Enzyme types), shown to be statistically significant ($p < 0.05$) from the ANOVA analysis (**Table 6**). There was no significant difference ($p > 0.05$) in enzyme loading varied from 5 to 15 w/w% compared to other experimental variables. The substrate molar ratio of 1:4, 1:5 and 1:6 contributed the least statistically significant because of the *F* values. However, considering the economy of the process, we decided to use the amount of 10 % of the lipase and 1:4 of the substrate molar ratio in further studies. Hence, the optimum conditions for the maximum incorporation rate should be adjusted to enzyme type of Lipozyme TL IM Immobead 150, molar substrate molar ratio of 1:4 and 10 w/w% enzyme loading at 50 ℃ and 4 hours reaction time.

Table 5. The L9 orthogonal array design for enzymatic acidolysis reaction.

Code	Enzyme Types	Enzyme Loading (w/w%)	Substrate Molar Ratio (TAG/NA)	Response variables
				Incorporation of nervonic acid (w/w%)
1	Lipozyme TL IM	5	1 : 4	47.41 ± 2.12
2	Lipozyme TL IM	5	1 : 5	48.51 ± 1.51
3	Lipozyme TL IM	5	1 : 6	47.46 ± 2.28
4	Heterologour Immobead 150	10	1 : 5	19.49 ± 2.58
5	Heterologour Immobead 150	10	1 : 6	32.18 ± 2.89
6	Heterologour Immobead 150	10	1 : 4	37.69 ± 4.15
7	Lipozyme TL IM Immobead 150	15	1 : 6	49.88 ± 5.53
8	Lipozyme TL IM Immobead 150	15	1 : 4	48.86 ± 1.911
9	Lipozyme TL IM Immobead 150	15	1 : 5	51.91 ± 6.65

All reactions were conducted in triplicate after the preliminary experiments. TAG, Triacylglycerol; NA, Nervonic acid. Mean ± STD, n=3. NA, Nervonic acid; TAG, triacylglycerol.

Table 6. Range analysis and Analysis of Variance (ANOVA) of enzymatic acidolysis reaction factors for the L9 (3^3) orthogonal experiment.

	Incorporation of nervonic acid (w/w%)		
	A	B	C
k1	47.79	38.93	44.65
k2	29.79	43.18	39.97
k3	50.22	45.69	43.17
Best level	A3	B2	C1
R	20.43	6.76	4.68
Order		ABC	
SS	747.50	70.08	34.39
F value	21.74*	2.04	1.00

Factors, A, Enzyme Types; B, Enzyme Loading [w/w%]; C, Substrate Molar Ratio; Range analysis, k-averaged value of each level of the factors (k1, k2, k3 for level 1, 2, 3, respectively), the biggest k value indicates the best level for each factor; R, range between the maximum and minimum k value, a larger R value suggests a more important role of the factor in the encapsulation process; order, influential order of the factors, determined by the descending order of R value; SS, sum of squares; *F* value, obtained from ANOVA Fisher's F-test, F (2,2) 95% = 19; *, $p < 0.05$.

4.3. TLC Analysis of Lipid Mixture and Purification of Structure Lipid

Thin-layer chromatography (TLC) is a technique that has been routinely used for the separation and identification of lipids. Structured lipids in the final mixtures were separated and analyzed for their TAG content using TLC. All content of lipid compounds such as free fatty acids (FFA), monoacylglycerol (MAG), diacylglycerols (DAG), and triacylglycerol (TAG) were resolved easily in a single step using this technique. The separation is attained using a solvent system (hexane: diethyl ether: acetic acid; 700: 300: 15, v/v/v) where hexane with acetic acid migrates free fatty acids while diethyl ether functions to control the separation of saturated and polyunsaturated TAGs (Patel et al., 2015).

The TLC chromatogram developed after the optimized acidolysis reaction showed the presence of TAG, FFA, DAG and MAG bands (**Fig.13**). These bands were identified based on literature (Caballero et al., 2014). The results suggested the successful incorporation of NA into the TAG, as the NA was substituted on *sn*-1,3 positions of the glycerol backbone and released a high amount of free fatty acids as shown in the large fractions of **Fig.13**. A similar result by Caballero et al. (2014) reported the TLC analysis of interesterification reaction samples using avocado oil and caprylic acid as substrates, and the bands on TLC plates demonstrated that the caprylic acid was successfully substituted on *sn*-1,3 positions.

Initially, the titration method was applied to neutralize the FFA in the NA-TAG oil mixture using 0.5N aq. NaOH to react with the free fatty acid to form sodium salts. According to literature (Kavidia et al., 2018), oil mixture and sodium salts of fatty acids can be separated by liquid-liquid extraction by hexane and methanol-glycerin mixture. We have adopted a similar approach for separating the NA-TAG oil from the free fatty acids in the lipid mixture and using the TLC to check for purified NA-TAG. However, according to the TLC results, the titration method did not remove the free fatty acids successfully after checking the pKa values of the FFAs and NA which are protonated in the medium.

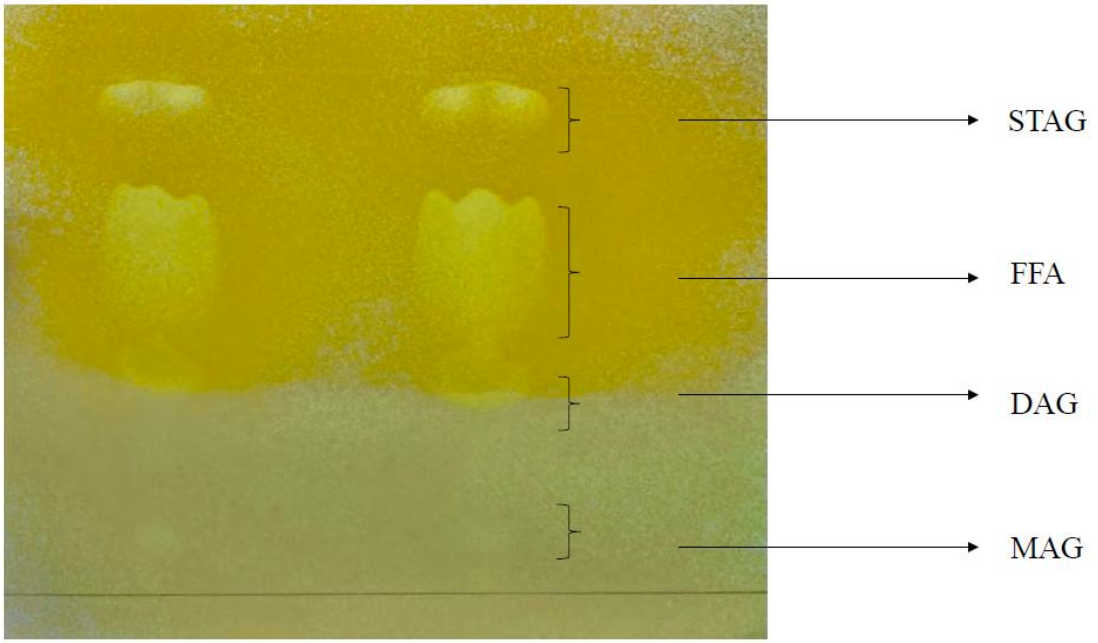

Figure 13 . Thin layer chromatography of NA-TAG oil mixture obtained from optimized acidolysis reaction before purification. The two lanes indicate duplicate samples from experiments. STAG, Structure triacylglycerols; FFA, Free fatty acids; DAG, Diacylglycerols; MAG, Monoacyglycerols.

As an alternative, column chromatography was selected to purify the structure lipid produced. The main benefit of column chromatography is that the stationary phase is inexpensive. We started with 90 g silica gel as the stationary phase, but no good separation of NA-TAG oil was achieved. After some initial trials, we found the use of 120 g silica gel as a stationary phase gave good separation of NA-TAG oil. This may be due to the higher amount of silica gel increasing the surface area for adsorption and better separation.

The identification of purified NA-TAG oil and FFA were carried out on TLC plates of silica-gel. From the column chromatography experiments, the purified NA-TAG fractions could be eluted from the column after 30 minutes, and the elution lasted for 7 minutes. Approximately 190 mL fraction was collected during these 7 minutes of elution. From **Fig. 14**, TLC Plate A shows fractions collected after 30 mins of column chromatographic separation. It can be seen that no free fatty acid bands were observed on the plate, and mostly purified NA-TAG oil was present.

After the elution of the NA-TAG oil for 7 mins, free fatty acids started to show up in the fractions collected (**Fig. 14**, Plate B). Plate C showed no more purified NA-TAG oil presence for the remaining fractions collected. Hence, it is clear that column chromatography could successfully separate the NA-TAG oil from the free fatty acids to give purified NA-TAG. The purified oil was evaporated in a rotary evaporator at 50 ℃ to remove the solvent. The purification process was repeated multiple times to collect purified NA-TAG oil for encapsulation in the nanostructured lipid carriers (NLCs).

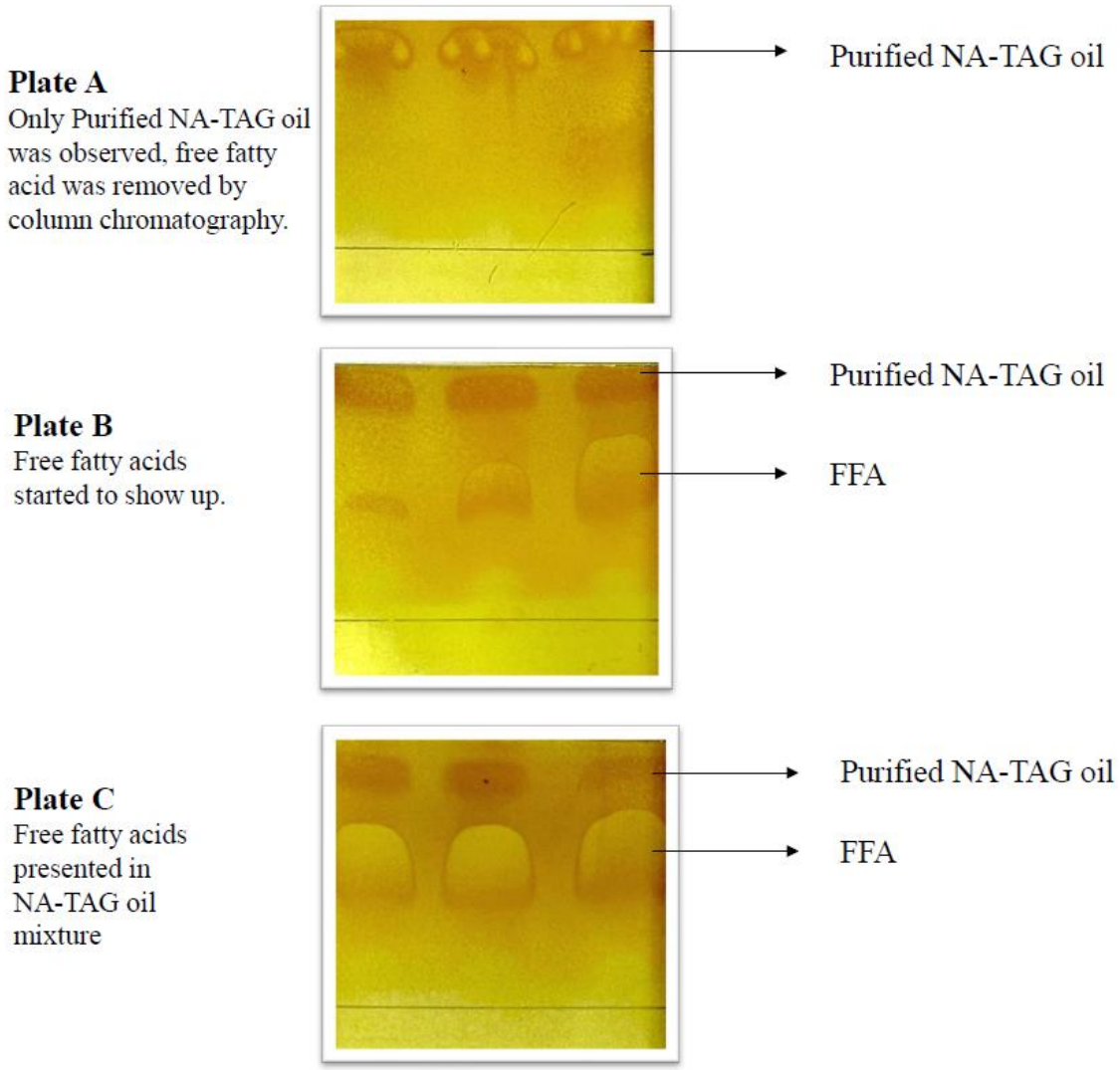

Figure 14. Thin-layer chromatography (TLC) plate separation of purified NA-TAG oil mixture by column chronography. Plate A, TLC analysis for samples collected from 30 to 37 mins; Plate B, TLC analysis for samples collected from 38 to 40 mins; and Plate C, TLC analysis showing samples collected at 41 mins. The three bands shown on each TLC plate indicate triplicate experiments. NA, Nervonic acid; TAG, Triacylglycerol; FFA, Free fatty acids.

4.4. Fatty Acid Composition

Table 7 summarizes the fatty acid composition of the soybean oil used for experiments and the purified NA-TAG oil obtained after the optimized acidolysis and oil purification by column chromatography.

Oils and fats are composed of mono-, di-, and triglycerides with varying chain lengths and degrees of unsaturation in their fatty acids (Elmowafy & Al-Sanea, 2021). The soybean oil used for this study has seven fatty acids, with oleic and linoleic acid being the major ones. The sample has an average of 11% palmitic (C16:0), 4.7% stearic acid (C18:0), 22% oleic (C18:1), 54% linoleic acid (C18:2), 7.3% linolenic acid (C18:3) acids, 0.4% Behenic acid (C22:0) and 0.16% lignoceric acid (C24:0). The palmitic and stearic fractions are low saturated fatty acids and constitute 15.7% of the soybean oil. Behenic and lignoceric acid are also saturated fatty acids but only constitute 0.56% of the soybean oil. The unsaturated fatty acids (22% monounsaturated, 61.5% polyunsaturated) was the predominant fatty acid in soybean oil. The ratio between MUFA and PUFA is a frequently used criterion to show the oxidative potential of fatty acid compositions, indicating the stability of oil (Hsieh & Kinsella, 1989; Toorani et al., 2019). The unsaturated fatty acids in soybean oil included two essential fatty acids, linoleic (54.27%) and linolenic (7.3%), which are not produced in the human body (Toorani et al., 2019).

The fractionation, hydrogenation and interesterification of an oil or oil blend are three modification processes that change their physical properties (Dijkstra, 2016), including the FA profile. The mole ratio mixture of soybean oil and nervonic acid (C24: 1) selected in the optimization was 1:4, and the reaction was performed at an optimal temperature of 50 ℃ for 4 hours. The immobilized Lipozyme TL IM immobead 150 lipase was chosen as a biocatalyst for incorporating NA (C24:1) into soybean oil because it would place this FA at *sn*-1,3 positions on the TAG molecule for maximum metabolic benefit. The changes in the fatty acid composition were due to the rearrangement of the fatty acids. As expected, the FA composition of soybean oil was significantly changed after modification (**Table 7**). After a 4-hour acidolysis reaction, there was an average of 65.57 ± 0.99 w/w% incorporation of C24:1 into the soybean oil. The purified

NA-TAG oil has a significant increase in MUFA, as nervonic acid became the primary FA in the modified structured lipid. These results demonstrate that the acidolysis reaction was efficient for nervonic acid incorporation.

After the incorporation of nervonic acid (C24:1), the amounts of the main saturated and unsaturated TGs decreased. The total mono-unsaturated fatty acid contents in the incorporation were 72.696%, higher than saturated fatty acid contents (9.583%) and poly-unsaturated fatty acid (17.721%). The two major unsaturated fatty acids (palmitic acid, Stearic acid) decreased around 30% of the initial amount at 3.47% and 1.55%, respectively. Thereby, the modified oils have lower saturated fatty acids. The monosaturated fatty acid of oleic was reduced to 7.126%. Linoleic and linolenic acid content decreased to 15.93% and 1.791%, respectively

The behenic and lignoceric acid increased after the acidolysis reaction. This is due to the nervonic acid already having these two fatty acids. Dietary behenic acid (22:0) enhanced from 0.4 to 0.872 % after incorporation. Despite its low bioavailability compared with oleic acid, behenic acid is a cholesterol-raising fatty acid in humans (Cater & Denke, 2001). On the other hand, nervonic acid (24:1) contains a monounsaturated analog of lignoceric acid (C24:0). The structure lipid mixture showed increased lignoceric acid from an initial 0.164% to 3.69%.

Table 7. Fatty acid composition of soybean oil and the structure lipid with nervonic acid incorporation.

	Fatty Acids	**FA profile of Soybean oil (w/w%)**	**FA profile of NA-TAG structure lipid (w/w%)**
Palmitic acid	C16:0	10.97 ± 0.01	3.468 ± 0.02
Stearic acid	C18:0	4.704 ± 0.01	1.553 ± 0.02
Oleic acid	C18:1	22.21 ± 0.03	7.126 ± 0.25
Linoleic acid	C18:2	54.27 ± 0.07	15.93 ± 0.01
Linolenic acid	C18:3	7.278 ± 0.01	1.791 ± 0.01
Behenic acid	C22:0	0.400 ± 0.00	0.872 ± 0.87
Lignoceric acid	C24:	0.164 ± 0.00	3.690 ± 0.08

	0		
	C24:		
Nervonic acid	1	0.000	65.57 ± 0.99
Total FA		**100.0**	**100.0**
Total Saturated FA		**16.24**	**9.583**
MUFA		22.21	72.69
PUFA		61.55	17.73
Total Unsaturated FA		**83.76**	**90.42**

FA, Fatty Acid; SFA, Saturated fatty acids; USFA, Unsaturated fatty acids; MUFA, Monounsaturated fatty acids; PUFA, Polyunsaturated fatty acids.

4.5. Preparation and Characterization of NA-TAG-loaded NLCs

As mentioned in the literature, NLCs have constantly sparked the development of valuable and safe drug delivery systems due to their physicochemical and biocompatible qualities (Elmowafy & Al-Sanea, 2021). The physicochemical properties of NLCs were investigated to understand their influences on the NLCs formation and stability.

As the first step, lipid screening was performed as part of formulation development to generate formulations with improved properties. Formulation variables and processes were optimized to obtain minimum particle size, minimum polydispersity index, maximum zeta potential, and entrapment efficiency. Preliminary lipid screening and processing conditions studies focused on creating a suitable lipid matrix of appropriate dimensions. Hence, this section aims to study the preparation of an optimised NLCs formulation as a potential tool for encapsulating NA-TAG oil. The NLCs's physicochemical properties were investigated, including particle size, polydispersity index (PDI), and zeta potential (ZP). Thermal analysis and storage stability studies of NA-TAG-loaded lipid carriers were evaluated. All formulations were measured at room temperature (25 ℃) to maintain the colloidal stability of the system.

4.5.1 Preliminary Experiments

4.5.1.1 Selection of Liquid and Solid Lipids

A different formulation of NLCs was selected based on different raw materials, including lipid (both liquid and solid lipid) and surfactant, to determine the optimum NLCs formulation. We have chosen a few commonly used liquid and solid lipids from the literature review to start with the NLCs formulation. Among the liquid lipid examined in the literature, natural oils are generally more tolerable and biocompatible than synthetic lipids (Cirri et al., 2018). The solubility of NA-TAG was observed in soybean oil and olive oil. According to the observations, NA-TAG showed a higher solubility in soybean oil than olive oil.

To select an appropriate solid lipid type, the concentration of surfactant (Tween 80) and oil (soybean oil) were kept constant in the formulation. The particle size, polydispersity PDI and zeta potential of NLCs with stearic acid (SA) and GMS were measured. As shown in **Table 8A**, 9 % of solid lipid was encapsulated, and the GMS gave much smaller particle size at 138.7 ± 9.655 nm than SA (1222 ± 171.9 nm) ($p < 0.05$). The PDI value was 0.26, indicating a narrow particle size distribution, and the zeta potential was much higher than NLCs prepared with SA. PDI value less than 0.3 is considered optimum in most studies; PDI greater than 0.7 shows a wide particle distribution (Babazadeh et al., 2017). The dispersion of GMS with higher zeta potential values indicates that the systems were more physically stable than those containing SA. Thus, GMS was selected as an appropriate solid lipid for the following stages. Solid lipids play an essential role in developing physically stable NLCs particles. As the homogenous lipids, Stearic acid was prone to form crystals, which was undesirable in NLCs structures (Rousseau, 2000). The amphiphilic nature of GMS might contribute to a chemical reaction with the liquid lipid, stabilizing the NLCs dispersion. From the above trials, we found that the NA-TAG structure lipid has good solubility in soybean oil (liquid lipid), and GMS served a suitable solid lipid to give potential good stability to the NLCs preparation.

4.5.1.2 Miscibility of Solid-Liquid Lipid System

Miscibility of solid and liquid lipid in the lipid phase at specific concentrations is a prerequisite for the optimized NLCs structures (Cirri et al., 2018), as this can be the main reason for the instability of formulations. The miscibility between GMS and soybean oil was initially evaluated by preparation of solid lipid nanoparticles (SLN) in different liquid to aqueous phase ratios (w/w) of 10:90, 20:80 and 30:70 (**Table 8B$_1$)**, and 10:90 to establish the miscibility of the two lipids; according to the frequent ratio reported in literature while controlling other factors constant. When the lipid phase increased from 10 to 30 %, the particle size increased significantly from 79.01 nm to 154.0 nm ($p < 0.05$). The incorporation of lipid phase can cause massive crystal order disturbance; the resulting matrix of lipid particles reveals great imperfections in the crystal lattice and leaves enough space to accommodate the drug molecules, which leads to increased drug entrapment efficiency (Jenning et al., 2000; Azmi et al., 2020). From the results, the liquid to aqueous phase ratios of 10:90 w/w was selected as a proper candidate for the preparation of

NLCs. This finding agreed with Loo et al. (2012), in which NLCs with high lipid concentrations were physically less stable than those with low lipid concentrations due to their propensity to recrystallise more rapidly. A similar study also reported that the lipid to aqueous phase ratio of 10:90 w/w was suitable to improve the miscibility and minimize the toxicity risks simultaneously (Cirri et al., 2018). Similar results reported that the stock emulsions were also prepared by homogenizing the 10 wt% oil phases with the 90 wt% aqueous phases to create a fine emulsion (Zhang et al., 2015). However, another study reported that the results of 85:15 w/w in the ratio was the most appropriate concentration of optimum NLCs formulations(Babazadeh et al., 2017). However, at 30% w/w liquid lipid, a plateau in size was reached, with no further particle size variations. Similar results were reported by Sakellari et al. (2021). Therefore, there was no significance if the liquid lipid ratio was over 30%. In the orthogonal optimization (**Table 9**), we investigated the ratio at 10:90, 15:85 and 20: 30 to discuss the effects.

As shown in **Table 8B$_2$**, the solid lipids (GMS) and liquid lipid (soybean oil) with the best-solubilizing potential for 1% concentration of NA-TAG were mixed in different ratios of 1:2, 1:1, 2:1, 3:2 and 2:3 in different tubes to observe the solubility and miscibility of the two lipids in NLCs. The liquid to aqueous phase ratio of 10:90 and aqueous phases was kept constant. From visual inspection, the solubility and miscibility of these five formulations of NLCs were good (they did not show any precipitation by observations). Formulations with glyceryl monostearate (GMS) and tween 80 exhibited a significant increase from 157.83 nm to 1959.89 nm in particle size nm ($p < 0.05$). It was observed that particle size decreased by increasing the concentration of GMS from 3% to 6% in the lipid phase. The liquid to solid lipid ratio of 2:1 means a particle size of 157.83 nm and PDI 0.19. The PDI value measures the narrowness of particle size distribution (Babazadeh et al., 2017). The readings were below 0.2 and indicated homogeneity of the formulations. According to Mitri et al. (2011), the polydispersity parameter provides important indications about the homogeneity of NLCs samples, with values below 0.25 reflecting relatively homogeneous nanoparticles with a low predisposition to aggregation (Mitri et al., 2011). The ratio of 2:1 showed a zeta potential of -25.31 mV compared to other lipids to the solid ratios in the 10% lipid phase. Zeta potential is the indication of the stability of colloidal dispersion. In the general concept, minimum particle aggregation is associated with charged

particles due to repulsion. Therefore, the lipid to solid lipid ratio at 2:1 was selected as one of the optimized variables for further study.

4.5.1.3 Selection of Surfactant Type and Concentration

The third step was choosing the appropriate surfactant types and concentrations. GMS and soybean oil were kept unchanged, and three types of surfactants, including Poloxamer 407, Tween 20, and Tween 80, were assessed. Surfactants play two significant roles in the NLCs preparation; 1) formation and stabilization of pre-emulsion (colloidal stabilization) and 2) preventing particle aggregation (Babazadeh et al., 2017). It was found that when surfactant Poloxamer 407 was present in the formulations, the phase stage of NLCs emulsion tuned to a solid phase, and no further analysis of physicochemical properties could be performed. Thus, the NLCs formulation with poloxamer 407 was discarded (Data in **Appendix 5**). On the other hand, the formulation with Tween 20 led to a significantly higher PDI exceeding 0.6 (**Appendix 5**), which suggests the formation of a poorly uniform system and a great tendency to aggregation phenomena (Cirri et al., 2018).

Regarding the EE%, the Tween 80-based NLCs was transparent by observation. As shown in **Table 8C**, the formulation with Tween 80 had the significantly smallest particle size, PDI and the highest physical stability of zeta potential, which indicated the formation of homogeneous and stable nano-dispersions (Aditya et al., 2014; Zhang et al., 2015). The type and concentration of surfactants can affect the zeta potential of particles in a colloidal system (Talebi et al., 2021). Han et al. (2008) reported that using Tween 80 makes the NLCs formulations more stable for more than one year compared to other surfactants including lecithin and poloxamer 188.

Surfactant concentrations can also significantly impact the quality of NLCs. As the surfactant was absorbed on the surface of nanoparticles, making them sterically repulsive to one another (Rai et al., 2021). It was observed that particle size significantly decreased from 157.83 nm to 90.12 nm ($p < 0.05$) when increasing the concentration of Tween 80 from 1% to 3% (in **Table 8C**). This occurred because the sufficient surfactant lowered surface tension and stabilised newly

formed surfaces during homogenization, resulting in smaller particles (Babazadeh et al., 2017). In addition, surfactant concentrations might also potentially contribute to the small PDI value. For example, high quantities of tween 80 allow for easier dispersion, less agglomeration and coalescence, and hence a reduction in PDI (Azmi et al., 2020). However, if the amount of surfactant used is insufficient, uncovered surface areas of lipid nanoparticles in NLCs would result in flocculation, aggregation, and gelation (Pezeshki et al., 2019; Azmi et al., 2020). Larger particles produced by coalescence may take longer to crystallize as a lipid matrix (Babazadeh et al., 2017). Similar findings by Huang (2017) et al. discovered that surfactant concentration is an important parameter affecting the surfactant functionality in colloidal systems. Hence, increasing the concentration of surfactants, the more negatively charged NLCs were prepared, and the smallest droplet sizes were formed with 3% Tween 80 to obtain a stable lipid nanoparticles emulsion.

4.5.1.4 Selection of NA-TAG Concentration

NLCs would protect the encapsulated active ingredients and enhance their functionality and stability (Karimi et al., 2015). While we wanted to include more active ingredients in the NLCs formulation, the amount of active ingredient, in this case, the NA-TAG, can potentially impact the particle size and PDI of NA-TAG-loaded NLCs. Thus, selecting the optimum NA-TAG concentrations for the NLCs formulation was important. The solid to liquid lipid ratio of 2:1 and the aqueous phase were kept constant to study this. As shown in **Table 8D**, when NA-TAG oil loaded increased from 10% to 30% in the liquid phase, the PS increased significantly from 148.5 nm to 1474 nm ($p < 0.05$). This suggested that the excess oil content would expulse during crystallization, resulting in aggregation and particle size growth (Wang et al., 2014). However, when the NA-TAG oil accounts for more than 3%, the phase states were solid by observation, and the particle size became large because the solid did not melt in the dilution. The results might be that when the oil droplets are incorporated into the surfactant micelles at higher concentrations, they cannot further disperse the oil droplets (Mehmood, 2015). PDI also increased significantly from 0.17 to 0.752, which indicated a broad particle size distribution. This could be attributed to the increased viscosity, which means more energy was needed to

disintegrate the particles (Huang et al., 2017). Moreover, zeta potential reduced from -34.7 to -23.0 mV. In general, lipid nanoparticles are negatively charged on the surface. The results of the factorial orthogonal design also suggest that the concentration NA-TAG significantly influenced the ZP of the NLCs (Gonzalez-Mira et al., 2010). The stability of emulsions decreases with the increase of NA-TAG oil concentrations from 1% to 3%. This can be due to the increase of interfacial tension with the addition of higher oil contents (Mehmood, 2015). Similar trends were observed in the study by Das et al. (2011) and Azmi et al. (2020). Their results showed that particle size and PDI increased as the number of active ingredients increased. In a similar study, Mehmood (2015) reported that canola oil as the active ingredient could not dissolve further when increasing the concentrations in NLCs system.

Table 8. Preliminary experiments for NLCs preparation.

Formulation code	Liquid lipid (Soybean oil) (w/w%)	Solid lipid (w/w%)		NA-TAG (%w/w)	Lipid to aqueous phase	Surfactant type (w/w%)	Aqueous Water (w/w%)	Response variables		
		Stearic Acid	GMS			Tween 80		Particle Size (nm)	PDI	Zeta potential (mV)
A. Selection of solid lipid trials (SLNs)										
NLCs 9:1	-	9	-	1	10 : 90	1	89	1222 ± 171.9	0.76 ± 0.072	-18.1 ± 6.47
NLCs 8:2	-	8	-	2	10 : 90	2	88	1469 ± 242.9	0.80 ± 0.076	-10.5 ± 4.51
NLCs 7:3	-	7	-	3	10 : 90	3	87	2324 ± 142.1	0.77 ± 0.692	-9.25 ± 0.24
NLCs 9:1	-	-	9	1	10 : 90	1	89	138.7 ± 9.655^{c}	0.26 ± 0.45^{b}	-28.0 ± 3.46^{a}
NLCs 8:2	-	-	8	2	10 : 90	2	88	564.1 ± 669.0	-	-19.10 ± 1.01
NLCs 7:3	-	-	7	3	10 : 90	3	87	-	-	-
B_1. Miscibility of solid-liquid lipid systems (SLNs)										
$NLCs_{M1}$	4	-	6	-	10 : 90	3	87	79.01 ± 0.7772^{c}	0.23 ± 0.14^{b}	-28.2 ± 2.63^{a}
$NLCs_{M2}$	8	-	12	-	20 : 80	3	77	98.42 ± 0.9459^{c}	0.22 ± 0.009^{b}	-36.7 ± 2.32^{a}
$NLCs_{M3}$	12	-	18	-	30 : 70	3	67	154.0 ± 1.093^{c}	0.16 ± 0.010^{b}	-41.9 ± 3.56^{a}
B_2. Liquid to solid lipid ratio in lipid phase trials (NLCs)										
$NLCs_{1:1}$	4.5	-	4.5	1	10 : 90	1	89	2457.00 ± 27.98	0.90 ± 0.18	-24.8 ±1.29
$NLCs_{1:2}$	3	-	6	1	10 : 90	1	89	1938.33 ± 125.27	0.98 ± 0.04	-23.8 ± 0.71
$NLCs_{2:1}$	6	-	3	1	10 : 90	1	89	157.83 ± 2.65^{c}	0.19 ± 0.02^{b}	-25.3 ± 1.45^{a}
$NLCs_{2:3}$	3.6	-	5.4	1	10 : 90	1	89	1959.89 ± 211.42	0.94 ± 0.1	-23.7 ± 0.73
$NLCs_{3:2}$	5.4	-	3.6	1	10 : 90	1	89	308.42 ± 8.95	0.43 ± 0.04	-27.9 ± 1.01
C. Surfactant Concentration (Tween 80)										
$NLCs_{T1}$	6	-	3	1	10 : 90	1	89	157.83 ± 2.65	0.19 ± 0.02	-25.3 ± 1.45
$NLCs_{T2}$	6	-	3	1	10 : 90	2	88	102.51 ± 1.25	0.12 ± 0.05	-30.1 ± 2.54
$NLCs_{T3}$	6	-	3	1	10 : 90	3	87	90.12 ± 0.85^{c}	0.11 ± 0.01^{b}	-42.5 ± 1.18^{a}
D. NA-TAG concentrations										
$NLCs_{NT1}$	6	-	3	1	10 : 90	3	87	148.5 ± 3.446^{c}	0.17 ± 0.01^{b}	-34.7 ± 2.00^{a}
$NLCs_{NT2}$	5.333	-	2.667	2	10 : 90	3	87	612.2 ± 229.6	0.706 ± 0.06	-27.6 ± 1.06
$NLCs_{NT3}$	4.667	-	2.333	3	10 : 90	3	87	1474 ± 229.6	0.752 ± 0.94	-23.0 ± 0.784

SLNs, solid lipid nanoparticles; NLCs, nanostructured lipid carriers. Values are presented as mean SD ± (n=3). Different letters are significantly ($p < 0.05$).

4.5.2 Optimization of NLCs Containing NA-TAG oil

NLCs is derived from the oil-in-water (O/W) emulsions (Babazadeh et al., 2017). The NLCs formulations contained GMS as solid lipid, Tween 80 as the surfactant, and soybean oil as the lipid phase was optimized using the L9 (3^3) orthogonal optimization design.

The orthogonal optimisation design was applied to examine the effect of three independent variables, namely lipid phase to aqueous phase ratio (10:90, 15:85 and 20:80 w/w%), aqueous surfactant concentrations (1-3 w/w%) and NA-TAG (1-2 w/w%) concentrations, on four response variables of particle size, polydispersity index, zeta potential and the entrapment efficiency of the NA-TAG loaded NLCs. As shown in **Table 9**, the minimum particle size was 85.84 nm. However, the best homogenization conditions cannot be chosen only based on particle size. For the range analysis (**Table 10**), the significance of each factor was evaluated by calculating the *F* value to ensure the selected level was significantly better than other levels (Wu et al., 2012). Compared to a comprehensive experimental design, this approach requires only fewer experiments. For instance, other than 64 groups, only nine groups of tests were required to investigate four factors with a three-level design (Peng et al., 2019). Hence, the experimental process has been considerably shortened to decrease solvent waste and energy consumption.

The percentage of encapsulation efficiency was the most significant factor influencing the experiment in the orthogonal design optimization (**Table 9**). Entrapment efficiencies of NA-TAG in all the NLCs were observed as > 90% which indicated that NA-TAG oil could be well entrapped in lipid nanoparticles. From the range analysis, the optimized encapsulation conditions to obtain the maximum EE% was A1B1C3 (**Table 10**). However, only factors A (NA-TAG mix concentration) and C (aqueous surfactant concentration) were shown to be statistically significant ($p < 0.05$) from the ANOVA analysis (**Table 10**). Therefore, the optimal conditions for the maximum EE% should be adjusted to A1B1C3 (NA-TAG mix concentration, 1%; lipid phase to aqueous phase ratio, 10:90; and aqueous surfactant concentration, 3%). The influence of the parameters on the EE% of NLCs decreased in the order of C (aqueous surfactant concentration) > A (NA-TAG mix concentration) > B (lipid phase to aqueous phase ratio)

according to the *F* values. The most significant parameter (at the 95% confidence level) was surfactant concentration in the aqueous phase of the NLCs formulations, followed by the NA-TAG mix concentration. There was no significant difference in lipid phase to aqueous phase ratio (at the 95% confidence level) compared to other experimental variables.

As shown in **Table 10**, the optimized encapsulation conditions to obtain the minimum particle size and polydispersity index of NLCs by range analysis were A2B1C3 and A2B3C1, respectively. The optimized lipid encapsulation to achieve the maximum zeta potential of NLCs by range analysis was A1B2C3. However, according to the *F* values, there was no significant difference (at the 95% confidence level) in the factors ABC on particle size, polydispersity index and zeta potential. In addition, compared to factor B (lipid phase to aqueous phase ratio) among four response variables, B1 was used twice to obtain the highest entrapment efficiency and smallest particle size. Thus, based on a balanced evaluation of all factor levels, the lipid phase to aqueous phase ratio of 10:90 was selected in the optimized NLCs formulations.

The orthogonal design has been successfully applied in the NLCs optimization of aimed conditions from various variables. Based on this analysis, and considering the highest encapsulation efficiency, the cost of energy and the feasibility of the experiment, the optimum conditions of NA-TAG-loaded NLCs were determined as follows: aqueous surfactant concentration 3%, NA-TAG mix concentration 1%, and lipid phase to aqueous phase ratio 10:90. Therefore, the criteria which were selected for the optimization of NA-TAG NLCs was the minimum amount of oil and maximum amount of surfactant concentration, to achieve the maximum stability of NLCs.

Furthermore, the optimized NLCs were suitable for application in liquid food products due to their ultrasmall size and transparency among the lipid nanocarriers. All the produced nanocarriers have a high rate of EE%. The properties of optimized NA-TAG-loaded NLCs obtained by the hot high-shear homogenization and hot melt probe sonication technique, followed by recrystallisation were analyzed in **Table 11**.

The results (**Table 11**) indicated that the size of the NLCs prepared by the hot high-shear homogenization technique was 191.3 ± 3.28 nm, markedly greater than the size of the NLCs prepared by the sonication method, which was around 85.13 ± 0.43 nm ($p < 0.05$). Moreover, the NLCs prepared by recrystallisation was 82.11 ± 0.14 nm, slightly smaller than those obtained from the hot melt probe sonication method. Sonication can be used as a processing step in reducing droplet size to produce significant uniform particles (Lu et al., 2018). The ultrasonic method with mechanical stirring would reduce the energy consumption, and the emulsions obtained were more stable with smaller particle sizes (Babazadeh et al., 2017). In addition, the oil particle sizes could be reduced to less than 100 nm, to produce a transparent emulsion with optical clarity, suitabkle to be applied in beverages (Mirhosseini et al., 2008). Despite the significant disadvantages associated with high-energy in producing ultra-small nanoparticles, we could produce NLCs of < 100 nm using HPH by optimizing compositional and processing parameters (Aditya et al., 2014).

The physical stability of NLCs could be evaluated by measuring zeta potential. The zeta potential was usually used to determine the stability of the emulsion system. The particle dispersion became less stable when the zeta potential decreased (Loo et al., 2012). It was found that the particle size of the NLCs without sonication (Formulation H: GMS: Soybean oil: NA-TAG, 6:3:1) was dramatically shifted toward larger sizes with slightly increased zeta potential. The zeta potential of NLCs prepared without sonication was - 44.20 ± 1.35 mV, whereas the NLCs prepared with sonication slightly increased to - 46.9 ± 1.11 mV, indicating the particle dispersion was more stable.

The PDI was at 0.268 ± 0.01 ($p > 0.05$) for the NLCs prepared by probe sonication-based method, indicating good dispersion of uniformly sized lipid vesicles. After recrystallization, the optimized NLCs achieved the highest encapsulation efficiency (99.82%) ($p > 0.05$). Thus, the PDI and EE% show no significant differences among samples prepared from different methods.

Thus, the sonication and recrystallization steps effectively reduced the particle size and enhanced physical stability. The optimized NA-TAG NLCs have a smaller size, lower PDI, and relatively

higher zeta potential and encapsulation efficiency, indicating that this preparation method is suitable for encapsulating the optimized and purified NA-TAG oil.

Table 9. Results for NA-TAG loaded NLCs from lipid encapsulation using the L9 (3^3) orthogonal design with Tween 80 as surfactant

Formulation Code	Purified NA-TAG (%) A	Lipid phase to aqueous phase ratio(w/w%) B	Aqueous Surfactant Concentrations (%) C	Response variables				Phase State
				Entrapment efficiency (%)	Particle size (nm)	Polydispersity index	Zeta Potential (mV)	
1	1	10:90	1	98.5 ± 0.07	105.8 ± 0.71	0.266 ± 0.00	-55.2 ± 0.51	Liquid
2	1	15:85	2	97.5 ± 0.12	108.9 ± 1.36	0.280 ± 0.01	-59.2 ± 1.11	Liquid
3	1	20:80	3	98.9 ± 0.06	104.5 ± 0.72	0.289 ± 0.01	-58.1 ± 1.06	Liquid
4	1.5	10:90	2	94.4 ± 0.57	94.69 ± 0.29	0.256 ± 0.02	-48.1 ± 0.73	Liquid
5	1.5	15:85	3	96.7 ± 0.23	93.02 ± 0.46	0.288 ± 0.00	-57.8 ± 1.80	Liquid
6	1.5	20:80	1	96.6 ± 0.16	115.8 ± 0.93	0.248 ± 0.00	-58.4 ± 1.02	Semi-liquid lotion
7	2	10:90	3	98.5 ± 0.09	85.84 ± 0.34	0.278 ± 0.03	-42.7 ± 1.00	Liquid
8	2	15:85	1	96.8 ± 0.13	113.1 ± 1.12	0.266 ± 0.03	-60.4 ± 3.48	Liquid
9	2	20:80	2	94.8 ± 0.63	121.4 ± 0.59	0.258 ± 0.05	-59.9 ± 0.57	Semi-liquid lotion

Factors, A, NA-TAG concentration%; B, Lipid phase to aqueous phase ratio (w/w%) (10:90, 15:85 and 20:80); C, Aqueous Surfactant Concentrations (%).

Table 10. Range analysis and analysis of variance (ANOVA) of lipid encapsulation factors and levels from the orthogonal experiment.

	Entrapment encapsulation efficiency (%)			Particle size (nm)			Polydispersity index			Zeta Potential (mV)		
	A	B	C	A	B	C	A	B	C	A	B	C
k1	98.30	97.13	97.30	106.4	95.44	111.6	0.278	0.267	0.260	- 57.50	- 48.67	- 58.00
k2	95.90	97.00	95.57	101.2	105.0	108.3	0.264	0.278	0.265	- 54.77	- 59.13	- 55.73
k3	96.70	96.77	98.03	106.8	113.9	94.45	0.267	0.265	0.285	- 54.33	- 58.80	- 52.87
Best level	A1	B1	C3	A2	B1	C3	A2	B3	C1	A1	B2	C3
R	7.20	1.10	7.40	5.61	18.5	17.1	0.01	0.01	0.03	3.17	10.47	5.13
Order		CAB			BCA			CAB			BCA	
SS	8.960	0.207	9.627	58.97	511.2	495.9	0.0003	0.0003	0.0011	17.69	212.3	39.71
F value	43.35*	1.00	46.58*	1.00	8.67	8.41	1.12	1.00	3.53	1.00	12.01	2.25

Factors, A, NA-TAG mix%; B, Lipid phase to aqueous phase ratio (w/w%) (10:90, 15:85 and 20:80); C, Aqueous Surfactant Concentrations (%); Range analysis, k-averaged value of each level of the factors (k1, k2, k3 for level 1, 2, 3, respectively), the biggest k value indicates the best level for each factor; R, range between the maximum and minimum k value, a larger R value suggests a more important role of the factor in the encapsulation process; order, influential order of the factors, determined by the descending order of R value; SS, sum of squares; *F* value, obtained from ANOVA Fisher's *F*-test (2,2) 95% = 19; *, $p < 0.05$.

1

Table 11. Formulation and characterization of optimized NA-TAG-loaded NLCs under different preparation methods.

Formulation						Particle size (nm)	Polydispersity index[1]	Zeta potential (mV)	Entrapment efficiency (%)[1]
Code	GMS	Soybean Oil	NA-TAG	T80	DW				
Hot high-shear Homogenization method									
H	0.6	0.3	0.1	0.3	8.7	191.3 ± 3.28[a]	0.2887 ± 0.01	-44.20 ± 1.35[a]	97.79 ± 0.65
Hot melt probe Sonication method									
S	0.6	0.3	0.1	0.3	8.7	85.13 ± 0.43[b]	0.2680 ± 0.01	-46.90 ± 1.11[a]	98.28 ± 0.23
Recrystallization									
R	0.6	0.3	0.1	0.3	8.7	82.11 ± 0.14[b]	0.2623 ± 0.00	-50.47 ± 0.40[b]	99.82 ± 0.01

Values are presented as mean SD ± (n=3). Values within a row with different letters are significantly ($p < 0.05$).
[1] shows no significant differences among samples ($p > 0.05$). SD, Standard deviation; GMS, Glyceryl monostearate; T80, Tween 80; DW, Distilled water.

4.6. Freeze Drying of optimized NLCs and Their Properties

Formed powders are easier to handle, store and transport than the bulk liquid forms for further applications in food and pharmaceuticals (Nowak & Jakubczyk, 2020). Drying converts liquid to solid and is widely used in the food industry to transfer dehydrated emulsions to lipid particles. This method decreases the water content to a level that can inhibit the growth of microorganisms, extending the shelf life. Freeze-drying, also known as lyophilization, is an excellent method for storing nanoparticles since it preserves them from hydrolysis and Ostwald ripening while facilitating transport (Zhu et al., 2015). Lyophilization was hypothesized to have advantages for sensitive components because of its low temperature and vacuum condition during the drying process, and thus, retain the quality of the dried product in terms of biological safety, nutritional and organoleptic properties.

The lyophilization method aimed to produce good quality NLCs. The optimum conditions for freeze-drying emulsions were selected from the orthogonal optimisation experimental design. They were lyophilized to verify the suitability of our produced nanocarriers to use in the solid foodstuff. The physical properties of the lyophilized NLCs can be analyzed by differential scanning calorimeter (DSC) analysis. The interaction of the components in wall materials was investigated using Fourier transforms infrared (FT-IR) spectroscopy.

4.6.1 Differential Scanning Calorimetry (DSC)

Differential scanning calorimetry is widely used to provide information on the physical properties of a compound or formulation by detecting the heat loss or gain resulting from physical or chemical changes inside a sample (Averina et al., 2011). DSC provides qualitative and quantitative information on lipid particles' melting and crystallization behaviour, which may affect the bioavailability in the delivery system (Talebi et al., 2021). Due to a continuous crystallisation process, solid lipid nanoparticles formulated based solely on solid lipids or a blend of solid lipids have limited bioactive component loading and its release during storage. When the liquid lipids are incorporated into the solid lipids, the particles have a less crystalline structure (Shahparast et al., 2019). Furthermore, the advantages of NLCs over other traditional colloidal systems are essentially due to the liquid state of the lipid in the

nanoparticle system that improves the physical stability of the systems and the protection of the loaded drugs (Gonzalez-Mira et al., 2010). For these reasons, it is essential to conduct a DSC study to examine the thermal properties of the formulated NLCs in this research. **Fig. 15** shows the thermal behaviour of incorporated NA-TAG oil, an optimized formulation of NA-TAG nanostructured lipid carriers (NLCs), unloaded NLCs and the GMS at the temperature of 10 - 300 °C.

The NA-TAG oil exhibited an endothermic peak at 150.4 °C, when the NA-TAG oil fabricated into the NLCs, the melting peak reduced to 53.00 °C (**Fig. 15)**. Moreover, the characteristic peaks of NA-TAG oil completely disappeared in NLCs. A similar DSC study with the progesterone (PG)-loaded NLCs was reported (Elmowafy et al., 2018a). The absence of the main endothermic peak of PG confirmed the existence in the amorphous state, which enhanced PG solubility (Elmowafy et al., 2018a). Talebi and coworkers (2021) had similar results - the absence of a vitamin D3 melting peak and only one melting peak in the DSC curve of nano-niosomes containing vitamin D3. Similarly, the niosomes containing Candesartan showed that the Candesartan melting peak was absent from the DSC curves comparing to the loaded niosomes, indicating that the active drug was encapsulated inside the nanoparticles in an amorphous state (Sezgin-Bayindir et al., 2014).

Comparing the lyophilized NPs with or without NA-TAG (**Fig. 15**), the DSC thermograms indicated that the melting peak in the NLC without NA-TAG showed a slight shift from 53 °C to 52.09 °C. The incorporation of NA-TAG increased the enthalpy and the melting peak slightly (0.91 °C, 5.74 J/g, respectively, **Table 12**). This might be attribute to the physical interaction between NA-TAG structure and other NLCs compounds such as surfactants, the interactions may change their thermal properties. Similar interactions were reported for omega-3 fish oil/ α-tocopherol-loaded NLCs to improve the stability of the fish oil, where the peak melting point in the NLCs loaded without α-tocopherol showed a shift from 54.66°C to 53.02°C (Shahparast et al., 2019). In addition, the increased melting temperature of the NA-TAG-loaded NLCs could indicate an increase in crystallite size and order compared with the unloaded NLCs sample (Elmowafy et al., 2019) due to forming of a more imperfection crystal structure with the addition of NA-TAG oil.

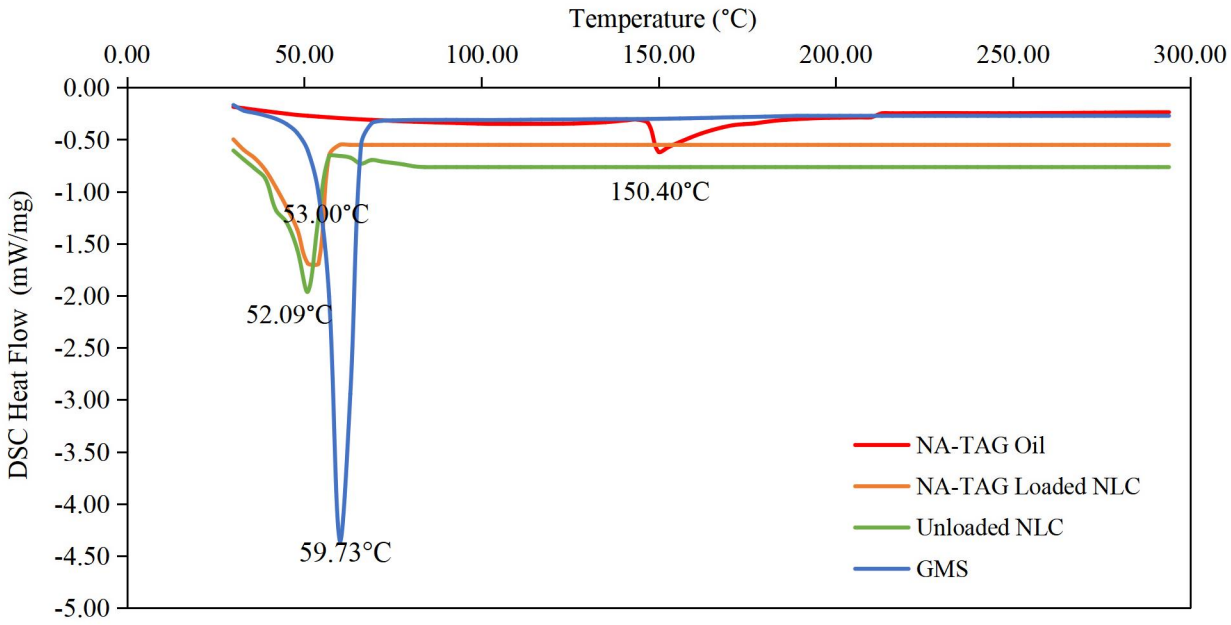

Figure 15. Differential scanning calorimetry thermogram of NA-TAG oil, NA-TAG nanostructured lipid carrier (NLCs), unloaded NLCs and the solid lipid GMS. GMS, Glyceryl monostearate; NA, Nervonic acid; TAG, triacylglycerol.

The melting behaviour of the lipid core in NLCs as measured by DSC was also useful in understanding the mixing state of GMS with the NA-TAG oil. From **Table 12**, GMS as a solid lipid has an onset temperature of 55.61 °C and a sharp endothermic peak at 59.73 °C indicating crystalline transition (Huang et al., 2017). When the GMS was formulated in the inner phase of the NA-TAG-loaded NLCs, the onset temperature and melting peak exhibited at 42 °C and 53 °C, respectively, lower than those of GMS. There was an almost 7°C drop in melting peak from that of GMS to NA-TAG-loaded NLCs. When solid lipid GMS was present in NLCs matrix, the lipid core surface contributed to this reduction in melting peak. Similar results reported a drop in the DSC melting temperature around 12 °C from GMS to when they were present in nanoparticles (Rai et al., 2021). Other similar dropping results also found that around 4 °C from the solid lipid Precirol ATO 5 to the NLCs formulations, which was potentially explained by the Precirol ATO 5 interaction or surface-active effect of NLCs (Elmowafy et al., 2019).

The width of the peak shoulders was measured by the difference between the onset temperature and melting point. From **Fig. 15** and **Table 12**, the peak shoulders of solid lipid GMS shifted to broader peaks in the NA-TAG-loaded NLCs, which have further confirmed

concurrent melting and consequent interaction between the NLCs lipid matrix. As a result of the presence of complex glycerides in NLCs, DSC thermograms usually exhibited broader peak shoulders (Elmowafy et al., 2019). Elmowafy and coworkers (2018a) reported similar findings when studying the effect of fatty alcohol containing NLCs for oral progesterone delivery, where they observed the shift into broader peaks comparing to the solid lipid stearic acid. A broader peak indicates massive crystal order disturbance (lattice defects) and forms less ordered of NLC structure. The less ordered structures in NLC may provide more space for drug/bioactive molecules, improving overall drug/bioactive loading capacity (Hu et al., 2006).

Table 12. Melting temperature and enthalpy of the NA-TAG oil, NA-TAG-loaded NLCs, unloaded NLCs and the solid lipid GMS.

Sample	Onset temperature (°C)	Melting Peak (°C)	Enthalpy ΔH (J/g)
NA-TAG Oil	148.4 ± 2.51	150.4 ± 3.51	20.55 ± 3.26
NA-TAG Loaded NLCs	42.00 ± 0.78	53.00 ± 0.07	81.78 ± 0.25
Unloaded NLCs	41.22 ± 0.07	52.09 ± 0.08	76.04 ± 0.14
GMS	55.61 ± 1.51	59.73 ± 0.79	172.8 ± 2.71

Values are presented as mean SD ± (n=3). SD, Standard deviation; GMS, Glyceryl monostearate; NLCs, nanostructured lipid carrier; TAG, Triacylglycerol; NA, Nervonic acid.

Since DSC is valid for studying the degrees of crystallinity of nanoparticles, this information could help explain the encapsulation efficiency as indicated by the other author (Rai et al., 2021). Moreover, a larger temperature differential indicates a greater lipid crystal disorder, and this leads to a maximum encapsulation efficiency (EE) for the NLCs (Shahparast et al., 2019). Furthermore, the peak depression of nanoparticles can also be correlated to the amount of added liquid lipid, as a higher concentration of liquid lipid would induce a broader solid lipid peak (Hu et al., 2006; Fang et al., 2013). The crystallinity degree of nanoparticles decreases with increasing liquid lipid ratio in the particles (Hu et al., 2006; Fang et al., 2013). Thus, the liquid oil was the main factor in lowering the crystallinity and enhancing the less-

ordered structure of NLCs, allowing for more spaces to encapsulate the drug/bioactive with high loading (Hu et al., 2006; Fang et al., 2013).

Thermodynamic parameters such as enthalpy and melting temperature are critical because they indicate the complexation and kinetics of active material release, and also potentially reflect the stability of the nanoliposomes during storage (Talebi et al., 2021). The degree of crystallinity of NLCs could be calculated from the ratio of NLCs enthalpy to bulk lipid enthalpy, which was calculated based on the total weight used (Fang et al., 2013). From **Table 12**, the reduction in melting enthalpy from 172.8 J/g in GMS to 81.78 J/g in the NA-TAG loaded NLCs could be associated with the deformity in the crystal structure of lipid. Similar findings were reported in a study involving the encapsulation of Omega-3 fish oil in NLC (Shahparast et al., 2019).

DSC provides an useful insight into the melting and recrystallization behaviour of the solid lipids from NLCs (Fang et al., 2013). The disappeared of the endothermic peak of NA-TAG oil in NA-TAG-loaded NLCs has confirmed that the NA-TAG oil was successfully encapsulated in NLCs lipid matrix. NLCs without NA-TAG oil showed a depression of the melting peaks from 53 °C to 52.09 °C. The results suggested that there was physical interaction between the NA-TAG oil and NLCs. The loading of NA-TAG in NLCs leads to crystal order disturbance, resulting in more space to include drug molecules in the applications. The results present the evidence that the components in the optimized NLCs have good compatibility with the NLCs lipid matrix and created a new composition with new thermal properties.

4.6.2 Fourier-Transform Infrared (FT-IR) Spectroscopy Analysis

Fourier transforms infrared (FT-IR) spectroscopy is an appropriate technique for determining the interaction between components and rheological properties in the nanocarrier structure (Hashemi et al., 2020). The FT-IR studies were carried out for the soybean oil, purified NA-TAG oil, solid lipid GMS, and the NLCs with and without NA-TAG to understand the possible chemical interactions between NA-TAG and other carrier components in the NLCs formulation.

The structural characteristics of the five samples were confirmed by FT-IR spectroscopy in the range of 400 to 4000 cm^{-1}, as shown in **Fig. 16** and **Table 13**. The characteristic peaks of soybean oil (line I) and NA-TAG oil (line II) were well captured and exhibited different IR bands. The peak at 3008.66 cm^{-1} for soybean oil and at 3006.73 cm^{-1} for NA-TAG oil were both attributed to =C-H stretching, which indicates the presence of unsaturated fatty acids in oils (Man & Rohman, 2013; Morris et al., 2021). The soybean oil was rich in the total unsaturated FAs at 83.76 %, while the NA-TAG oil was higher in unsaturated fatty acids at 90.42 % (**Table 7**). The bands at 2921.87 cm^{-1} and 2852.44 cm^{-1} were attributed to stretching vibrations of -CH groups. However, the two oils revealed some differences in peak intensities, which can be observed in the ester stretching region around 1700 - 1750 cm-1 and in carbonyl stretching 1085 - 1200 cm^{-1}. The soybean oil had only one peak during the region around 1700 – 1750 cm^{-1} at 1743.48 cm^{-1}; no bands were observed for soybean oil at 1708.00 cm^{-1}. Whereas NA-TAG oil revealed two peaks, one at 1745.41 cm^{-1} due to C=O stretching of the carboxylic acids (ester) with strong intensity, the other at 1708.00 cm^{-1} indicated the C=C with low weak intensity (Lumakso et al., 2015; Morris et al., 2021). This result might be attributed to the alkene (-C=C-) that came from the monounsaturated nervonic acid in the incorporated NA-TAG oil. The FT-IR distinguishes the two oil types and accounts for their structure difference.

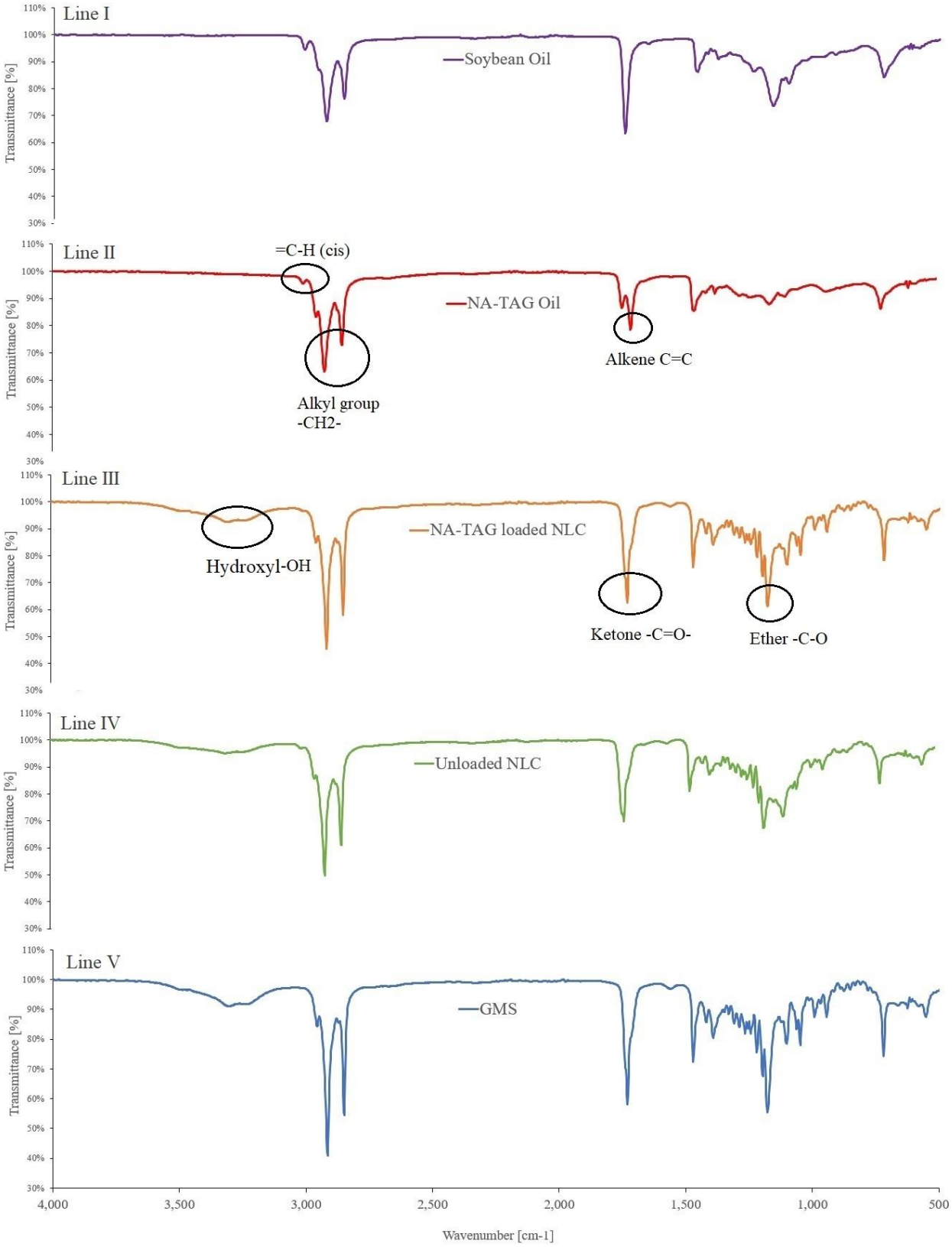

Figure 16. Fourier transform infrared (FTIR) spectroscopy of different materials. (I) soybean oil, (II) NA-TAG oil, (III) NA-TAG loaded NLCs, (IV) unloaded NLCs without NA-TAG, and (V) solid lipid GMS as surfactant in the NLCs.

Furthermore, the NA-TAG-loaded NLCs (line III) and unloaded NLCs (line IV) showed all characteristic peaks related to the functional groups (hydroxyl, methyl, ester) of NA-TAG oil. Similar results were also observed for the turmeric encapsulation in NLCs (Karimi et al., 2018). In addition, line III, IV and V showed strong hydroxy stretching at 3309.52 cm^{-1}, 3311.45 cm^{-1} and 3301.81 cm^{-1}, respectively. These O-H stretching confirmed a stable intermolecular hydrogen bonding (between NA-TAG oil and NLCs components. The hydrogen bondings enhance NA-TAG solubility in the NLCs formulation (Elmowafy et al., 2018a).

Table 13. The frequency ranges, vibration and absorptions of functional groups for soybean oil, NA-TAG oil, NA-TAG-loaded NLCs, unloaded NLCs and solid lipid GMS.

Common Name	Wavenumber (cm^{-1})					Structural Characteristics
	Soybean Oil	NA-TAG Oil	NA-TAG loaded NLCs	Blank NLCs	GMS	
Hydroxyl (-OH)	-	-	3309.52	3311.45	3301.81	Hydroxyl groups stretching
=C-H (cis)	3008.66	3006.73	-	-	-	= C-H (cis) stretching vibrations
Alkyl group $-CH_2-$	2923.80	2921.87	2914.85	2916.09	2914.15	Alkanes ($-CH_2-$) asymmetric stretching
Alkane CH_2	2852.44	2852.44	2848.58	2848.58	2848.58	C-H symmetrical stretching
Ketone (RCOR) -C=O-	1743.48	1745.41	1729.98	1729.98	1729.98	C=O stretching of carboxylic acids (esters), strong intensity
Alkene C=C (cis)	-	1708.00	-	-	-	C=C stretching vibrations, Weak intensity
Alkyl group $-CH_2-$	1458.04	1458.04	1469.61	1469.61	1469.61	Bending
Ether (-C-O-)	1159.11	1159.11	1178.39	1176.46	1178.39	C-O-C covalent stretching vibration, two bands or more
Group-CH-CH-	-	-	1101.24	1097.39	-	Bending and Deformation Vibrations
Alkyl group $-CH_2-$	719.38	721.31	719.38	719.38	719.38	CH_2 bending

According to the present results, FT-IR analysis showed no chemical bonding or interactions among the NA-TAG oil in the NLCs system; only physical interactions occurred. Other discussions on FT-IR analysis also confirm the current findings. Hashemi et al. (2020)

reported that CLA encapsulated in the NLCs system showed no chemical bonding. Karimi et al. (2018) stated that the production of NLCs-containing turmeric extract was compatible without the chemical reaction within the lipid matrix. Also, Pezeshki et al. (2019), in their study on the presence of beta-carotene in the NLCs system, demonstrated that there were no chemical reactions between the components of the system and the active ingredient. Similarly, no chemical reaction was observed between the lipid phase and resveratrol in the NLCs, according to the FT-IR results of Sun et al. (2014). Ghate et al. (2016) also reported that the FT-IR spectra indicated no interactions between tretinoin with the NLCs formulation excipients.

4.7. Storage Stability of Lyophilized NA-TAG-Loaded NLCs

For most commercial applications, emulsion-based delivery systems must maintain stability throughout their shelf life (Change & McClementsm, 2014; Puglia et al., 2014). The stability test ensures the product will maintain its desired chemical, physical and microbiological quality. Lyophilized powder is a freeze-dried powder. A short-term stability test was conducted for the lyophilized NA-TAG-loaded NLCs. Three storage temperatures were selected: at high temperature (45 °C), room temperature (25 °C) and refrigerator temperatures (4 °C). Factors affecting the shelf life of NLCs were determined to include the physicochemical properties of nanoparticles (i.e., particle size, polydispersity index, zeta potential), encapsulation efficiency, primary and secondary oxidative stability and water activity.

4.7.1 Physical Stability

Short-term physical stability is essential for NLCs during storage. Photon correlation spectroscopy (PCS) and laser diffraction are the most powerful methods for routine measurement of particle size. PCS is also known as dynamic light scattering yielding the particle size and the polydispersity index (PDI). It measures the fluctuation of the scattered light intensity produced by particle movement. As shown in **Fig. 17** to **19**, the particle size and PDI of liquid optimized NLCs at day 0 have a relatively small value compared to the powder form after lyophilization. Even though the nanocarrier size increased from 82.11 ± 0.14 to 252.5 ± 1.76 nm after freeze-dried, they were well within the required size to enhance bio-accessibility and bioavailability (Najjar & Stubenrauch, 2009). After lyophilisation, the PDI of the NLC slightly increased from 0.2623 to 0.39, indicating its ability to disperse uniformly (Aditya et al., 2014).

4.7.1.1 PS, PDI and Zeta Potential

The particle size of NLCs showed a gradual growth trend in the three storage temperatures. The particle size of the lipid carrier dispersions increased sharply when they were stored at 45 °C (**Fig. 17**). Only a slight increase to 328.1 ± 1.95 nm in particle size (PS) was observed when the sample was stored at 4 °C. At 25 °C, there was a negligible increase in particle size to 463.0 ± 2.13 nm. It seems that the NLCs were fit for storage at 25 °C and 4 °C as no signs

of instability in the form of phase separation or creaming and no significant change of PS ($p > 0.05$) were detected during the storage period. The results suggested that the NLCs containing NA-TAG were stable against Ostwald ripening, flocculation, and coalescence at room and refrigerated temperatures. The concentration gradient to the environment is minimised by a narrow particle size distribution, which inhibits the Ostwald ripening process (mass transfer from small particles to larger particles) (Tian et al., 2015; Hashemi et al., 2020; Talebi et al., 2021). However, due to the kinetic energy depression of nanoparticles at lower temperatures, NLCs stored at 4 °C were more stable than those stored at 25 °C.

In contrast, NLCs stored at high temperatures such as 45 °C showed a slower increase in particle size for the first 25 days or so. After that, the PS increased rapidly from 252.5 ± 1.76 to 1351 ± 10.76 nm at the end of 42 days' storage. These results suggested that some droplet growth occurred due to either coalescence or Ostwald ripening during storage (Change & McClementsm, 2014). Also, the structure of NLCs might be impaired, and bioactive entrapped were unstable (described later in **Section 4.7.2**). A similar stable trend of particle size was observed in other NLCs preparations stored at 4 or 25 °C (Wang et al., 2014; Soleimanian et al., 2018).

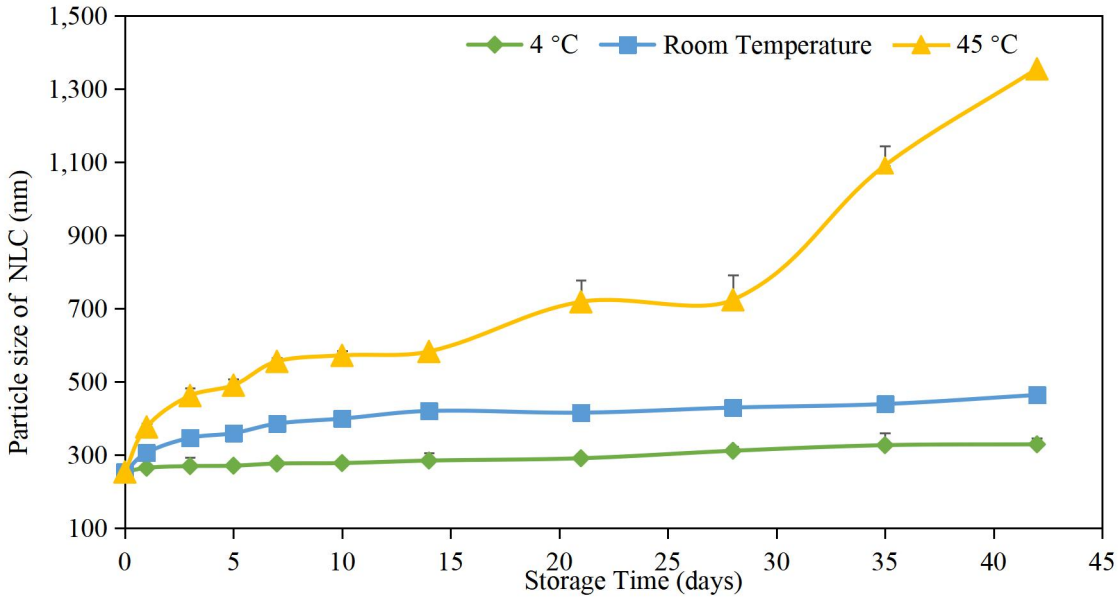

Figure 17. Changes of lyophilized NLCs in the particle size during storage at 4 °C, room temperature (25 °C) and 45 °C throughout 42 days of stability study. Experiments were performed in triplicate (n = 3).

The polydispersity index (PDI) was used to measure the broadness of molecular weight distribution. The PDI value provides a measure of particle size distribution, which ranges from 0 (monodisperse) to 1.0 (very broad distribution) (Azmi et al., 2020). The change of PDI values can be observed in **Fig. 18**, that all the temperatures indicated an increasing trend. However, the PDI value remained above 0.200, implying a relatively broad sample particle distribution (Azmi et al., 2022). On day 0, the PDI of NA-TAG NLCs remained at 0.39 (above 0.3), which indicates the poor physical stability of this colloidal system and relatively homogeneous nanocarriers among all the temperatures. These results would be in agreement with the zeta potential results.

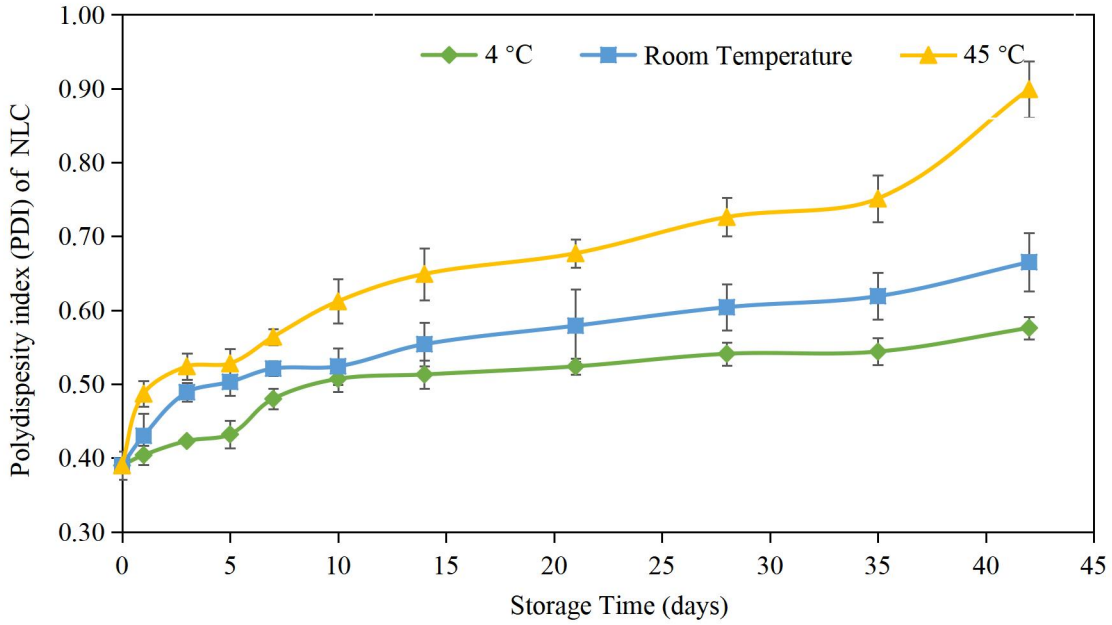

Figure 18. Changes of lyophilized NLCs in the polydispersity index during storage at 4 °C, room temperature (25 °C) and 45 °C throughout 42 days of stability study. Experiments were done in triplicate (n = 3).

The electrical charge on the droplets affects the functional performance and stability of emulsions. As shown in **Fig. 19**, the ζ-potential on NA-TAG NLCs did not change significantly (around - 50 mV) at refrigerator temperature (4 °C) for 6 weeks ($p > 0.05$). At low temperatures, the high stability of developed nanoparticles against particle aggregation could be related to their high zeta potential value (Soleimanian et al., 2018). The good stability could be attributed to the small particle size, the slow lipid transition, and the steric effect in the NLCs system (Sun et al., 2014; Azmi et al., 2022).

At storage of 25 °C and 45 °C for 42 days, the particle size and PDI were increased, and the absolute electrical charge was significantly decreased to - 41.6 and - 30.12 mV ($p < 0.05$), respectively. On the same storage day, samples at 4 °C and 25 °C did not show a significant difference ($p > 0.05$) during the storage time. The reduced electrical charge value was associated with physical instabilities such as agglomeration, aggregation, and gelation (Sun et al., 2014). Hence, these results indicate that electrostatic interaction could be one of the main factors determining the stability of the NA-TAG-loaded NLCs. In addition, storage at high temperatures can cause the breakdown of hydrogen bonds in surfactant, resulting in decreased NLCs stability at 25 °C and 45 °C.

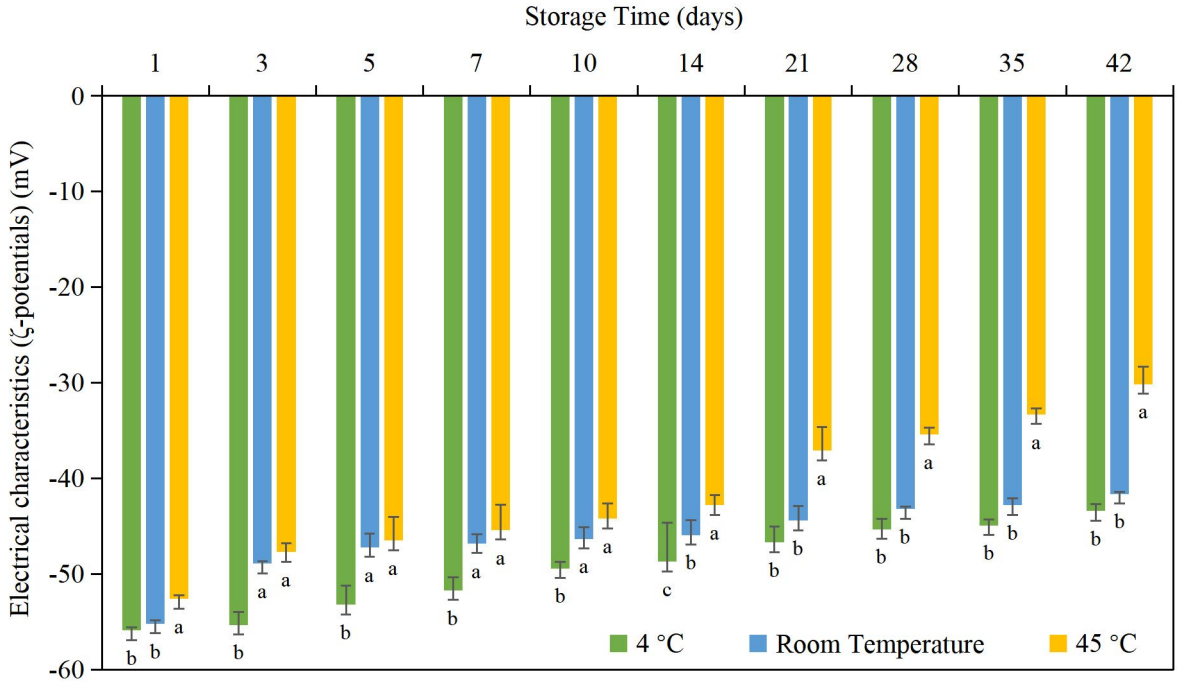

Figure 19. Changes of lyophilized NLCs in electrical characteristics during storage at 4 °C, 25 °C and 45 °C throughout 42 days of stability study. Experiments were done in triplicate (n = 3). Error bars represent the standard deviation. Different letters (a-c) indicate the significant difference between the different temperatures at the same storage day (one-way ANOVA, Tukey's HSD, $p < 0.05$).

4.7.1.2 Entrapment Efficiency of NA-TAG-loaded NLCs

From the results (**Table 14**), the ratio and concentration of 3% Tween 80 and 3% GMS in this experiment were adequate to stabilize the NLCs. The data showed that the NA-TAG loaded NLCs had high stability throughout the storage period. for storage at 4 °C, EE% decreased

from 95.89 to 91.96%. There was no substantial change in the attributes studied for 42 days storage. At 25 °C and 45 °C, the EE% was reduced to 90.22% and 81.24%, respectively. However, there is no significant difference in the EE% at different temperatures during the storage time ($p > 0.05$). The NLCs developed showed high EE% values irrespective of storage temperature and time. At the end of 42 days of storage, over 81% of NA-TAG remained in the NLCs stored at 45°C and ~ 90-92% at room and refrigerated temperatures, indicating that the fabricated NLCs effectively protected the loaded NA-TAG oil. Samples stored at 45 °C always had the lowest EE% among all the storage temperatures. In contrast, sample at 4 °C had the highest EE%. Given that the high temperature may disturb the structural molecules, a more logical explanation may be that at 45 °C, less ordered lattice defects will form with more space for molecules (Aditya et al., 2014). In an earlier study, a similar reduction in EE % was observed (Kumer et al., 2016). From **Table 14**, caking or clumping occurred during the storage of powders at 45 °C. Caking produces permanent clumps due to particle stickiness, resulting in a loss of functionality and lower quality (Bell & Labuza, 2000), reducing the product's shelf-life.

Overall, storage at 4 °C was favoured for enabling the good physicochemical stability of the lyophilized NLCs. It was concluded that higher temperatures increase the incidences of particle coalescence, leading to aggregation and more kinetic energy, and thus the rapid increase of particle size by accelerating the collision of particles (Talebi et al., 2021). During the study duration of 6 weeks, the developed nanocarriers were found to be substantially stable at 4 °C. Therefore, the refrigerated condition (4 °C) were considered the optimum storage conditions for lyophilized NLCs samples. Keeping the products at refrigerated temperature (4 °C) is suggested to prolong the encapsulated NLCs products' shelf-life. Good physical stability of lipid nanoparticles at 4 and 25 °C, with no significant modification in the particle size, was also found by other researchers (Li et al., 2015; Zhu et al., 2015; Soleimanian et al., 2018; Razak et al., 2018). There was also no noticeable change in the PDI, zeta potential and EE% of formulations during the storage period ($p > 0.05$) at refrigerated temperature, which was in agreement with results reported for other NLCs preparations (Wang et al., 2014; Zhu et al., 2015).

Table 14. The entrapment efficiency (%) of lyophilized NLCs for 42 days of storage trials.

Time (day)	4°C ± 1°C/ RH 60 ± 5%		25°C ± 2°C/ RH 60 ± 5%		45°C ± 1°C/ 75 ± 5%	
	Physical appearance	Entrapment efficiency ± SD (%)	Physical appearance	Entrapment efficiency ± SD (%)	Physical appearance	Entrapment efficiency ± SD (%)
0	White-fine powders with bright crystal throughout storage	95.89 ± 0.12^{c}	White-fine powders with bright crystal throughout storage	95.89 ± 0.12^{b}	White-fine powders with bright crystal initially; caking, clumping and aggregation occurred at the end of the storage	95.89 ± 0.12^{a}
1		95.56 ± 0.11^{c}		94.83 ± 0.03^{b}		94.22 ± 0.01^{a}
3		95.51 ± 0.16^{c}		94.62 ± 0.01^{b}		93.28 ± 0.34^{a}
5		95.23 ± 0.01^{c}		94.44 ± 0.42^{b}		92.15 ± 0.13^{a}
7		95.12 ± 0.22^{c}		94.36 ± 0.12^{b}		91.36 ± 0.28^{a}
10		94.83 ± 0.13^{c}		93.22 ± 0.56^{b}		90.23 ± 0.17^{a}
14		94.01 ± 0.32^{c}		93.01 ± 0.32^{b}		89.28 ± 0.63^{a}
21		93.89 ± 0.63^{c}		92.46 ± 0.62^{b}		87.94 ± 0.56^{a}
28		92.73 ± 0.56^{c}		91.25 ± 0.41^{b}		85.12 ± 0.45^{a}
35		92.41 ± 0.33^{c}		90.87 ± 0.51^{b}		83.89 ± 0.65^{a}
42		91.96 ± 0.65^{c}		90.22 ± 0.15^{b}		81.24 ± 0.71^{a}

Values are presented as mean SD ± (n=3). Values within a row with different letters are significantly (one-way ANOVA, Tukey's HSD, $p < 0.05$). Values within a column with same letters are insignificantly different ($p > 0.05$). RH: Relative humidity, SD: Standard deviation.

4.7.1.3 Water Activity (a_w)

Water activity is an important means of predicting and controlling the shelf-life of food products. It is crucial to determine critical water activity levels for a product and how sensitive it is to changes in water activity to ensure the microbiological safety of a product. This part of the study evaluated the lyophilized NA-TAG-loaded NLCs during storage at 4, 25 and 45 °C for 6 weeks.

As shown in **Fig. 20**, the initial a_w of the lyophilized NA-TAG loaded NLCs was 0.435, indicating the water in the product has 43.5% of the energy that pure water would have at day 0. The overall a_w in all temperatures was lower than 0.5, which suggested that microorganisms are not likely to have the potential growth for microbial spoilage (Wason et al., 2022). However, products in this range do not have an unlimited shelf life. Chemical degradation, textural alterations, and moisture migration are the most likely failure modes between a_w of 0.40 and 0.70 (Wason et al., 2022).

At refrigerated temperature (4 °C), the a_w was stable until the last day of the storage. However, for samples with low a_w between 0.20 and 0.40, texture alterations, caking, and clumping of powders are the most likely failure reasons in the deterioactive reactions (Wason et al., 2022). NLCs samples stored at 25 °C had a_w range of 0.364 to 0.227 from day 3 to day 21. At 45 °C, the NLCs had a_w ranged from 0.375 to 0.226 from day 1 to day 10. When the a_w was less than 0.2, the chemical instability characterized by a higher rancidity rate would be the major failure. The samples stored at 25°C had the a_w of 0.191 after day 28. At 45 °C, the sample's a_w was 0.197 after day 14. These changes in a_w values explained the caking and clumping of powders (Bell & Labuza, 2000). At 45 °C storage, the a_w of the NLCs significantly decreased at the end of 42 days compared to the samples stored at lower temperatures. This could be due to the loss of moisture at a higher temperature.

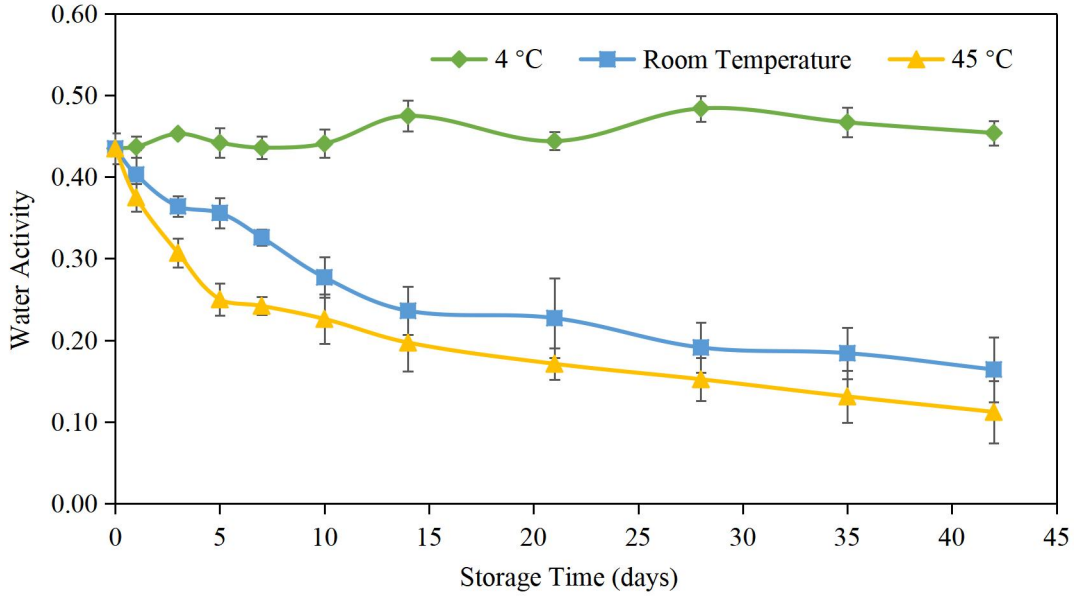

Figure 20. Water activity (a_w) of lyophilized NA-TAG loaded NLC stored at 4 °C, room temperature (25 °C) and 45 °C for 6 weeks. Data points and error bars represent means (n=3) ± standard deviations.

Changes in water activity influence both structure and texture of food products. To extend shelf life, any product must be manufactured to its ideal water activity during transport and storage.-Therefore, monitoring the influence of water activity and storage temperature on the freeze-dried NA-TAG-loaded NLCs will help design an effective thermal process control to ensure a better product shelf-life.

4.7.2 Chemical Stability

Lipid oxidation process involves a complex series of chemical reactions between fatty acids and oxygen, which results in oxidative degradation of lipids to produce off-flavours in the oil, such as rancidity (Tura et al., 2022). Thus, it is essential to ensure that the NLCs are of good quality during storage, as oxidative stability is essential in determining its use in food and pharmaceuticals. This section aimed to investigate the oxidative stability of NA-TAG-loaded NLCs during storage at 4 ºC, 25 ºC and 45 ºC for 6 weeks. The peroxide value (PV) and thiobarbituric acid value (TBA) were monitored during the storage.

4.7.2.1 Primary Lipid Oxidation Products

Peroxide value (PV) is an indication of primary oxidation and detection of the initial evidence of rancidity in unsaturated fat and oil deterioration. The results (**Fig. 21**) show that changes in primary oxidative extent in different temperatures of the loaded NA-TAG oil had a similar increasing trend during storage. At day 0, all the temperatures were insignificant ($p > 0.05$) and presented the lowest PV with 5.624 mEq/kg of oil, indicating high protection of oil oxidation in the NLCs system. The temperature was one of the most important factors influencing the product's quality during storage. Higher PV values would indicate a shorter shelf life and be unsuitable for consumption (Chew, 2020). Thus, to assure food safety and quality during storage, it was crucial to develop models to describe and predict the quality of the product in a wide range of temperatures (Kaczmarek & Muzolf-Panek, 2021).

The current results suggested that storage of NA-TAG loaded NLCs at 4 ºC and 25 ºC exhibited insignificantly differences in the change of peroxide values ($p > 0.05$), which indicated that these two temperatures have better inhibition against the formation of primary lipid oxidation products compared to 45 ºC. The peroxide value of NA-TAG-loaded NLCs at 4 ºC ranging from initial to 12.469 mEq/kg after 6 weeks. At 25 ºC, the peroxide value increased gradually to 14.003 mEq/kg. The oxidation process at 45 °C exhibited a significantly high peroxide value at 24.44 mEq/kg ($p < 0.05$), causing a decrease in oxidative stability. A high PV value could indicate the increased hydroperoxide radical formation or reduced decomposition (Gordon, 2004). Moreover, during the same storage day, PV for samples stored at 45 °C was significantly different to those stored at 25 and 4 °C ($p < 0.05$). Primary oxidative degradation can be accelerated at higher temperatures. Storage temperature at 45 °C promoted the primary oxidation to give higher PV values, which might be due to the unsaturated compounds in the NLCs formulation being susceptible to autoxidation at higher temperatures (Chandran et al., 2016). Hence, the NLCs produced should not be stored at 45 °C.

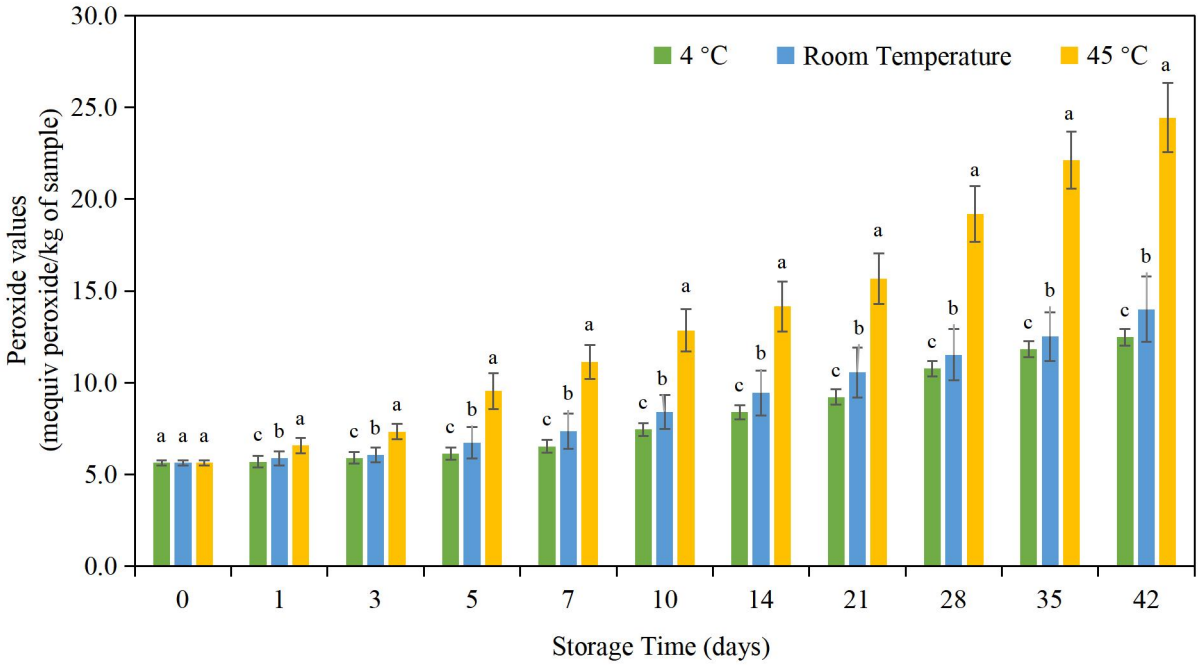

Figure 21. The peroxide value of lyophilized NLCs stored at 4 °C, room temperature (25 °C) and 45 °C for a period of 6 weeks. Error bars represent the standard deviation. Different letters (a-c) indicate the significant difference between the different temperatures at the same storage day (one-way ANOVA, Tukey's HSD, $p < 0.05$).

At 4 ºC, the PV steadily increased from an initial 5.624 to 9.209 mEq/kg during the storage time of 21 days. The PV had a steady increase indicating the formation of hydroperoxides during fat oxidation. At 25 °C, the PV gradually increased to 9.434 mEq/kg on day 14 while at 45 ºC, the PV significantly increased to 9.543 mEq/kg on day 5 ($p < 0.05$). Generally, the PV of fresh oil is less than 10 mEq/kg oil and this could be related to a chemically protective effect of the solid core of the nanoparticles that inhibited the oxygen from reaching the oil (Chew, 2020). The results agreed with the findings reporting the high oxidative stability of fish oil at high preparation temperatures (Soleimanian et al., 2018). If the PV was greater than 10 meq/kg, the oil was considered bad (Banks, 2007) and the product should be placed on quality hold pending comprehensive analysis and quality assessment before being directed to disposal (Liu & Wu, 2010). During the storage time of 35 days, the PV had reached 22.133 mEq/kg at 45 ºC. The rancid taste could be predictable with higher PV. According to the literature (Gordon, 2004), a rancid taste was usually noticeable when PV was between between 20 and 30 mEq/kg. The NLCs at 45 ºC with higher PV will have a shorter shelf life and be unsuitable for consumption.

Generally, high temperature will promote primary oxidation, which increases the PV. The inappropiate storage temperature would affect the quality of the NLCs. In addition, the oils with higher PV might have adverse health effects, such as stimulating cardiovascular and inflammatory diseases by increasing reactive oxygen species and secondary oxidation products (Chew, 2020).

4.7.2.2 Secondary Lipid Oxidation Products

Although the PV measurement was a helpful approach to monitoring the oxidative deterioration of fats and oils, it is usually combined with a method of secondary lipid oxidation products to provide more specific evaluation of lipid oxidation (Gordon, 2004). Reaction with thiobarbituric acid (TBA) has been one of the most extensively accepted assays for measuring the secondary products of lipid peroxidation in emulsions (Wang et al., 2015). The thiobarbituric reactive substances (TBARs) assay was used to monitor malondialdehyde (MDA), a marker of secondary oxidative products (Wang et al., 2015; Reitznerová et al., 2017). The objective of this section was to compare the methods of MDA detection in lyophilized NLCs in various storage time and temperature conditions.

As shown in **Fig. 22**, the initial content of TBARs was 1.034 ± 0.044 mol/kg oil ($p > 0.05$). The NLCs composition, such as the presence of solid lipid GMS, might affect the most effective oxidative stability at the initial storage. This shell might function as a physical barrier that prevents oxidation by restricting oxygen access (Shahparast et al., 2019). Materials with good emulsifying capacity could surround the core materials, providing superior oil oxidation protection in processing (Fäldt & Bergenståhl, 1994). During the storage time, the protective shell might be missing so that the oxygen could interact to a greater degree of TBARs content, such as higher MDA concentrations. Shahparast (2019) et al. generated the same results by encapsulating fish oil in the NLCs.

Furthermore, the MDA increased to 4.498 mol/kg after 42 days of incubation at 4 °C, which was insignificant ($p > 0.05$) for the change of MDA. The incorporation of NA-TAG oil at 4 °C in the dispersed lipid phase retards the lipid peroxidation via the mainly chain-breaking mechanism of NA-TAG targeting radicals formed inside the lipid core during lipid autoxidation. The formation of the antioxidant interface at lower temperatures appears to be a

promising strategy to preserve emulsified oil against oxidation rather than admixing antioxidants into the oil core (Wang et al., 2015). At 25 °C, it had been varied to 6.879 mol/kg ($p > 0.05$). The MDA content was increased to 7.826 mol/kg at 45 °C till the end of storage ($p < 0.05$). The higher values obtained with the TBA test have been attributed to several other lipid oxidation products, such as alkenes, alkadienals, aldehydes, and ketones, which would not be suitable for feed (Gordon, 2004). In addition, the changes of TABRs between the different temperatures at the same storage day were not as significant as those of PV. For example, at day 1, there was not a significant difference between 25 and 45 °C (**Fig. 27**). This suggests that the storage stability condition, NLCs had a more substantial influence on the generation of primary oxidation products measured by PV, than on the production of secondary oxidation products measured by TBARs. This result can be attributable to the protective shell created by encapsulation, inhibiting oxygen from reaching the lipid surface of NLCs (Shahparast et al., 2019).

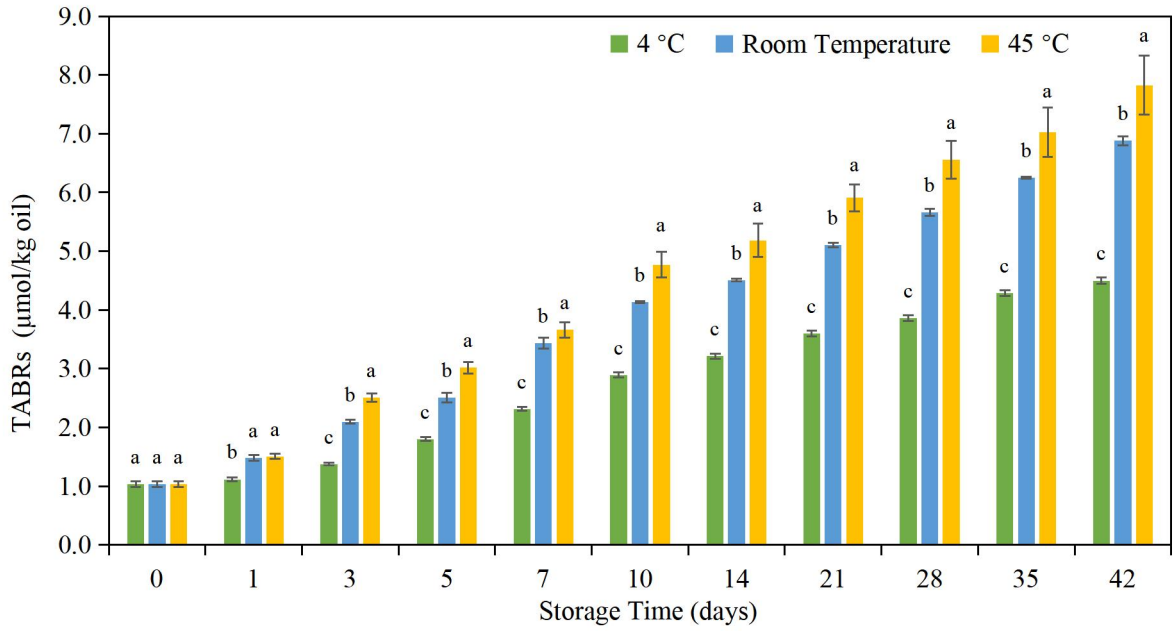

Figure 22. Formation of thiobarbituric acid reaction substances (TBARs) in lyophilized NLCs during storage at 4 °C, room temperature (25 °C) and 45 °C for 42 days. Data points represent means (n=3) ± standard deviations. Error bars represent the standard deviation. Different letters (a-c) indicate the significant difference between the different temperatures at the same storage day (one-way ANOVA, Tukey's HSD, $p < 0.05$).

The current results show that lipid oxidation accumulated significantly during a storage time of 42 days at the three storage temperatures under investigation. Again, the oxidation changes in the NLCs were lower at 4 ºC than the 25 °C and 45 ºC ($p < 0.05$). In addition, the PV and TBARs values were correlated with the storage period's length and temperature. The results indicated that encapsulation of NA-TAG oil in the NLCs reduced the primary oxidative products more effectively than the secondary products. Adding an antioxidant might prevent the increase in both primary and secondary products, which could be investigated in future studies. A study by Shahparast et al. (2019) had confirming this point. They reported that omega-3 fish oil encapsulated with an antioxidant, i.e., tocopherol, in NLCs has achieved good oxidative stability for the oil.

4.8. *In vitro* Digestion of Lyophilized NA-TAG-loaded NLCs

The digestion behaviour of the lyophilized NLCs was investigated using an *in vitro* model to simulate the stomach and the upper small intestine in a fasting state. This section expressed the extent of lipolysis obtained by titrating the fatty acids released as a percentage of total digestible fatty acids. In sequence, the lipolysis of core materials was conducted using either simulated gastric fluid (SGF) or simulated intestinal fluid (SIF). The objective of the experiment was to establish the application of the *in vitro* digestion model for characterizing the profiles of FFA release generated by the pH-stat method. In addition, we also wanted to use the *in vitro* digestion model to quantify the influence of lipid droplet characteristics on the rate and extent of digestion.

4.8.1 Physical Stability of NLCs

The physical stabilities of the NA-TAG NLCs were examined as they passed through the simulated GIT. The mean droplet size, particle size distributions (PSDs) and ζ-potentials of the emulsions were determined after each GI phase. It is known that the particle size and size distribution are critical characteristics for the evaluation of the physical stability of colloidal systems (Babazadeh et al., 2017).

Initial phase

Initially, the mean particle diameter and particle size distribution measured by light scattering remained relatively small (261.2 ± 7.02 nm, **Fig. 23**). The mean particle size was appreciably smaller for the NA-TAG loaded NLCs, which could be attributed to more efficient droplet disruption during homogenisation. It was suggested that NLCs could be stable to droplet aggregation at relatively high pH values (pH 6 and 7) but exhibited a significant increase in particle size when stored under more acidic conditions (pH 2.5) (Mao & McClements, 2012).

Gastric/Stomach phase

After passing through the stomach phase, the particle size distribution of the emulsions are maintained monomodal but the mean particle diameters increased slightly to 290.37 ± 6.89 nm (**Fig. 23**). These results suggest that some droplet aggregation or flocculation occurred within the gastric fluids.

Moreover, several reasons might have contributed to the aggregation under gastric conditions. Firstly, the combined effects of various SGF constituents, such as pepsin, could be attributed to droplet aggregation during the gastric stage (Mao & McClements, 2012). The pepsin would induce a reduced steric and electrostatic repulsion, which contributed to the aggregation effect (Liang et al., 2018). Secondly, the increasing particle size suggested that coalescence and aggregation phenomena occurred when the pH was reduced from 7 to 2.5 in the gastric stage. These findings suggest that incubating the emulsions within the highly acidic environment of the stomach might destabilize the lipid carriers and not break down the aggregates formed in the initial stage, which may even have encouraged further droplet aggregation as a consequence of attractive forces, such as Van der Waals and hydrophobic interactions (Choi et al., 2011; Rao et al., 2013; Cirri et al., 2018). As shown in **Fig. 23**, the particle size distributions (PSDs) of the emulsions stored at pH 7 did not change appreciably and maintained a single narrow peak centred with a growth of the broad size-distribution tails skewed toward large particle size. The broadening for the emulsions stored at pH 2.5 in the stomach phase suggested that these emulsions were highly unstable to droplet growth and likely caused coalescence formation (Anarjan et al., 2011). The oil molecules diffusing from small to large droplets cause droplet development (Tian et al., 2015; Change & McClementsm, 2014). Thus, the PSD data indicated an increased fraction of larger particles in those samples that aggregated.

The small intestine phase

At the end of the gastric digestion phase, the pH of samples were adjusted to neutral to mimic the small intestine. The presence of pancreatic lipases at pH 7.0 helped to hydrolyse the triacylglycerol molecules (Singh et al., 2009).

At this stage, the NA-TAG-loaded emulsions contained larger particles, giving a mean droplet size of 300.4 ± 2.32 nm (**Fig. 23**). The large particles observed might be attributed to the lipid carriers that were not fully digested by the intestinal enzymes that formed mixed micelles composed of lipid degradation products (Aditya et al., 2014). Moreover, increasing droplet coalescence and flocculation might have taken place to form larger particles. Any sedimentation or flocculation brought on by lipid disintegration in the stomach may delay the delivery of nutrients to the small intestine, reducing satiety and increasing food intake. The lipid droplet size impacted stomach motility and the release of gut hormones, which might contribute to obesity (Li & McClements, 2010; Aditya et al., 2014; Zhang et al., 2015). Furthermore, some droplet coalescence may occur throughout the lipid digestion process due to alterations in the composition of the interfacial or oil phase, resulting in an overall increase in oil droplet size. The NA-TAG molecules present within the oil droplets might be converted into long-chain free fatty acids due to the hydrolysis by pancreatic lipase. Long-chain FFAs are known to accumulate at the surfaces of lipid droplets during lipid digestion (Rao et al., 2013).

On the other hand, the PSDs of the emulsions changed from monomodal under the stomach digestion phase to a broad and bimodal distribution in the small intestinal phase (**Fig. 23**). This suggested that more bigger particles presenting in the small intestine stage, presumably due to the action of the digestive enzymes. As the digestion products that leave the lipid phase might be assembled into other types of colloidal structures, such as mixed micelles (tiny), vesicles (large), insoluble calcium salts (large), undigested protein aggregates or undigested lipid droplets in the small intestine stage. The similar result had been reported by Rao et al., (2013) and Wang et al., (2019). It is challenging to ascertain their precise nature in such a compositionally complex system (Zhang et al., 2015; Wang et al., 2019).

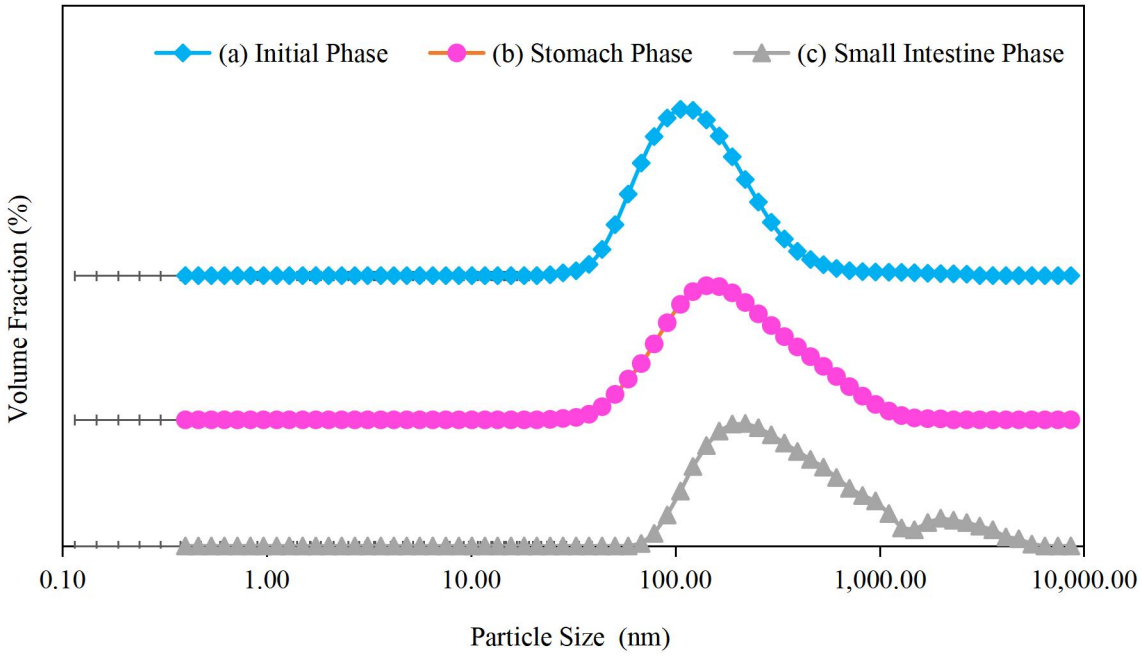

Figure 23. Influence of *in vitro* digestion on the particle size distribution of NA-TAG loaded NLCs emulsions as they passed through different regions of a simulated GIT: (a) initial; (b) stomach; (c) small intestine.

In general, the initial and stomachs play a small role in this digestive process, as the enzymatic digestion of lipids primarily occurs within the small intestine. The above results suggest that the particle size within the human GI tract was important because it might have an influence on the rate and extent of lipid digestion.

4.8.2 Surface Charge Characterization

The changes in the electrical charge characteristics of the particles in the emulsions were measured as they passed through the different stages of the GIT model to provide information about alterations in the droplets' interfacial properties (Hur et al., 2009; Zhang et al., 2015).

Initial phase

The stability and interactions of the droplet surface charges with other components are determined by their magnitude (Liang et al., 2018). We measured the electrical charges at the

surface of the lipid droplets before and after passage through the simulated GIT model. As shown in **Fig. 24**, the initial phase had relatively high negative charges at -50.2 mV. The electrical charge on the lipid droplets might be attributed to the emulsions stabilized by the nature of the surfactant tween 80 that had absorbed into the oil droplet surfaces (Rao et al., 2013; Liang et al., 2018). Thus, the initial electrical charges of tween 80-stabilized emulsions containing different droplet sizes showed relatively high negative charges. Several studies have found that lipid droplets stabilized by Tween 80 are negatively charged at neutral pH (Hur et al., 2009).

Gastric/Stomach phase

After exposure to the stomach region, there was an appreciable reduction in the magnitude of the electrical charge on the particles to -11.7 ± 3.39 mV (**Fig. 24**). The observed change in electrical charge on the droplets within the stomach mimics the highly acidic conditions at pH 2 and high ionic strength, which would change the droplets' electrical characteristics (Hur et al., 200; Mao & McClements, 2012). The relative low magnitudes of the electrical charges on the lipid droplets would be insufficient to create strong electrostatic repulsion between them, which would then contribute to the instability of the emulsions under acidic conditions and partly explain the fact that extensive droplet aggregation occurred (Choi et al., 2011; Liang et al., 2018).

Moreover, the NaCl, as the salt ions present in the SGF can cause electrostatic interactions or bind to droplet surfaces causing charge neutralisation or bridging effects. Thus, salt ions promote droplet flocculation in digestion emulsions (Mao & McClements, 2012). In addition, SGF contained pepsin, an enzyme capable of catalyzing the hydrolysis of proteins under acidic conditions. A similar study explored the gastric digestibility of an O/W emulsion stabilized by a globular protein (β-lactoglobulin) (Singh et al., 2009). However, in some studies, the surface potentials of the samples were slightly positive after passing to the stomach stage. The positive ζ-potential would be expected at +0.9 mV as the pH of the acidic gastric fluid (pH 2.5) was fairly below the isoelectric points (Liang et al., 2018).

The small intestine phase

The electrical charge at -28.77 mV on the particles after incubation in the small intestine phase was much higher than after the gastric stage but still lower than the initial stages. The observed change in electrical charge on the lipid droplets can be attributed to similar factors as mentioned earlier: changes in solution conditions (pH and ionic strength). Generally, the emulsion with a zeta potential > 30 mV is physically stable (Huang et al., 2017). Although the zeta-potential charges in the stomach are less than 30 mV, they are still above the required zeta potential to stabilize the nanoparticles by electrostatic and steric interactions (Aditya et al., 2014). In this study, steric stability is reported to be provided by surfactant Tween 80 (Kumar et al., 2016).

Furthermore, the high negative charge in the small intestine stage might be attributed to the presence of impurities after digestion. For instance, anionic or cationic impurities in the lipid phase could adsorb to the oil-water interface and contribute to the overall interfacial charge, including bile salts, undigested lipid droplets, mixed micelles, vesicles, and calcium salts, free fatty acids produced by hydrolysis (Mao & McClements, 2012; Rao et al., 2013; Zhang et al., 2015; Liang et al., 2018). These anionic colloidal species might have come from the initial phase (e.g., peptides, free fatty acids, or phospholipids) or the gastrointestinal fluids (e.g., bile salts and phospholipids) (Mao & McClements, 2012; Zhang et al., 2015). It would be predicted to reduce the strength of the electrostatic repulsion between the oil droplets, thereby promoting aggregation (McClements, 2004). Several other studies have found a change in negative charge in the particles present in the digestion after incubation in simulated small intestine conditions (Hur et al., 2009; Li & McClements, 2010; Mao & McClements, 2012; Rao et al., 2013; Zhang et al., 2015; Liang et al., 2018; Santos et al., 2019; Wang et al., 2019).

Due to electrostatic screening and ion binding effects, the bile salts in SIF would decrease the ζ -potential on the droplets (McClements, 2004). Consequently, the hydrolysis of lipids is enhanced. This could decrease the rate of digestion since bile salts are required to solubilise lipid digestion products for continuous lipase activity (Beysseriat et al., 2006).

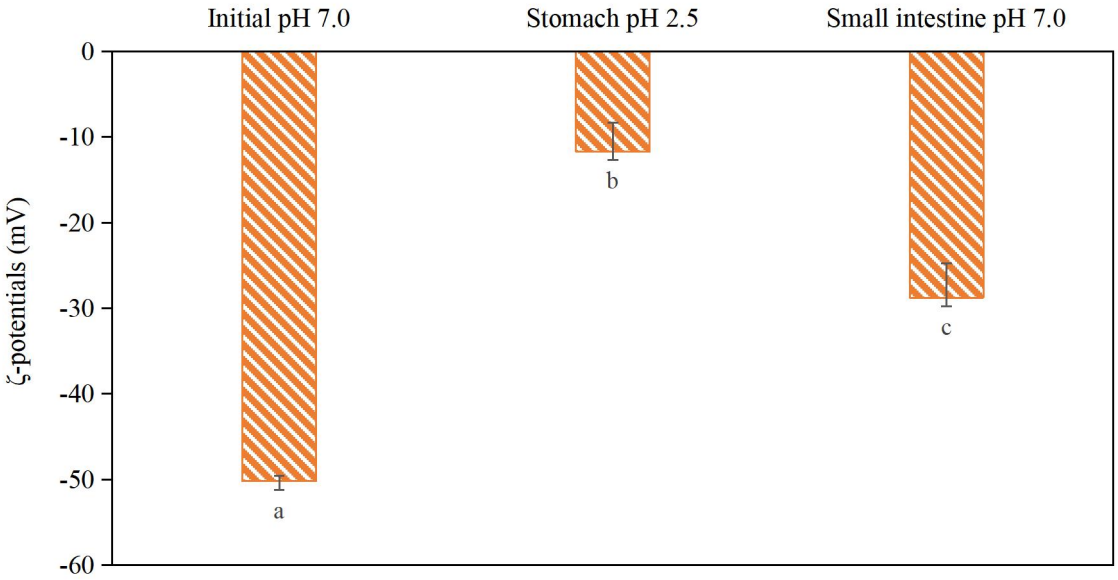

Figure 24. Influence of *in vitro* digestion on the droplet surface charge characteristics (ζ-potentials) of NA-TAG-loaded NLCs emulsions at different GIT stages. Error bars represent standard deviation. Bars represent the standard deviation. Different letters (a-c) indicate the significant difference between the different phase (one-way ANOVA, Tukey's HSD, $p < 0.05$).

4.8.3 Lipid Digestion

It is well-known that pancreatic lipases will produce free fatty acids (FFA) during the lipid hydrolysis of the droplet core in the small intestine. After the emulsions were subjected to simulated digestion, the rate and extent of lipid digestion was examined using an automatic titration ("pH-state") method. The volume of NaOH (0.1 M) titrated into the samples to maintain a constant pH (7.0) was measured as a function of digestion time (120 min) during the small intestine stage (**Fig. 25**).

As described previously (**Section 3.11.1**), the amount of free fatty acids released was calculated from the titration curves (Li & McClements, 2010). The release profiles of NA-TAG from the NLCs formulation were compared with NA-TAG oil as a control. The amount of FFA released from the NA-TAG structure lipid over time was then calculated from these profiles (**Fig. 25**).

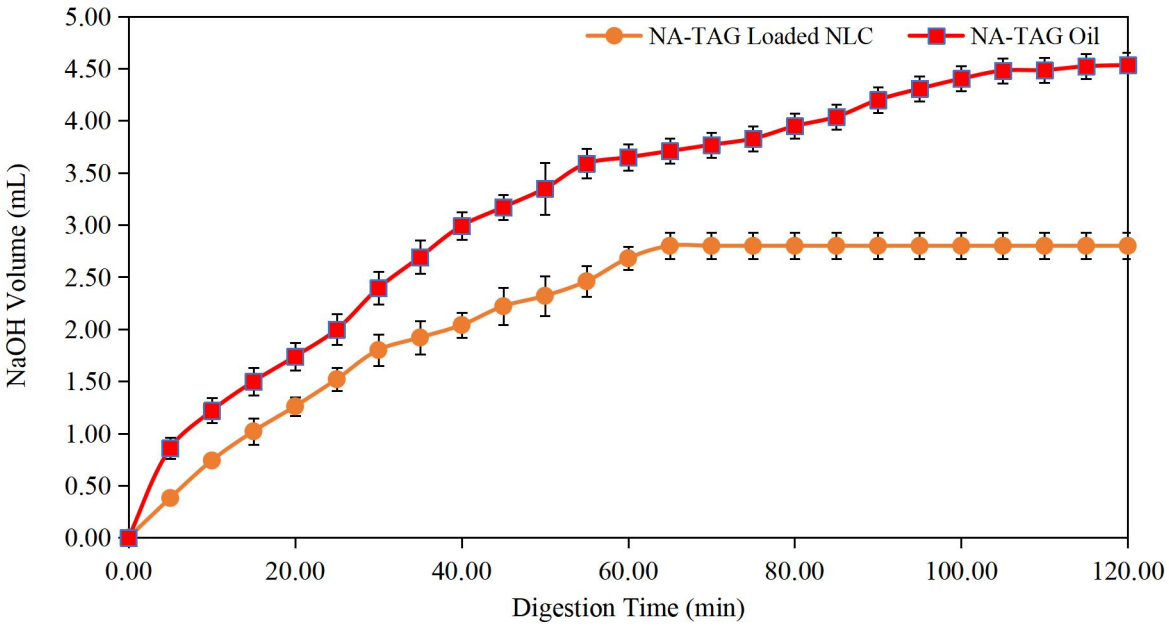

Figure 25. The volume of NaOH (0.1 M) required to maintain a constant pH (7.00) in the NA-TAG-loaded NLCs emulsions after passing through different GIT stages as measured using a pH-stat. Data points and error bars represent means (n=3) ± standard deviations.

From **Fig. 26**, the purified NA-TAG oil exhibited a fast release pattern with approximately 70% release amount of FFA dissolved during the duration of 2 h. On the other hand, NLCs containing NA-TAG showed a sustained release property with a slower release rate. In the initial stage, approximately 30 % of FFA was released in the first 40 min of the digestion. The NA-TAG near the surface of NLCs could be quickly released into the surrounding liquid, accounting for the initial burst release (Sun et al., 2014). In some of these systems, the addition of bile salts can remove the surface-active components from the emulsion droplet surfaces, promoting lipase binding to the interfacial layer and accelerating the lipolysis rate through the removal of FFA digestion products from the droplet surface rapidly by solubilization in mixed micelles (Singh et al., 2009; Hur et al., 2009; Li & McClements, 2010). In addition, unentrapped NA-TAG might be present in the NLCs dispersion, which could also lead to the initial burst release (Azmi et al., 2020).

Furthermore, around 32 to 46 % of FFA have a sustained release at a longer time of 60 min. *In vitro* slow diffusion of encapsulated NA-TAG in the hydrophobic core of NLCs might partially result in sustained release of NA-TAG in the later phase (Liu & Wu, 2010; Sun et al., 2014). This might be due to the *in vitro* release of the active component from the NLCs dispersion being biphasic, with the first burst action followed by a steady release of the active ingredient (Mishra et al., 2010; Huang et al., 2015). These findings suggested that the unique structure of NA-TAG might regulate the release of free fatty acids and maintain a relatively steady amount throughout a prolonged digestion time. A similar release trend with the *in vitro* release study of virgin coconut oil based NLCs loaded with *ficus deltoidea* (FD) extract was reported by Azmi et al. (2020). Another study (Kumer et al., 2016) also observed a similar *in vitro* release pattern for quercetin from NLCs.

Overall, the FFA release from NLCs was retarded, containing a substantial surface area to which a part of NA-TAG might be dissolved in the liquid shell composed of surfactants, and the remaining parts of NA-TAG might be located in the skeletal structure (Sun et al., 2014; Huang et al., 2017). A relatively constant final value of 46.8% of FFA released was attained. The lower FFA% released in NLCs compared to NA-TAG oil might be attributed to the fact that the digestion products of emulsions (long chain FFAs) tend to accumulate at the oil-water interface, thereby limiting the lipase access to the droplet surfaces (Zhang et al., 2015). Similar results were obtained in β-carotene emulsions using a simulated gastrointestinal tract model (Rao et al., 2013). Moreover, there are several possible reasons for this. Firstly, it is likely that some digestion of the NA-TAGs had already occurred within the stomach before entering the small intestine, or it could have been because the presence of long-chain fatty acids at the droplet surfaces inhibited lipid surface hydrolysis (Porter et al., 2007). Secondly, the low fatty acid released might also be attributed to the small intestine colloidal particle structure that may have been resistant to digestion. In addition, in the NLCs system, the NA-TAG molecules were surrounded by soybean oil molecules, which might prevent the lipase from reaching the ester bonds in the NA-TAGs. In a similar study by Rao (2013) et al., lemon oil inhibited TAG digestion in the lipid phase.

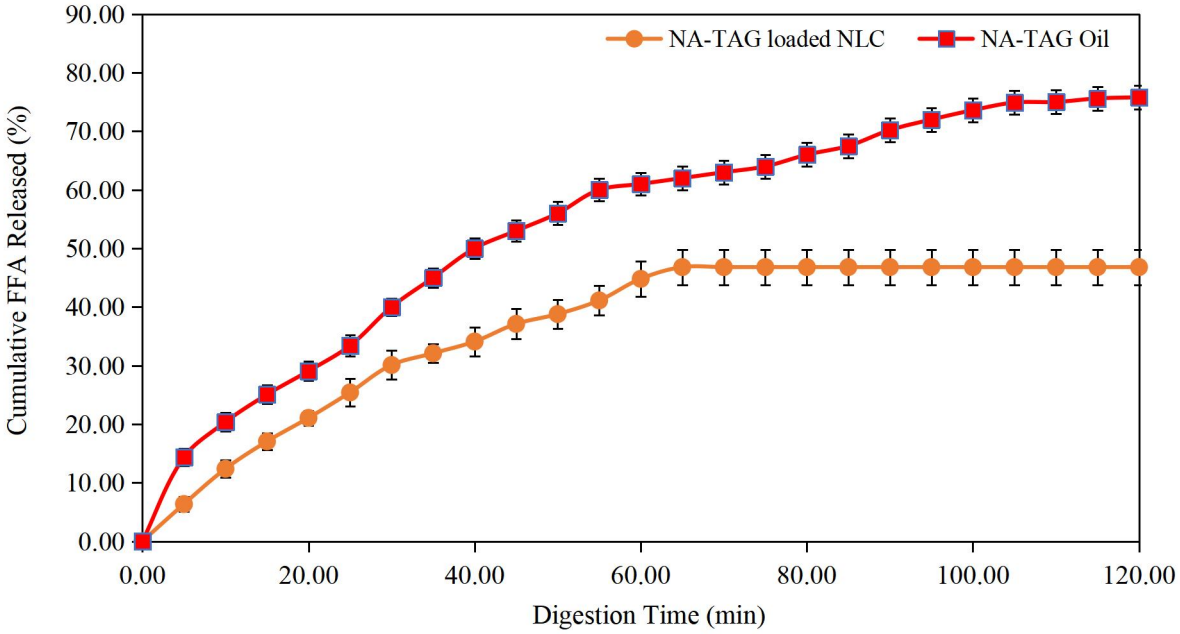

Figure 26. The cumulative fatty acids released profile from the NA-TAG-loaded NLCs compared to the NA-TAG oil (n=3) after passing through different GIT stages as measured using a pH-stat. Data points and error bars represent means (n=3) ± standard deviations.

Chapter Five

Summary, Conlcusion and Future work

5.1. Summary

This is the first study investigating the synthesis of triacylglycerol and nervonic acid via acidolysis reaction and its optimization. Furthermore, the physicochemical properties of NA-TAG-loaded NLCs were characterized to understand their influences on the formation and stability, followed by an in vitro digestion to provide information on the release characteristics of NA from the NLCs. The following summarises the research of different sections and drawn conclusions based on the data obtained.

- Enzymatic acidolysis reaction to obtain optimized NA-TAG oil

Lipozyme TL IM immobead 150 from *Rhizomucor miehei* offered the highest catalytic efficiency, specificity and selectivity than the other four immobilized lipases under the same optimal conditions. The lipase successfully catalyzed the incorporation of nervonic acid into the specific *sn*-1 and *sn*-3 positions of TAG. The modified TAG with nervonic acid is named NA-TAG oil in this study.

The acidolysis reaction was optimized according to an orthogonal experimental design to obtain the maximum incorporation of NA into TAG. The following are optimum conditions for the maximum incorporation of NA into TAG: enzyme type, Lipozyme TL IM immobead 150; enzyme-to-substrate ratio, 1:4; enzyme loading, 10 w/w%; reaction temperature, 60 °C; and reaction time, 4 hours.

- Separation of purified NA-TAG oil by Column Chromatography

The recovery of purified structured lipid was performed by column chromatography. After chromatographic separation, the lipid factions were identified by TLC plates consisting of silica gel. The TLC developed showed TAG, FFA, DAG and MAG bands after acidolysis, confirming that NA was successfully incorporated into the TAG molecules to release FA from the glycerol backbone. The TLC plates also showed the presence of a certain number of purified NA-TAG, which were collected for Fatty acid composition and further NLCs study.

- Fatty acid composition

The fatty acid composition analysis showed that the purified NA-TAG oil constituted 65.57 ± 0.99 w/w% NA after the optimized acidolysis reaction. The faty acid composition of the soybean oil and the purified NA-TAG oil samples were deternined. Comparing to the soybean oil and NA-TAG oil, the total saturated fatty acids (SFA) decreased from 16.24 to 9.583 w/w%, while the total unsaturated fatty acid increased from 83.76 to 90.42 w/w%. Among the unsaturated FA, the monounsaturated fatty acid (MUFA) in the purified NA-TAG oil increased from 22.21 to 72.69 w/w% as the nervonic acid was incorporated and constituted the majority of MUFA, but the polyunsaturated fatty acid (PUFA) reduced from 61.55 to 17.73 w/w%.

- Preparation of optimized NA-TAG-loaded NLCs

NLCs have been successfully produced from the hot high-shear homogenization followed by the hot melt probe sonication method. Based on the preliminary experimental data, Tween 80 was chosen as the surfactant, and the solid to liquid lipid ratio selected was 2:1. Then, the formulation was optimized using a L9 orthogonal design to obtain NLCs with the highest NA incorporation, examining the effects on particle size, polydispersity index, zeta potential and entrapment efficiency. The best formulation was determined as follows: aqueous surfactant concentration of 3%, NA-TAG concentration of 1%, and lipid phase to aqueous phase ratio of 10:90. In addition, during the preparation of NLCs, the sonication and recrystallization methods are necessary as it was significantly decreased the particle size and enhanced the physical stability.

- Preparation of lyophilized NLCs and evaluation of their properties

The lyophilized NLCs was obtained via freeze-drying. The lyophilized NLC's physical property was studied using differential scanning calorimetry (DSC), while Fourier examined the interaction of the NLCs components transforms infrared spectroscopy (FT-IR). From DSC, the characteristic peaks of purified NA-TAG oil completely disappeared when NA-TAG oil was fabricated in the NLC formulations, indicating that the molecule of NA-TAG was encapsulated. The NA-TAG oil has good compatibility with the matrix of NLCs. The loading of NA-TAG oil in NLCs causes crystal order disturbance, resulting in more space for the incursion of bioactive molecules. FT-IR demonstrated that the NA-TAG oil has a different chemical structure from the soybean oil, as reflected by the alkene group (-C=C-) from the monounsaturated nervonic acid incorporated in the NA-TAG oil. Only physical interaction was observed, and no chemical bonding between NA-TAG oil and the NLCs components formed.

- Storage stability of lyophilized NLCs

The storage short-term stability test was carried out for 6 weeks at high temperatures (45 °C), room temperature (25 °C) and refrigerator temperatures (4 °C). Higher temperature storage at 45 °C would significantly damage the physical stability of the NLCs system ($p < 0.05$), as indicated by the dramatic increase of particle size from 252.5 ± 1.76 to 1351 ± 10.76 nm at the end of the storage. This might be due to some droplet growth during the storage. Similarly, the PDI of lyophilized NLCs indicated poor physical stability (above 0.70). The ζ-potential was reduced to -30.12 mV which was associated with the aggregation. Moreover, the entrapment efficiency of lyophilized NLCs did not show significantly difference among the temperature during the six weeks storage time ($p > 0.05$). Over 81% of NA-TAG remained in the NLCs stored at 45 °C and ~ 90-92% at room and refrigerated temperatures, indicating that the fabricated NLCs effectively protected the loaded NA-TAG oil. At 45 °C, caking or clumping of the lyophilized powders occurred at the end of storage time, which might lead to a loss of functionality and lower the quality. For chemical stability, the peroxide value increased significantly to 24.44 mEq/kg ($p < 0.05$), while the MDA content significantly increased to 7.826 mol/kg ($p < 0.05$) at 45 °C. On the other hand, storage at 4 °C and 25 °C showed better inhibition against the formation of primary and secondary lipid oxidation

products. The water activity of the NLCs was stable at around 0.40. Hence, the refrigerated conditions (4 °C) were considered the optimum storage conditions for lyophilized NLCs samples.

- *In vitro* digestion of lyophilized NLCs

At the initial phase, the particle size was 261.2 ± 7.02 nm, and the electrical charge was relatively high at -50.2 mV. After passing through the stomach phase, the particle size increased to 290.37 ± 6.89 nm and the electrical charge was reduced to -11.7 mV. In the small intestine phase, the emulsions contained larger particles at 300.4 ± 2.32 nm, and the electrical charge was at -28.77 mV. The particle size distribution of the emulsions changed from monomodal under the stomach phase to broad and bimodal under the small intestinal phase. The particle size of the samples increased after exposure to simulated GIT conditions, which was attributed to droplet aggregation. The electrical properties of the particles in the sample changed through the GIT, which was attributed to pH changes and formation of other types of colloidal particles (such as mixed micelles).

Moreover, the purified NA-TAG oil exhibited a fast release at approximately 70% of FFA in lipid digestion. In contrast, the NA-TAG-loaded NLCs exhibited a slower release pattern. Initially, around 30% of the FFA had been released quickly. After that, a sustained and steadily release of FFA was observed, which might be due to the slow diffusion of encapsulated NA-TAG in the hydrophobic core of NLCs. At the end of the digestion at 65 mins, 46% of FFA was released and remained constant. The results suggested that entrapped NA-TAG oil in NLCs changed the FFA release behaviour, which can further influence the cellular uptake and its bioactivities.

5.2. Conclusion

To conclude, the current study has provided scientific data for a comprehensive understanding of the synthesis and modification of structured lipid (NA-TAG oil) using the immobilize lipase Lipozyme TL IM immobead 150 as the enzymes. The NA-TAG oil was entrapped into nanostructured lipid carriers (NLCs) derived from oil/water (O/W) emulsions. This study leads to the following significant findings:

A new modified fat or structure lipid (i.e., NA-TAG oil) was produced for the first time, and the fatty acid composition was analyzed by gas chromatography. An orthogonal optimization design was applied by considering the reaction conditions during the lipase-catalyzed acidolysis reaction and successfully achieved the highest NA incorporation at 65.57 ± 0.99 w/w% in the structure lipid.

This study successfully entrapped the NA-TAG oil in the nanostructured lipid carriers (NLCs) by hot high-shear homogenization, followed by sonication and recrystallization. Lipid screening and an orthogonal optimization were applied to achieve NLCs with the particle size of 82.11 ± 0.14 nm and polydispersity index of 0.2623, the zeta potential of -50.47 ± 0.4 mV and encapsulation efficiency of 99.82 ± 0.01 %.

This study evaluated the physical and chemical stability of NLCs in short-term storage trials. The study showed encapsulation efficiency for the NA-TAG loaded NLCs was from 81% to 95.89% among different storage temperatures and was stable for at least 42 days.

The current study also explained the gastrointestinal fate of the optimized NLCs. A total of 46% of cumulative free fatty acids were released from NLCs after intestinal digestion. The results have important implications for the design of food products to control lipid absorption and the bio-accessibility of bioactive components within the GIT.

5.3. Future work

The following are proposed for future works building on the results of this thesis:

1) Selection of the substrate oil

Soy oil was used as the substrate in the enzymatic acidolysis reaction. Other oil, such as sunflower oil, olive oil, avocado oil and fish oil, can be considered as the substrate of the acidolysis reaction catalyzed by commercial immobilized lipases for incorporating NA in the TAGs in future.

2) Determination of other compounds in the lipid mixture from the TLC

The lipid mixtures were determined in **Section 4.3**. In the current study, the identification of the bands was based on literature (Caballero et al., 2014). The NA-TAG appear in first place of the chromatogram was scraped from the TLC plate, and their fatty acid composition identified by GC-FID. Further knowledge of the other bands, such as FFA, DAG and MAG, can be carried out using a suitable separation and quantification methodology such as the one reported in Narváez-Rivas & León-Camacho (2016) using acidity followed by gas-chromatographic method.

3) Identifying the purity of NA-TAG oil

From **Section 4.2** and **Section 4.3**, column chromatography separated the optimized NA-TAG oil from the acidolysis from the free fatty acid. The purity of the NA-TAG oil obtained from the TLC can be double-checked by nuclear magnetic resonance (NMR) spectroscopy.

4) Morphology characteristics of the lyophilized NLCs powder

Several key properties, including particle size, polydispersity index, zeta potential, and encapsulation efficiency of the lyophilized NLCs, were confirmed in **Section 4.6**. Scanning electron microscopy (SEM) can be used to get information regarding the morphology (shape

and surface characteristics) (Hashemi et al., 2020). SEM can be used to observe the crystal behaviour of the lyophilized NLCs powder. Also, the SEM can confirm the size of lyophilized powder and their changes during storage trial.

5) Improvements of the storage stability trials for the NLCs

For storage trials in **Section 4.7**, there are a few improvements can be made: 1) determination of PV using the standard AOCS procedure and compare with the values ontained by the current method used in this study; 2) use an antioxidant in the NLCs formulation and investigate the storage stability; 3) extend the storage trials to a longer period; and 4) obtain the kinetics data for mathematical modelling and estimate the shelf life of the NLCs.

6) The role of NA-TAG-loaded NLCs in industry applications

Application of NLCs for bioactive delivery have some advantages, but how these advantages are achieved is not entirely clear. **Section 4.8** discusses the digestion behaviour of the lyophilized NLCs using an *in vitro* digestion model to simulate the stomach and the upper small intestine in a fasting state. Research into these pathways can be extended to incorporate the NA-TAG-loaded NLCs in the food systems and study their properties. It might be advantageous to use *ex vivo* oral microbiota tests in future studies as LCs have been shown to affect gut microbiota *in vivo* and *in vitro* (Utembe et al., 2022).

References

Acosta, E. (2009). Bioavailability of nanoparticles in nutrient and nutraceutical delivery. *Current Opinion In* Colloid &Amp; *Interface Science*, *14*(1), 3-15. https://doi.org/10.1016/j.cocis.2008.01.002

Adamczak M. The application of lipases in modifying the composition, structure and properties
of lipids – A review. Pol J Food Nutr Sci. 2004;13/54(1):3–10.

Adhikari, P., & Hu, P. (2012). Enzymatic and Chemical Interesterification of Rice Bran Oil, Sheaolein and Palm Stearin and Comparative Study of Their Physicochemical Properties. *Journal Of Food Science*, *77*(12), C1285-C1292. https://doi.org/10.1111/j.1750-3841.2012.02977.x

Aditya, N., Macedo, A., Doktorovova, S., Souto, E., Kim, S., Chang, P., & Ko, S. (2014). Development and evaluation of lipid nanocarriers for quercetin delivery: A comparative study of solid lipid nanoparticles (SLN), nanostructured lipid carriers (NLC), and lipid nanoemulsions (LNE). *LWT - Food Science And Technology*, *59*(1), 115-121. https://doi.org/10.1016/j.lwt.2014.04.058

Al-Jassar, S., Mikajiri, S., & Roos, Y. (2020). Rehydration of whey protein isolate: Effect of temperature, water activity, and storage time. *LWT*, *133*, 110099. https://doi.org/10.1016/j.lwt.2020.110099

Akoh, C. C.; Xu, X. Enzymatic production of Betapol and other specialty fats. In *Lipid Biotechnology*; Kuo, C. C., Gardner, H. W., Eds.; Dekker; New York, 2002; pp 461-478

Alavizadeh, S., Akhtari, J., Badiee, A., Golmohammadzadeh, S., & Jaafari, M. (2015). Improved therapeutic activity of HER2 Affibody-targeted cisplatin liposomes in HER2-expressing breast tumor models. *Expert Opinion On Drug Delivery*, *13*(3), 325-336. https://doi.org/10.1517/17425247.2016.1121987

Anarjan, N., Mirhosseini, H., Baharin, B., & Tan, C. (2011). Effect of processing conditions on physicochemical properties of sodium caseinate-stabilized astaxanthin nanodispersions. *LWT - Food Science And Technology*, *44*(7), 1658-1665. https://doi.org/10.1016/j.lwt.2011.01.013

Anon (2001), Maximising the life of frying oil', Asia Pacific Food Industry, 13(6) 28-30.
Antolovich, M., Prenzler, P., Patsalides, E., McDonald, S., & Robards, K. (2001). Methods for testing antioxidant activity. *The Analyst*, *127*(1), 183-198. https://doi.org/10.1039/b009171p

Arifin, N., Soo-Peng, K., Long, K., Chin-Ping, T., Yusoff, M., & Oi-Ming, L. (2010). Modeling and Optimization of Lipozyme RM IM-Catalyzed Esterification of Medium- and Long-Chain Triacylglycerols (MLCT) Using Response Surface Methodology. *Food And Bioprocess Technology*, *5*(1), 216-225. doi: 10.1007/s11947-010-0325-5

Asbridge, D. (1995). Soybeans vs. Other Vegetable Oils as a Source of Edible Oil Products. *Practical Handbook Of Soybean Processing And Utilization*, 1-8. https://doi.org/10.1016/b978-0-935315-63-9.50005-x

Assadpour, E., & Jafari, S. (2019). Nanoencapsulation. *Nanomaterials For Food Applications*, 35-61. https://doi.org/10.1016/b978-0-12-814130-4.00003-8

Averina, E. S., Müller, R. H., Popov, D. V., & Radnaeva, L. D. (2011). Physical and chemical stability of nanostructured lipid drug carriers (NLC) based on natural lipids from Baikal region (Siberia, Russia). *Die Pharmazie*, *66*(5), 348–356.

Azadmard-Damirchi, S., & Dutta, P. (2010). Phytosterol Classes in Olive Oils and their analysis by Common Chromatographic Methods. *Olives And Olive Oil In Health And Disease Prevention*, 249-257. https://doi.org/10.1016/b978-0-12-374420-3.00027-9

Azmi, N., Hasham, R., Ariffin, F., Elgharbawy, A., & Salleh, H. (2020). Characterization, Stability Assessment, Antioxidant Evaluation and Cell Proliferation Activity of Virgin Coconut Oil-based Nanostructured Lipid Carrier Loaded with Ficus deltoidea Extract. *Cosmetics*, *7*(4), 83. https://doi.org/10.3390/cosmetics7040083

B. Sarmento, S. Martins, D. Ferreira, and E. B. Souto. (2007) "Oral insulin delivery by means of solid lipid nanoparticles," International Journal of Nanomedicine, vol. 2, no. 4, pp. 743– 749.

Babazadeh, A., Ghanbarzadeh, B., & Hamishehkar, H. (2017). Formulation of food grade nanostructured lipid carrier (NLC) for potential applications in medicinal-functional foods. *Journal Of Drug Delivery Science And Technology*, *39*, 50-58. https://doi.org/10.1016/j.jddst.2017.03.001

Banks, D. (2007). Industrial Frying. *Deep Frying*, 291-304. https://doi.org/10.1016/b978-1-893997-92-9.50020-7

BARTH, M., KERBEL, E., BROUSSARD, S., & SCHMIDT, S. (1993). Modified Atmosphere Packaging Protects Market Quality in Broccoli Spears Under Ambient Temperature Storage. *Journal Of Food Science*, *58*(5), 1070-1072. https://doi.org/10.1111/j.1365-2621.1993.tb06115.x

Brodkorb, A., Egger, L., Alminger, M., Alvito, P., Assunção, R., & Ballance, S. et al. (2019). INFOGEST static in vitro simulation of gastrointestinal food digestion. *Nature Protocols*, *14*(4), 991-1014. https://doi.org/10.1038/s41596-018-0119-1

Bell, L. N., & Labuza, T. P. (2000). Moisture sorption: practical aspects of isotherm measurement and use (Vol. Second). St. Paul, MN: American Association of Cereal Chemists.

Berlin: Springer-Verlag. Merrill, A., Schmelz, E., Wang, E., Dillehay, D., Rice, L., Meredith, F., & Riley, R. (1997). Importance of Sphingolipids and Inhibitors of Sphingolipid Metabolism as Components of Animal Diets. *The Journal Of Nutrition*, *127*(5), 830S-833S.https://doi.org/10.1093/jn/127.5.830s

Bettger, W., DiMichelle-Ranalli, E., Dillingham, B., & Blackadar, C. (2003). Nervonic acid is transferred from the maternal diet to milk and tissues of suckling rat pups. *The Journal Of Nutritional Biochemistry*, *14*(3), 160-165. https://doi.org/10.1016/s0955-2863(02)00280-2

Beysseriat, M., Decker, E., & McClements, D. (2006). Preliminary study of the influence of dietary fiber on the properties of oil-in-water emulsions passing through an in vitro human digestion model. *Food Hydrocolloids*, *20*(6), 800-809. https://doi.org/10.1016/j.foodhyd.2005.08.001

Bhagavan, N., & Ha, C. (2015). Enzymes and Enzyme Regulation. *Essentials Of Medical Biochemistry*, 63-84. https://doi.org/10.1016/b978-0-12-416687-5.00006-3

BHATT, S., SHARMA, J., KAMBOJ, R., KUMAR, M., SAINI, V. and MANDGE, S., 2021. Design and Optimization of Febuxostat-loaded Nano Lipid Carriers Using Full Factorial Design. *Turkish Journal of Pharmaceutical Sciences*, 18(1), pp.61-67.

Blamey JM, Fischer F, Meyer HP, Sarmiento F, Zinn M.(2017) .Enzymatic biocatalysis in chemical transformations: a promising and emerging field in green chemistry practice. In: *Biotech Microb Enzym* Academic Press; p. 347–403.

Bornscheuer, U. (2014). Enzymes in lipid modification: Past achievements and current trends. *European Journal Of Lipid Science And Technology*, *116*(10), 1322-1331. https://doi.org/10.1002/ejlt.201400020

BORNSCHEUER, U., ADAMCZAK, M., & SOUMANOU, M. (2012). Lipase-catalysed synthesis of modified lipids. *Lipids For Functional Foods And Nutraceuticals*, 149-182. Doi:10.1533/9780857097965.149

Bucio, S., Solaesa, Á., Sanz, M., Melgosa, R., Beltrán, S., & Sovová, H. (2015). Kinetic S t u d y for the Ethanolysis of Fish Oil Catalyzed by Lipozyme 435 in Different Reaction Media. *Journal Of Oleo Science*, *64*(4), 431-441. https://doi.org/10.5650/jos.ess14263

Caballero, E., Soto, C., Olivares, A., & Altamirano, C. (2014). Potential Use of Avocado Oil on Structured Lipids MLM-Type Production Catalysed by Commercial Immobilised Lipases. *Plos ONE*, *9*(9), e107749. doi: 10.1371/journal.pone.0107749

Carbonell-Capella, J., Buniowska, M., Barba, F., Esteve, M., & Frígola, A. (2014). Analytical

Methods for Determining Bioavailability and Bioaccessibility of Bioactive Compounds from Fruits and Vegetables: A Review. *Comprehensive Reviews In Food Science And Food Safety*, *13*(2), 155-171. https://doi.org/10.1111/1541-4337.12049

Cardoso, C., Afonso, C., Lourenço, H., Costa, S., & Nunes, M. (2015). Bioaccessibility assessment methodologies and their consequences for the risk–benefit evaluation of food. *Trends In Food Science &Amp; Technology*, *41*(1), 5-23. https://doi.org/10.1016/j.tifs.2014.08.008

CASTELL, J., GÓMEZ-LECHÓN, M., PONSODA, X., & BORT, R. (1997). In Vitro Investigation of the Molecular Mechanisms of Hepatotoxicity. *In Vitro Methods In Pharmaceutical Research*, 375-410. https://doi.org/10.1016/b978-012163390-5.50017-x

Cater, N., & Denke, M. (2001). Behenic acid is a cholesterol-raising saturated fatty acid in humans. *The American Journal Of Clinical Nutrition*, *73*(1), 41-44. https://doi.org/10.1093/ajcn/73.1.41

Chaiyasit, W., McClements, D., Weiss, J., & Decker, E. (2007). Impact of Surface-Active Compounds on Physicochemical and Oxidative Properties of Edible Oil. *Journal Of Agricultural And Food Chemistry*, *56*(2), 550-556. https://doi.org/10.1021/jf072071o

Chandra, P., Enespa, Singh, R., & Arora, P. (2020). Microbial lipases and their industrial applications: a comprehensive review. *Microbial Cell Factories*, *19*(1). https://doi.org/10.1186/s12934-020-01428-8

Chandran, J., Nayana, N., Roshini, N., & Nisha, P. (2016). Oxidative stability, thermal stability and acceptability of coconut oil flavored with essential oils from black pepper and ginger. *Journal Of Food Science And Technology*, *54*(1), 144-152. https://doi.org/10.1007/s13197-016-2446-y

Chang, Y., & McClements, D. (2014). Optimization of Orange Oil Nanoemulsion Formation by Isothermal Low-Energy Methods: Influence of the Oil Phase, Surfactant, and Temperature. *Journal Of Agricultural And Food Chemistry*, *62*(10), 2306-2312. https://doi.org/10.1021/jf500160y

Charles Bai, S., Hardy, R., & Hamidoghli, A. (2022). Diet analysis and evaluation. *Fish Nutrition*, 709-743. https://doi.org/10.1016/b978-0-12-819587-1.00010-0

Chen, Q., McGillivray, D., Wen, J., Zhong, F., & Quek, S. (2013). Co-encapsulation of fish oil with phytosterol esters and limonene by milk proteins. *Journal Of Food Engineering*, *117*(4), 505-512. https://doi.org/10.1016/j.jfoodeng.2013.01.011

Chew, S. (2020). Cold pressed rapeseed (Brassica napus) oil. *Cold Pressed Oils*, 65-80. https://doi.org/10.1016/b978-0-12-818188-1.00007-4

Choi, S., Decker, E., Henson, L., Popplewell, L., Xiao, H., & McClements, D. (2011).

Formulation and properties of model beverage emulsions stabilized by sucrose monopalmitate: Influence of pH and lyso-lecithin addition. *Food Research International*, *44*(9), 3006-3012. https://doi.org/10.1016/j.foodres.2011.07.007

Choudhury, N., Meghwal, M., & Das, K. (2021). Microencapsulation: An overview on concepts, methods, properties and applications in foods. *Food Frontiers*, *2*(4), 426-442. https://doi.org/10.1002/fft2.94

Cirri, M., Maestrini, L., Maestrelli, F., Mennini, N., Mura, P., Ghelardini, C., & Di Cesare Mannelli, L. (2018). Design, characterization and in vivo evaluation of nanostructured lipid carriers (NLC) as a new drug delivery system for hydrochlorothiazide oral administration in pediatric therapy. *Drug Delivery*, *25*(1), 1910-1921. https://doi.org/10.1080/10717544.2018.1529209

Costa, C., Osório, N., Canet, A., Rivera, I., Sandoval, G., Valero, F., & Ferreira-Dias, S. (2017).
Production of MLM Type Structured Lipids From Grapeseed Oil Catalyzed by Non-Commercial Lipases. *European Journal Of Lipid Science And Technology*, *120*(1), 1700320. https://doi.org/10.1002/ejlt.201700320

Cui, Ym., Wei, Dz. & Yu, Jt. (1997). Lipase-catalyzed esterification in organic solvent to resolve racemic naproxen. *Biotechnology Letters* 19, 865–868. https://doi.org/10.1023/A:1018333503317

Das, S., Ng, W., Kanaujia, P., Kim, S., & Tan, R. (2011). Formulation design, preparation and physicochemical characterizations of solid lipid nanoparticles containing a hydrophobic drug: Effects of process variables. *Colloids And Surfaces B: Biointerfaces*, *88*(1), 483-489. https://doi.org/10.1016/j.colsurfb.2011.07.036

Defang, O., Shufang, N., Wei, L., Hong, G., Hui, L., & Weisan, P. (2005). In Vitro and In Vivo
Evaluation of Two Extended Release Preparations of Combination Metformin and Glipizide. *Drug Development And Industrial Pharmacy*, *31*(7), 677-685. https://doi.org/10.1080/03639040500216410

Dijkstra, A. (2016). Soybean Oil. *Encyclopedia Of Food And Health*, 58-63. https://doi.org/10.1016/b978-0-12-384947-2.00638-3

Dorsey, B., & Jones, M. (2017). Healthy components of coffee processing by-products. *Handbook Of Coffee Processing By-Products*, 27-62. https://doi.org/10.1016/b978-0-12-811290-8.00002-5

Dumortier, G., Grossiord, J., Agnely, F., & Chaumeil, J. (2006). A Review of Poloxamer 407 Pharmaceutical and Pharmacological Characteristics. *Pharmaceutical Research*, *23*(12), 2709-2728. https://doi.org/10.1007/s11095-006-9104-4

Eh Suk, V., Mohd. Latif, F., Teo, Y., & Misran, M. (2020). Development of nanostructured

lipid carrier (NLC) assisted with polysorbate nonionic surfactants as a carrier for l-ascorbic acid and Gold Tri.E 30. *Journal Of Food Science And Technology*, *57*(9), 3259-3266. https://doi.org/10.1007/s13197-020-04357-x

Elmowafy, M., & Al-Sanea, M. (2021). Nanostructured lipid carriers (NLCs) as drug delivery platform: Advances in formulation and delivery strategies. *Saudi Pharmaceutical Journal*, *29*(9), 999-1012. https://doi.org/10.1016/j.jsps.2021.07.015

Elmowafy, M., Shalaby, K., Ali, H., Alruwaili, N., Salama, A., & Ibrahim, M. et al. (2019). Impact of nanostructured lipid carriers on dapsone delivery to the skin: in vitro and in vivo studies. *International Journal Of Pharmaceutics*, *572*, 118781. https://doi.org/10.1016/j.ijpharm.2019.118781

Elmowafy, M., Shalaby, K., Badran, M., Ali, H., Abdel-Bakky, M., & Ibrahim, H. (2018). Multifunctional carbamazepine loaded nanostructured lipid carrier (NLC) formulation. *International Journal Of Pharmaceutics*, *550*(1-2), 359-371. https://doi.org/10.1016/j.ijpharm.2018.08.062

Elmowafy, M., Shalaby, K., Badran, M., Ali, H., Abdel-Bakky, M., & El-Bagory, I. (2018). Fatty alcohol containing nanostructured lipid carrier (NLC) for progesterone oral delivery: In vitro and ex vivo studies. *Journal Of Drug Delivery Science And Technology*, *45*, 230-239. https://doi.org/10.1016/j.jddst.2018.03.007

Elsayed, M., Abdallah, O., Naggar, V., & Khalafallah, N. (2007). Lipid vesicles for skin delivery of drugs: Reviewing three decades of research. *International Journal Of Pharmaceutics*, *332*(1-2), 1-16. https://doi.org/10.1016/j.ijpharm.2006.12.005

Ermer, J., & Ploss, H. (2005). Validation in pharmaceutical analysis. *Journal Of Pharmaceutical And Biomedical Analysis*, *37*(5), 859-870. https://doi.org/10.1016/j.jpba.2004.06.018

Esteban, L., Jiménez, M., Hita, E., González, P., Martín, L., & Robles, A. (2011). Production of structured triacylglycerols rich in palmitic acid at sn-2 position and oleic acid at sn-1,3 positions as human milk fat substitutes by enzymatic acidolysis. *Biochemical Engineering Journal*, *54*(1), 62-69. doi: 10.1016/j.bej.2011.01.009

Esterbauer, H., Lang, J., Zadravec, S., & Slater, T. (1984). Detection of malonaldehyde by high-performance liquid chromatography. *Methods In Enzymology*, 319-328. https://doi.org/10.1016/s0076-6879(84)05041-2

Estevinho, B., & Rocha, F. (2017). A Key for the Future of the Flavors in Food Industry. *Nanotechnology Applications In Food*, 1-19. https://doi.org/10.1016/b978-0-12-811942-6.00001-7

F. Gibbs, Selim Kermasha, Inteaz Al, B. (1999). Encapsulation in the food industry: a review. *International Journal Of Food Sciences And Nutrition*, *50*(3), 213-224. https://doi.org/10.1080/096374899101256

F., & Riley, R. (1997). Importance of Sphingolipids and Inhibitors of Sphingolipid Metabolism

as Components of Animal Diets. *The Journal Of Nutrition*, *127*(5), 830S-833S.

Fäldt, P. and Bergenståhl, B. (1994). "*The Surface Composition of Spray-Dried Protein-Lactose Powders.*" Colloids and Surfaces A: Physicochemical and Engineering Aspects 90: 183-190.

Fan, Y., Meng, H., Hu, G., & Li, F. (2018). Biosynthesis of nervonic acid and perspectives for its production by microalgae and other microorganisms. *Applied Microbiology And Biotechnology*, *102*(7), 3027-3035. https://doi.org/10.1007/s00253-018-8859-y

Fang, C., A. Al-Suwayeh, S., & Fang, J. (2013). Nanostructured Lipid Carriers (NLCs) for Drug Delivery and Targeting. *Recent Patents On Nanotechnology*, *7*(1), 41-55. https://doi.org/10.2174/187221013804484827

Farbodi, M. (2017). Application of Taguchi Method for Optimizing of Mechanical Properties of Polystyrene-Carbon Nanotube Nanocomposite. *Polymers And Polymer Composites*, *25*(2), 177-184. https://doi.org/10.1177/096739111702500208

Fernandez-Lafuente, R. (2010). Lipase from Thermomyces lanuginosus: Uses and prospects as an industrial biocatalyst. *Journal Of Molecular Catalysis B: Enzymatic*, *62*(3-4), 197-212. https://doi.org/10.1016/j.molcatb.2009.11.010

Filho, D., Silva, A., & Guidini, C. (2019). Lipases: sources, immobilization methods, and industrial applications. *Applied Microbiology And Biotechnology*, *103*(18), 7399-7423. https://doi.org/10.1007/s00253-019-10027-6

Fu, X., Zheng, J., Ying, X., Yan, H., & Wang, Z. (2014). Investigation of Lipozyme TL IM-*Functional Lipids*. CRC Press, USA, pp. 489–512.

Gawrysiak-Witulska, M., Rudzińska, M., Wawrzyniak, J., & Siger, A. (2012). The Effect of Temperature and Moisture Content of Stored Rapeseed on the Phytosterol Degradation Rate. *Journal Of The American Oil Chemists' Society*, *89*(9), 1673-1679. https://doi.org/10.1007/s11746-012-2064-4

Ghate, V., Lewis, S., Prabhu, P., Dubey, A., & Patel, N. (2016). Nanostructured lipid carriers for the topical delivery of tretinoin. *European Journal Of Pharmaceutics And Biopharmaceutics*, *108*, 253-261. https://doi.org/10.1016/j.ejpb.2016.07.026

Ginzburg, A. (1981). THE FORMS AND ENERGY OF MOISTURE BINDING IN FOODS AS A BASIS FOR CHOOSING RATIONAL METHODS FOR PROCESSING AND STORAGE. *Water Activity: Influences On Food Quality*, 679-711. https://doi.org/10.1016/b978-0-12-591350-8.50031-0

Goh, S.H., Yeong, S.K. & Wang, C.W. (1993). Transesterification of cocoa butter by fungal lipases: Effect of solvent on 1,3-specificity. *J Am Oil Chem Soc* 70, 567.

Gonçalves, M., Amaral, J., Lopes, L., Fernandez-Lafuente, R., & Tardioli, P. (2021). Stabilization and operational selectivity alteration of Lipozyme 435 by its coating with polyethyleneimine: Comparison of the biocatalyst performance in the synthesis

of xylose fatty esters. *International Journal Of Biological Macromolecules*, *192*, 665-674. https://doi.org/10.1016/j.ijbiomac.2021.10.052

Gonzalez-Mira, E., Egea, M., Garcia, M., & Souto, E. (2010). Design and ocular tolerance of flurbiprofen loaded ultrasound-engineered NLC. *Colloids And Surfaces B: Biointerfaces*, *81*(2), 412-421. https://doi.org/10.1016/j.colsurfb.2010.07.029

Gordon, M. (2004). Factors affecting lipid oxidation. *Understanding And Measuring The Shelf-Life Of Food*, 128-141. https://doi.org/10.1533/9781855739024.1.128

Grant, W. (2004). Life at low water activity. *Philosophical Transactions Of The Royal Society Of London. Series B: Biological Sciences*, *359*(1448), 1249-1267. https://doi.org/10.1098/rstb.2004.1502

GROMOPHONE M A (1991), Anisidine value as a measure of latent deterioration of fats, *Grasas-y-Aceites*, 42(1) 8-13.

Ginzburg, A. (1981). THE FORMS AND ENERGY OF MOISTURE BINDING IN FOODS AS A BASIS FOR CHOOSING RATIONAL METHODS FOR PROCESSING AND STORAGE. *Water Activity: Influences On Food Quality*, 679-711. https://doi.org/10.1016/b978-0-12-591350-8.50031-0

Gunstone, F. (2006). Introduction: Modifying lipids – why and how?. *Modifying Lipids For Use In Food*, 1-8. https://doi.org/10.1533/9781845691684.1

H. Muller, R., Shegokar, R., & M. Keck, C. (2011). 20 Years of Lipid Nanoparticles (SLN & NLC): Present State of Development & Industrial Applications. *Current Drug Discovery Technologies*, *8*(3), 207-227. https://doi.org/10.2174/157016311796799062

Han, F., Li, S., Yin, R., Liu, H., & Xu, L. (2008). Effect of surfactants on the formation and characterization of a new type of colloidal drug delivery system: Nanostructured lipid carriers. *Colloids And Surfaces A: Physicochemical And Engineering Aspects*, *315*(1-3), 210-216. https://doi.org/10.1016/j.colsurfa.2007.08.005

Han, F., Yin, R., Che, X., Yuan, J., Cui, Y., Yin, H., & Li, S. (2012). Nanostructured lipid carriers (NLC) based topical gel of flurbiprofen: Design, characterization and in vivo evaluation. *International Journal Of Pharmaceutics*, *439*(1-2), 349-357. https://doi.org/10.1016/j.ijpharm.2012.08.040

Hashemi, F., Farzadnia, F., Aghajani, A., Ahmadzadeh NobariAzar, F., & Pezeshki, A. (2020). Conjugated linoleic acid loaded nanostructured lipid carrier as a potential antioxidant nanocarrier for food applications. *Food Science & Nutrition*, *8*(8), 4185-4195. https://doi.org/10.1002/fsn3.1712

HAWRYSH Z J, ERIN M K, KIM S S and HARDIN R T (1995), Sensory and chemical

stability of tortilla chips fried in canola oil, corn oil and partially hydrogenated soybean oil, *J Am Oil Chem* Soc, 72(10) 1123-1130.

He, H., Hong, Y., Gu, Z., Liu, G., Cheng, L., & Li, Z. (2016). Improved stability and controlled release of CLA with spray-dried microcapsules of OSA-modified starch and xanthan gum. *Carbohydrate Polymers*, *147*, 243-250. https://doi.org/10.1016/j.carbpol.2016.03.078

Holser, R. (2011). Encapsulation of Polyunsaturated Fatty Acid Esters with Solid Lipid Particles. *Lipid Insights*, *5*, LPI.S7901. https://doi.org/10.4137/lpi.s7901

Houde, A., Kademi, A., & Leblanc, D. (2004). Lipases and Their Industrial Applications: An Overview. *Applied Biochemistry And Biotechnology*, *118*(1-3), 155-170. https://doi.org/10.1385/abab:118:1-3:155

Hsieh, R., & Kinsella, J. (1989). Oxidation of Polyunsaturated Fatty Acids: Mechanisms, Products, and Inhibition with Emphasis on Fish. *Advances In Food And Nutrition Research*, 233-341. https://doi.org/10.1016/s1043-4526(08)60129-1

Hu, F., Jiang, S., Du, Y., Yuan, H., Ye, Y., & Zeng, S. (2006). Preparation and characteristics of monostearin nanostructured lipid carriers. *International Journal Of Pharmaceutics*, *314*(1), 83-89. https://doi.org/10.1016/j.ijpharm.2006.01.040

Hu, P., Xu, X., & Yu, L. (2017). Interesterified trans-free fats rich in sn-2 nervonic acid prepared using Acer truncatum oil, palm stearin and palm kernel oil, and their physicochemical properties. *LWT – Food Science And Technology*, *76*, 156-163. doi: 10.1016/j.lwt.2016.10.054

Huang, J., Wang, Q., Li, T., Xia, N., & Xia, Q. (2017). Nanostructured lipid carrier (NLC) as a strategy for encapsulation of quercetin and linseed oil: Preparation and in vitro characterization studies. *Journal Of Food Engineering*, *215*, 1-12. https://doi.org/10.1016/j.jfoodeng.2017.07.002

Huguet-Casquero, A., Xu, Y., Gainza, E., Pedraz, J., & Beloqui, A. (2020). Oral delivery of oleuropein-loaded lipid nanocarriers alleviates inflammation and oxidative stress in acute colitis. *International Journal Of Pharmaceutics*, *586*, 119515. https://doi.org/10.1016/j.ijpharm.2020.119515

Hur, S., Decker, E., & McClements, D. (2009). Influence of initial emulsifier type on microstructural changes occurring in emulsified lipids during in vitro digestion. *Food Chemistry*, *114*(1), 253-262. https://doi.org/10.1016/j.foodchem.2008.09.069

Irwin, J., & Hedges, N. (2004). Measuring lipid oxidation. *Understanding And Measuring The Shelf-Life Of Food*, 289-316. https://doi.org/10.1533/9781855739024.2.289

Iwasaki, Y., & Yamane, T. (2000). Enzymatic synthesis of structured lipids. *Journal Of Molecular Catalysis B: Enzymatic*, *10*(1-3), 129-140. doi: 10.1016/s1381-1177(00)00120-x

Iwasaki, Y., & Yamane, T. (2004). Enzymatic Synthesis of Structured Lipids. *Recent Progress Of Biochemical And Biomedical Engineering In Japan I*, 151-171. https://doi.org/10.1007/b94196

Jenning, V., Thünemann, A., & Gohla, S. (2000). Characterisation of a novel solid lipid nanoparticle carrier system based on binary mixtures of liquid and solid lipids. *International Journal Of Pharmaceutics*, *199*(2), 167-177. https://doi.org/10.1016/s0378-5173(00)00378-1

Jennings, B., & Akoh, C. (2001). Lipase catalyzed modification of fish oil to incorporate capric acid. *Food Chemistry*, *72*(3),273-278. https://doi.org/10.1016/s0308-8146(00)00266-1

Jensen, R., DeJong, F., & Clark, R. (1983). Determination of lipase specificity. *Lipids*, *18*(3), 239-252. doi: 10.1007/bf02534556

Jones, D., Caballero, S., & Davidov-Pardo, G. (2019). Bioavailability of nanotechnology-based bioactives and nutraceuticals. *Advances In Food And Nutrition Research*, 235-273. https://doi.org/10.1016/bs.afnr.2019.02.014

Karupaiah, T., & Sundram, K. (2007). Effects of stereospecific positioning of fatty acids in triacylglycerol structures in native and randomized fats: a review of their nutritional implications. *Nutrition &Amp; Metabolism*, *4*(1), 16. https://doi.org/10.1186/1743-7075-4-16

Kaczmarek, A., & Muzolf-Panek, M. (2021). Predictive Modeling of Changes in TBARS in the Intramuscular Lipid Fraction of Raw Ground Beef Enriched with Plant Extracts. *Antioxidants*, *10*(5), 736. https://doi.org/10.3390/antiox10050736

Kaczmarek, A., Cegielska-Radziejewska, R., Szablewski, T., & Zabielski, J. (2016). TBARS and microbial & nbsp;growth predictive models of pork sausage stored at different temperatures. *Czech Journal Of Food Sciences*, *33*(No. 4), 320-325. https://doi.org/10.17221/591/2014-cjfs

KAMIL J Y V A, YOU-JIN-JEON and SHAHIDI F (2002), `Antioxidative activity of chitosans of different viscosity in cooked comminuted flesh of herring (*Clupea harengus*)', *Food Chem*, 79(1) 69-77.

Karimi, N., Ghanbarzadeh, B., Hamishehkar, H., KEYVANI, F., Pezeshki, A., & Gholian, M.M. (2015). Phytosome and liposome: the beneficial encapsulation systems in drug delivery and food application.

Karimi, N., Ghanbarzadeh, B., Hamishehkar, H., Mehramuz, B., & Kafil, H. (2018). Antioxidant, Antimicrobial and Physicochemical Properties of Turmeric Extract-Loaded Nanostructured Lipid Carrier (NLC). *Colloid And Interface Science Communications*, *22*, 18-24. https://doi.org/10.1016/j.colcom.2017.11.006

Kasongo, W., Pardeike, J., Müller, R., & Walker, R. (2011). Selection and Characterization of
Suitable Lipid Excipients for use in the Manufacture of Didanosine-Loaded Solid Lipid Nanoparticles and Nanostructured Lipid Carriers. *Journal Of Pharmaceutical Sciences*, *100*(12), 5185-5196. https://doi.org/10.1002/jps.22711

Kaszuba, M., Corbett, J., Watson, F., & Jones, A. (2010). High-concentration zeta potential measurements using light-scattering techniques. *Philosophical Transactions Of The Royal Society A: Mathematical, Physical And Engineering Sciences*, *368*(1927), 4439-4451. https://doi.org/10.1098/rsta.2010.0175

Kaup, M., Froese, C., & Thompson, J. (2002). A Role for Diacylglycerol Acyltransferase during Leaf Senescence. *Plant Physiology*, *129*(4), 1616-1626. https://doi.org/10.1104/pp.003087

Kavadia, M., Yadav, M., Odaneth, A., & Lali, A. (2018). Synthesis of designer triglycerides by enzymatic acidolysis. *Biotechnology Reports*, *18*, e00246. https://doi.org/10.1016/j.btre.2018.e00246

Kawashima A, Shimada Y, Nagao T, Ohara A, Matsuhisa T, Sugihara A, Tominaga Y. 2002. Production of structured tag rich in 1,3-dicapryloyl-2--linolenoyl glycerol from borage oil.JAm Oil Chem Soc 79(9):871–7.

Kennedy, E. P. (1961). Biosynthesis of complex lipids. *Fed. Proc.* 20, 934–940.

Keppley, L., Walker, S., Gademsey, A., Smith, J., Keller, S., Kester, M., & Fox, T. (2020).

Kerwin, B. (2008). Polysorbates 20 and 80 Used in the Formulation of Protein Biotherapeutics:
Structure and Degradation Pathways. *Journal Of Pharmaceutical Sciences*, *97*(8), 2924-2935. https://doi.org/10.1002/jps.21190

Khan, A., Mudassir, J., Akhtar, S., Murugaiyah, V., & Darwis, Y. (2019). Freeze-Dried Lopinavir-Loaded Nanostructured Lipid Carriers for Enhanced Cellular Uptake and Bioavailability: Statistical Optimization, in Vitro and in Vivo Evaluations. *Pharmaceutics*, *11*(2), 97. https://doi.org/10.3390/pharmaceutics11020097

Khan, S., Shaharyar, M., Fazil, M., Hassan, M., Baboota, S., & Ali, J. (2016). Tacrolimus-loaded nanostructured lipid carriers for oral delivery-in vivo bioavailability enhancement. *European Journal Of Pharmaceutics And Biopharmaceutics*, *109*, 149-157. https://doi.org/10.1016/j.ejpb.2016.10.011

Khodadadi, M., Aziz, S., St-Louis, R., & Kermasha, S. (2013). Lipase-catalyzed synthesis and
characterization of flaxseed oil-based structured lipids. *Journal Of Functional Foods*, *5*(1), 424-433. https://doi.org/10.1016/j.jff.2012.11.015

Kim, Byung Hee & Akoh, Casimir C. (2015). Recent Research Trends on the Enzymatic Synthesis of Structured Lipids. *Journal of Food Science*, 90(8), C1713-C1724

Kim, I., Kim, H., Lee, K., Chung, S., & Ko, S. (2002). Lipase-catalyzed acidolysis of perilla oil with caprylic acid to produce structured lipids. *Journal Of The American Oil Chemists' Society*, *79*(4), 363-367. https://doi.org/10.1007/s11746-002-0489-3

Kinsella, J. E., Shimp, J. L., & Mai, J. (1978). The proximate composition of several species of fresh water fishes. Food and Life Sciences Bulletin, 69, 1–20.

Kumar, P., Sharma, G., Kumar, R., Singh, B., Malik, R., Katare, O., & Raza, K. (2016). Promises of a biocompatible nanocarrier in improved brain delivery of quercetin: Biochemical, pharmacokinetic and biodistribution evidences. *International Journal Of Pharmaceutics*, *515*(1-2), 307-314. https://doi.org/10.1016/j.ijpharm.2016.10.024

Lacatusu, I., Badea, N., Murariu, A., & Meghea, A. (2011). The encapsulation effect of UV molecular absorbers into biocompatible lipid nanoparticles. *Nanoscale Research Letters*, *6*(1). https://doi.org/10.1186/1556-276x-6-73

Lacey, D., & Hills, M. (1996). Heterogeneity of the endoplasmic reticulum with respect to lipid synthesis in developing seeds of Brassica napus L. *Planta*, *199*(4). https://doi.org/10.1007/bf00195185

Lauridsen, J. (1976). Food emulsifiers: Surface activity, edibility, manufacture, composition, and application. *Journal Of The American Oil Chemists' Society*, *53*(6Part2), 400-407. https://doi.org/10.1007/bf02605731

Lee, J.H., Lee, K.T., (2006). Structured lipids production. In: Akoh, C.C. (Ed.), *Handbook of Functional Lipids*. CRC Press, USA, pp. 489–512.

Lee, K., & Akoh, C. (1998). Structured lipids: Synthesis and applications. *Food Reviews International*, *14*(1), 17-34. doi: 10.1080/87559129809541148

Lee, Y., Tang, T., & Lai, O. (2012). Health Benefits, Enzymatic Production, and Application of Medium- and Long-Chain Triacylglycerol (MLCT) in Food Industries: A Review. *Journal Of Food Science*, *77*(8), R137-R144. doi: 10.1111/j.1750-3841.2012.02793.x

Li, M., Zahi, M., Yuan, Q., Tian, F., & Liang, H. (2015). Preparation and stability of astaxanthin solid lipid nanoparticles based on stearic acid. *European Journal Of Lipid Science And Technology*, *118*(4), 592-602. https://doi.org/10.1002/ejlt.201400650

Li, Q., Cai, T., Huang, Y., Xia, X., Cole, S., & Cai, Y. (2017). A Review of the Structure, Preparation, and Application of NLCs, PNPs, and PLNs. *Nanomaterials*, *7*(6), 122. https://doi.org/10.3390/nano7060122

Li, Q., Chen, J., Yu, X., & Gao, J. (2019). A mini review of nervonic acid: Source, production, and biological functions. *Food Chemistry*, *301*, 125286. https://doi.org/10.1016/j.foodchem.2019.125286

Li, Y., & McClements, D. (2010). New Mathematical Model for Interpreting pH-Stat Digestion
Profiles: Impact of Lipid Droplet Characteristics on in Vitro Digestibility. *Journal Of Agricultural And Food Chemistry*, *58*(13), 8085-8092. https://doi.org/10.1021/jf101325m

Liang, L., Zhang, X., Wang, X., Jin, Q., & McClements, D. (2018). Influence of Dairy Emulsifier Type and Lipid Droplet Size on Gastrointestinal Fate of Model Emulsions: In Vitro Digestion Study. *Journal Of Agricultural And Food Chemistry*, *66*(37), 9761-9769. https://doi.org/10.1021/acs.jafc.8b02959

Lichtenstein, A. (2013). Fats and Oils. *Encyclopedia Of Human Nutrition*, 201-208. doi: 10.1016/b978-0-12-375083-9.00097-0

Liu, C., & Wu, C. (2010). Optimization of nanostructured lipid carriers for lutein delivery. *Colloids And Surfaces A: Physicochemical And Engineering Aspects*, *353*(2-3), 149-156. https://doi.org/10.1016/j.colsurfa.2009.11.006

Liu, F., Wang, P., Xiong, X., Zeng, X., Zhang, X., & Wu, G. (2021). A Review of Nervonic Acid Production in Plants: Prospects for the Genetic Engineering of High Nervonic Acid Cultivars Plants. *Frontiers In Plant Science*, *12*. https://doi.org/10.3389/fpls.2021.626625

Liu, L., & Kong, F. (2021). Measuring chemical deterioration of foods. *Chemical Changes During Processing And Storage Of Foods*, 637-679. https://doi.org/10.1016/b978-0-12-817380-0.00013-0

Liu, S., Dong, X., Wei, F., Wang, X., Lv, X., & Zhong, J. et al. (2015). Ultrasonic pretreatment
in lipase-catalyzed synthesis of structured lipids with high 1,3-dioleoyl-2-palmitoylglycerol content. *Ultrasonics Sonochemistry*, *23*, 100-108.https://doi.org/10.1016/j.ultsonch.2014.10.015

Loo, Basri, M., Ismail, Lau, Tejo, B., & Kanthimathi, M. et al. (2012). Effect of compositions in nanostructured lipid carriers (NLC) on skin hydration and occlusion. *International Journal Of Nanomedicine*, 13. https://doi.org/10.2147/ijn.s35648

Loo, C. h., Basri, M., Ismail, R., Lau, H., Tejo, B., Kanthimathi, M., Hassan, H., & Choo, Y. (2013). Effect of compositions in nanostructured lipid carriers (NLC) on skin hydration and occlusion. *International journal of nanomedicine*, *8*, 13–22. https://doi.org/10.2147/IJN.S35648

Lu, W., Huang, D., Wang, C., Yeh, C., Tsai, J., Huang, Y., & Li, P. (2018). Preparation, characterization, and antimicrobial activity of nanoemulsions incorporating citral essential oil. *Journal Of Food And Drug Analysis*, *26*(1), 82-89. https://doi.org/10.1016/j.jfda.2016.12.018

Lumakso, F., Rohman, A., M., H., Riyanto, S., & Yusof, F. (2015). DETECTION AND

QUANTIFICATION OF SOYBEAN AND CORN OILS AS ADULTERANTS IN AVOCADO OIL USING FOURIER TRANSFORM MID INFRARED (FT-MIR) SPECTROSCOPY AIDED WITH MULTIVARIATE CALIBRATION. *Jurnal Teknologi*, *77*(1). https://doi.org/10.11113/jt.v77.3640

Man, Y., & Rohman, A. (2013) Analysis of canola oil in virgin coconutoil using FTIR spectroscopy and chemometrics. *Journal of Food and Pharmaceutical Sciences*, 1:5–9.

Mao, Y., & McClements, D. (2012). Influence of electrostatic heteroaggregation of lipid droplets on their stability and digestibility under simulated gastrointestinal conditions. *Food &Amp; Function*, *3*(10), 1025. https://doi.org/10.1039/c2fo30108c

Mao, Y., & McClements, D. (2012). Influence of electrostatic heteroaggregation of lipid droplets on their stability and digestibility under simulated gastrointestinal conditions. *Food &Amp; Function*, *3*(10), 1025. https://doi.org/10.1039/c2fo30108c

Martin, J., Bougnoux, P., Antoine, J., Lanson, M., & Couet, C. (1993). Triacylglycerol structure of human colostrum and mature milk. *Lipids*, *28*(7), 637-643.https://doi.org/10.1007/bf02536059

Martinek, K. (1993). Need for themostability, its benefits and main strategies for thermo stabilization. In M. N. Gupta (Ed.), Thermostability of enzymes (pp. 76–82).

Matsuno, R., & Adachi, S. (1993). Lipid encapsulation technology - techniques and applications to food. *Trends In Food Science & Technology*, *4*(8), 256-261. https://doi.org/10.1016/0924-2244(93)90141-v

Matte, C., Bussamara, R., Dupont, J., Rodrigues, R., Hertz, P., & Ayub, M. (2014). Immobilization of *Thermomyces lanuginosus* Lipase by Different Techniques on Immobead 150 Support: Characterization and Applications. *Applied Biochemistry And Biotechnology*, *172*(5), 2507-2520. https://doi.org/10.1007/s12010-013-0702-4

McClements DJ (2004). Food Emulsions: Principles, Practice, and Techniques. CRC Press, Boca Raton, FL.

Mehmood, T. (2015). Optimization of the canola oil based vitamin E nanoemulsions stabilized
by food grade mixed surfactants using response surface methodology. *Food Chemistry*, *183*, 1-7. https://doi.org/10.1016/j.foodchem.2015.03.021

Mehnert, W., & Mäder, K. (2012). Solid lipid nanoparticles. *Advanced Drug Delivery Reviews*, *64*, 83-101. https://doi.org/10.1016/j.addr.2012.09.021

Meyer, A. S., Heinonen, M., & Frankel, E. N. (1998). Antioxidant interactions of catechin,

cyanidin, caffeic acid, quercetin, and ellagic acid on human LDL oxidation. Food Chemistry, 61(1–2), 71–75.

Mirhosseini, H., Tan, C., & Taherian, A. (2008). Effect of glycerol and vegetable oil on physicochemical properties of Arabic gum-based beverage emulsion. *European Food Research And Technology*, *228*(1), 19-28. https://doi.org/10.1007/s00217-008-0901-3

Mishra, B., Patel, B., & Tiwari, S. (2010). Colloidal nanocarriers: a review on formulation technology, types and applications toward targeted drug delivery. *Nanomedicine: Nanotechnology, Biology And Medicine*, *6*(1), 9-24. https://doi.org/10.1016/j.nano.2009.04.008

Mitri, K., Shegokar, R., Gohla, S., Anselmi, C., & Müller, R. (2011). Lipid nanocarriers for dermal delivery of lutein: Preparation, characterization, stability and performance. *International Journal Of Pharmaceutics*, *414*(1-2), 267-275. https://doi.org/10.1016/j.ijpharm.2011.05.008

Moghimi, R., Ghaderi, L., Rafati, H., Aliahmadi, A., & McClements, D. (2016). Superior antibacterial activity of nanoemulsion of Thymus daenensis essential oil against E. coli. *Food Chemistry*, *194*, 410-415. https://doi.org/10.1016/j.foodchem.2015.07.139

Mohammadi, M., Pezeshki, A., Mesgari Abbasi, M., Ghanbarzadeh, B., & Hamishehkar, H. *Molecular Catalysis B: Enzymatic*, *10*(1-3), 129-140. doi: 10.1016/s1381-1177(00)00120-x

Mohammadi, M., Pezeshki, A., Mesgari Abbasi, M., Ghanbarzadeh, B., & Hamishehkar, H. (2017). Vitamin D3-Loaded Nanostructured Lipid Carriers as a Potential Approach for Fortifying Food Beverages; in Vitro and in Vivo Evaluation. *Advanced Pharmaceutical Bulletin*, *7*(1), 61-71. https://doi.org/10.15171/apb.2017.008

Morais, A., Alencar, É., Xavier Júnior, F., Oliveira, C., Marcelino, H., & Barratt, G. et al. (2016). Freeze-drying of emulsified systems: A review. *International Journal Of Pharmaceutics*, *503*(1-2), 102-114. https://doi.org/10.1016/j.ijpharm.2016.02.047

Moreira, D., de Pádua Gandra, R., Zuin, J., Ract, J., Ribeiro, A., & Macedo, J. et al. (2020). Synthesis and characterization of structured lipid rich in behenic acid by enzymatic interesterification. *Food And Bioproducts Processing*, *122*, 303-310.https://doi.org/10.1016/j.fbp.2020.06.005

Morris, M., Ye, X., & Doona, C. (2021). Soybean Oil and Nonthermal Plasma Pretreatment to

Dye Para-Aramid Woven Fabrics with Disperse Dye Using a Glycerol-Based Dye Bath. *Journal Of The American Oil Chemists' Society*, *98*(4), 463-473. https://doi.org/10.1002/aocs.12477

Mu, H., Xu, X., & Høy, C. (1998). Production of specific-structured triacylglycerols by lipase-catalyzed interesterification in a laboratory-scale continuous reactor. Journal Of The American Oil Chemists' Society, 75(9), 1187-1193. https://doi.org/10.1007/s11746-998-0133-5

Müller, R., Radtke, M., & Wissing, S. (2002). Solid lipid nanoparticles (SLN) and nanostructured lipid carriers (NLC) in cosmetic and dermatological preparations. *Advanced Drug Delivery Reviews*, *54*, S131-S155. https://doi.org/10.1016/s0169-409x(02)00118-7

Muñío, M., Robles, A., Esteban, L., González, P., & Molina, E. (2009). Synthesis of structured
lipids by two enzymatic steps: Ethanolysis of fish oils and esterification of 2-monoacylglycerols. *Process Biochemistry*, *44*(7), 723-730. https://doi.org/10.1016/j.procbio.2009.03.002

Muñío, M., Robles, A., Esteban, L., González, P., & Molina, E. (2009). Synthesis of structured
lipids by two enzymatic steps: Ethanolysis of fish oils and esterification of 2-monoacylglycerols. Process Biochemistry, 44(7), 723-730. doi: 10.1016/j.procbio.2009.03.002

MURTHI T N, SHARMA M, DEVDHARA V D, CHATTERJEE S and CHAKRABORTY B
K (1987), `Storage stability of edible oils and their blends', *J Food Sci and Technol-India*, 24(2) 84-87.

Najjar, R., & Stubenrauch, C. (2009). Phase diagrams of microemulsions containing reducing agents and metal salts as bases for the synthesis of metallic nanoparticles. *Journal Of Colloid and Interface Science*, *331*(1), 214-220. https://doi.org/10.1016/j.jcis.2008.11.035

Naseri, N., Valizadeh, H., & Zakeri-Milani, P. (2015). Solid Lipid Nanoparticles and Nanostructured Lipid Carriers: Structure, Preparation and Application. *Advanced pharmaceutical bulletin*, *5*(3), 305–313. https://doi.org/10.15171/apb.2015.043

Narváez-Rivas, M., & León-Camacho, M. (2016). Fatty Acids: Determination and Requirements. *Encyclopedia Of Food And Health*, 609-614. https://doi.org/10.1016/b978-0-12-384947-2.00278-6

Ni, L., Zheng, Y., Hara, M., Pan, D., & Luo, X. (2015). Structural basis for Mob1-dependent activation of the core Mst–Lats kinase cascade in Hippo signaling. *Genes &Amp; Development*, *29*(13), 1416-1431. https://doi.org/10.1101/gad.264929.115

Nor Aini, I., & Miskandar, M. (2007). Utilization of palm oil and palm products in shortenings
and margarines. *European Journal Of Lipid Science And Technology*, *109*(4), 422-432. doi:10.1002/ejlt.200600232

Nowak, D., & Jakubczyk, E. (2020). The Freeze-Drying of Foods—The Characteristic of the Process Course and the Effect of Its Parameters on the Physical Properties of Food Materials. *Foods*, *9*(10), 1488. https://doi.org/10.3390/foods9101488

Ortiz, C., Ferreira, M., Barbosa, O., dos Santos, J., Rodrigues, R., & Berenguer-Murcia, Á. et al. (2019). Novozym 435: the "perfect" lipase immobilized biocatalyst?. *Catalysis Science & Technology*, 9910), 2380-2420. http://doi.org/10.1039/c9cy00415g

Overview. *Applied Biochemistry And Biotechnology*, *118*(1-3), 155-170. Packaging Protects Market Quality in Broccoli Spears Under Ambient Temperature Storage. *Journal Of Food Science*, *58*(5), 1070-1072. https://doi.org/10.1111/j.1365-2621.1993.tb06115.x

Pang, S., Yusoff, M., & Gimbun, J. (2014). Assessment of phenolic compounds stability and retention during spray drying of Orthosiphon stamineus extracts. *Food Hydrocolloids*, *37*, 159-165. https://doi.org/10.1016/j.foodhyd.2013.10.022

Parada, J., & Aguilera, J. (2007). Food Microstructure Affects the Bioavailability of Several Nutrients. *Journal Of Food Science*, *72*(2), R21-R32. https://doi.org/10.1111/j.1750-3841.2007.00274.x

Pasqualone, A., Delcuratolo, D., & Gomes, T. (2011). Focaccia Italian Flat Fatty Bread. *Flour And Breads And Their Fortification In Health And Disease Prevention*, 47-58. https://doi.org/10.1016/b978-0-12-380886-8.10005-4

Patel, A., Sindhu, D., Arora, N., Singh, R., Pruthi, V., & Pruthi, P. (2015). Biodiesel production from non-edible lignocellulosic biomass of Cassia fistula L. fruit pulp using oleaginous yeast Rhodosporidium kratochvilovae HIMPA1. Bioresource Technology, 197, 91-98. https://doi.org/10.1016/j.biortech.2015.08.039

Peng, Y., Bishop, K., & Quek, S. (2019). Extraction Optimization, Antioxidant Capacity and Phenolic Profiling of Extracts from Flesh, Peel and Whole Fruit of New Zealand Grown Feijoa Cultivars. *Antioxidants*, *8*(5), 141. https://doi.org/10.3390/antiox8050141

Pezeshki, A., Ghanbarzadeh, B., Mohammadi, M., Fathollahi, I., & Hamishehkar, H. (2014). Encapsulation of Vitamin A Palmitate in Nanostructured Lipid Carrier (NLC)-Effect of Surfactant Concentration on the Formulation Properties. *Advanced pharmaceutical bulletin*, *4*(Suppl 2), 563–568. https://doi.org/10.5681/apb.2014.083

Pezeshki, A., Hamishehkar, H., Ghanbarzadeh, B., Fathollahy, I., Keivani Nahr, F., Khakbaz Heshmati, M., & Mohammadi, M. (2019). Nanostructured lipid carriers as a favorable delivery system for β-carotene. *Food Bioscience*, *27*, 11-17. https://doi.org/10.1016/j.fbio.2018.11.004

Pilz, J., Meineke, I., & Gleiter, C. (2000). Measurement of free and bound malondialdehyde in plasma by high-performance liquid chromatography as the 2,4-dinitrophenylhydrazine derivative. *Journal Of Chromatography B: Biomedical Sciences And Applications*, *742*(2), 315-325. https://doi.org/10.1016/s0378-4347(00)00174-2

Porsgaard, Trine.,(2006). Clinical Studies with Structured Triacylglycerols. In: Akoh, C.C. (Ed.), *Handbook of Functional Lipids*. CRC Press, USA, pp. 419-429

Porter, C., Trevaskis, N., & Charman, W. (2007). Lipids and lipid-based formulations: optimizing the oral delivery of lipophilic drugs. *Nature Reviews Drug Discovery*, *6*(3), 231-248. https://doi.org/10.1038/nrd2197

Pradhan, M., Singh, D., Murthy, S., & Singh, M. (2015). Design, characterization and skin permeating potential of Fluocinolone acetonide loaded nanostructured lipid carriers for topical treatment of psoriasis. *Steroids*, *101*, 56-63. https://doi.org/10.1016/j.steroids.2015.05.012

Przybylski, R., Wu, J., & Eskin, N. (2013). A Rapid Method for Determining the Oxidative Stability of Oils Suitable for Breeder Size Samples. *Journal Of The American Oil Chemists' Society*, *90*(7), 933-939. https://doi.org/10.1007/s11746-013-2240-1

Puglia, C., Damiani, E., Offerta, A., Rizza, L., Tirendi, G., & Tarico, M. et al. (2014). Evaluation of nanostructured lipid carriers (NLC) and nanoemulsions as carriers for UV-filters: Characterization, in vitro penetration and photostability studies. *European Journal Of Pharmaceutical Sciences*, *51*, 211-217. https://doi.org/10.1016/j.ejps.2013.09.023

Rai, N., Madni, A., Faisal, A., Jamshaid, T., Khan, M., Khan, M., & Parveen, F. (2021). Glyceryl Monostearate based Solid Lipid Nanoparticles for Controlled Delivery of Docetaxel. *Current Drug Delivery*, *18*(9), 1368-1376. https://doi.org/10.2174/1567201818666210203180153

Rao, J., Decker, E., Xiao, H., & McClements, D. (2013). Nutraceutical nanoemulsions: influence of carrier oil composition (digestible versus indigestible oil) on β-carotene bioavailability. *Journal Of The Science Of Food And Agriculture*, *93*(13), 3175-3183. https://doi.org/10.1002/jsfa.6215

Razak, N., Hamid, N., & Shaari, A. (2018). Effect of storage temperature on moisture content of encapsulated Orthosiphon stamineus spray-dried powder. *AIP Conference Proceedings*. https://doi.org/10.1063/1.5066835

Reitznerová, A., Šuleková, M., Nagy, J., Marcinčák, S., Semjon, B., Čertík, M., & Klempová, Relevance and challenges in modeling human gastric and small intestinal digestion. *Trends In Biotechnology*, *30*(11), 591-600. https://doi.org/10.1016/j.tibtech.2012.08.001

Rey, L., May, J.C., 2004. Freeze-Drying/Lyophilization of Pharmaceutical and Biological Products, second ed. Taylor & Francis group, New York.

Romero, M., Calvo, L., Alba, C., Daneshfar, A., & Ghaziaskar, H. (2005). Enzymatic synthesis of isoamyl acetate with immobilized Candida antarctica lipase in n-hexane. *Enzyme And Microbial Technology*, *37*(1), 42-48. https://doi.org/10.1016/j.enzmictec.2004.12.033

Rousseau, D. (2000). Fat crystals and emulsion stability — a review. *Food Research International*, *33*(1), 3-14. https://doi.org/10.1016/s0963-9969(00)00017-x

Roy, S., Dhobale, M., Dangat, K., Mehendale, S., Wagh, G., Lalwani, S., & Joshi, S. (2014). Differential levels of long chain polyunsaturated fatty acids in women with preeclampsia delivering male and female babies. *Prostaglandins, Leukotrienes And Essential Fatty Acids*, *91*(5), 227-232. https://doi.org/10.1016/j.plefa.2014.07.002

Ruiz, J., Antequera, T., Andres, A., Petron, M., & Muriel, E. (2004). Improvement of a solid phase extraction method for analysis of lipid fractions in muscle foods. Analytica Chimica Acta, 520(1-2), 201 205. https://doi.org/10.1016/j.aca.2004.04.059

Rychlicka, M., Niezgoda, N., & Gliszczyńska, A. (2018). Lipase-Catalyzed Acidolysis of Egg-Yolk Phosphatidylcholine with Citronellic Acid. New Insight into Synthesis of Isoprenoid-Phospholipids. *Molecules*, *23*(2), 314. https://doi.org/10.3390/molecules23020314

Ray, S., & Bhattacharyya, D. (1995). Comparative nutritional study of enzymatically and chemically interesterified palm oil products. *Journal Of The American Oil Chemists' Society*, *72*(3), 327-330. https://doi.org/10.1007/bf02541091

Sagalowicz, L., & Leser, M. (2010). Delivery systems for liquid food products. *Current Opinion In Colloid & Interface Science*, *15*(1-2), 61-72. https://doi.org/10.1016/j.cocis.2009.12.003

Sakellari, G., Zafeiri, I., Batchelor, H., & Spyropoulos, F. (2021). Formulation design, production and characterisation of solid lipid nanoparticles (SLN) and nanostructured lipid carriers (NLC) for the encapsulation of a model hydrophobic active. *Food Hydrocolloids For Health*, *1*, 100024. https://doi.org/10.1016/j.fhfh.2021.100024

Salminen, H., Aulbach, S., Leuenberger, B., Tedeschi, C., & Weiss, J. (2014). Influence of surfactant composition on physical and oxidative stability of Quillaja saponin-stabilized lipid particles with encapsulated ω-3 fish oil. *Colloids And Surfaces B: Biointerfaces*, *122*, 46-55. https://doi.org/10.1016/j.colsurfb.2014.06.045

SANDHU K S, BAL A and AHLUWALIA P (2002), `Studies on suitability of cultivar, frying medium and packaging for potato chips', *J Food Sci Agric*, 39(4) 394-402.

Santos, D., Saraiva, J., Vicente, A., & Moldão-Martins, M. (2019). Methods for determining

bioavailability and bioaccessibility of bioactive compounds and nutrients. *Innovative Thermal And Non-Thermal Processing, Bioaccessibility And Bioavailability Of Nutrients And Bioactive Compounds*, 23-54. https://doi.org/10.1016/b978-0-12-814174-8.00002-0

Seifi, H., & Sadrameli, S. (2016). Bound cleavage at carboxyl group-glycerol backbone position in thermal cracking of the triglycerides in sunflower oil. *Journal Of Analytical And Applied Pyrolysis*, *121*, 1-10. doi: 10.1016/j.jaap.2016.06.006

Sellami, M., Ghamgui, H., Frikha, F., Gargouri, Y., & Miled, N. (2012). Enzymatic transesterification of palm stearin and olein blends to produce zero-trans margarine fat. BMC Biotechnology, 12(1), 48. doi: 10.1186/1472-6750-12-48

Sellappan S, Akoh C. 2000. Enzymatic acidolysis of tristearin with lauric and oleic acids to produce coating lipids. J Am Oil Chem Soc 77(11):1127–34.

Severino, P., Andreani, T., Macedo, A., Fangueiro, J., Santana, M., Silva, A., & Souto, E. (2012). Current State-of-Art and New Trends on Lipid Nanoparticles (SLN and NLC) for Oral Drug Delivery. *Journal Of Drug Delivery*, *2012*, 1-10. https://doi.org/10.1155/2012/750891

Sezgin-Bayindir, Z., Antep, M., & Yuksel, N. (2014). Development and Characterization of Mixed Niosomes for Oral Delivery Using Candesartan Cilexetil as a Model Poorly Water-Soluble Drug. *AAPS Pharmscitech*, *16*(1), 108-117. https://doi.org/10.1208/s12249-014-0213-9

Shahavi, M., Hosseini, M., Jahanshahi, M., Meyer, R., & Darzi, G. (2015). Clove oil nanoemulsion as an effective antibacterial agent: Taguchi optimization method. *Desalination And Water Treatment*, *57*(39), 18379-18390. https://doi.org/10.1080/19443994.2015.1092893

Shahparast, Y., Eskandani, M., Rajaei, A., & Yari Khosroushahi, A. (2019). Preparation, Physicochemical Characterization and Oxidative Stability of Omega-3 Fish Oil/α-Tocopherol-co-Loaded Nanostructured Lipidic Carriers. *Advanced pharmaceutical bulletin*, *9*(3), 393–400. https://doi.org/10.15171/apb.2019.046

Sharma, O., & Bhat, T. (2009). DPPH antioxidant assay revisited. *Food Chemistry*, *113*(4), 1202-1205. https://doi.org/10.1016/j.foodchem.2008.08.008

Sharma, R., Chisti, Y., & Banerjee, U. (2001). Production, purification, characterization, and applications of lipases. *Biotechnology Advances*, *19*(8), 627-662. https://doi.org/10.1016/s0734-9750(01)00086-6

Sheaolein and Palm Stearin and Comparative Study of Their Physicochemical Properties. *Journal Of Food Science*, *77*(12), C1285-C1292. https://doi.org/10.1111/j.1750-3841.2012.02977.x

Shimada, Yuji., (2006). Enzymatic Modification of Lipids for Functional Foods and Nutraceuticals. In: Akoh, C.C. (Ed.), *Handbook of Functional Lipids*. CRC Press, USA, pp.437-451

Shishir, M., Xie, L., Sun, C., Zheng, X., & Chen, W. (2018). Advances in micro and nano-encapsulation of bioactive compounds using biopolymer and lipid-based transporters. *Trends In Food Science & Technology*, *78*, 34-60. https://doi.org/10.1016/j.tifs.2018.05.018

SHUANG, D., JIANG-KE, Y., & YUN-JUN, Y. (2009). OPTIMIZATION OF LIPASE-CATALYZED ACIDOLYSIS OF SOYBEAN OIL TO PRODUCE STRUCTURED LIPIDS. *Journal Of Food Biochemistry*, *33*(3), 442-452. doi: 10.1111/j.1745-4514.2009.00227.x

Singh, H., Ye, A., & Horne, D. (2009). Structuring food emulsions in the gastrointestinal tract to modify lipid digestion. *Progress In Lipid Research*, *48*(2), 92-100. https://doi.org/10.1016/j.plipres.2008.12.001

Sitompul, J., Gusdinar, T., Anggadiredja, K., Rahman, H., & Tursino, T. (2018). Synthesis of Structured Triglycerides Based on Canarium Oil for Food Application. *Journal Of Engineering And Technological Sciences*, *50*(1), 87. doi: 10.5614/j.eng.technol.sci.2018.50.1.6 *Society*, *79*(4), 363-367. https://doi.org/10.1007/s11746-002-0489-3

Soleimanian, Y., Goli, S., Varshosaz, J., & Sahafi, S. (2018). Formulation and characterization of novel nanostructured lipid carriers made from beeswax, propolis wax and pomegranate seed oil. *Food Chemistry*, *244*, 83-92. https://doi.org/10.1016/j.foodchem.2017.10.010

Souto, E. B., Souto, S. B., Campos, J. R., Severino, P., Pashirova, T. N., Zakharova, L. Y., Silva, A. M., Durazzo, A., Lucarini, M., Izzo, A. A., & Santini, A. (2019). Nanoparticle Delivery Systems in the Treatment of Diabetes Complications. *Molecules (Basel, Switzerland)*, *24*(23), 4209. https://doi.org/10.3390/molecules24234209

Suganya, V., & Anuradha, V. (2017). Microencapsulation and Nanoencapsulation: A Review. *International Journal Of Pharmaceutical And Clinical Research*, *9*(3). https://doi.org/10.25258/ijpcr.v9i3.8324

Sun, M., Nie, S., Pan, X., Zhang, R., Fan, Z., & Wang, S. (2014). Quercetin-nanostructured lipid carriers: Characteristics and anti-breast cancer activities in vitro. *Colloids And Surfaces B: Biointerfaces*, *113*, 15-24. https://doi.org/10.1016/j.colsurfb.2013.08.032

Reitznerová, A., Šuleková, M., Nagy, J., Marcinčák, S., Semjon, B., Čertík, M., & Klempová, T. (2017). Lipid Peroxidation Process in Meat and Meat Products: A Comparison Study of Malondialdehyde Determination between Modified 2-Thiobarbituric Acid Spectrophotometric Method and Reverse-Phase High-Performance Liquid

Chromatography. *Molecules (Basel, Switzerland)*, *22*(11), 1988. https://doi.org/10.3390/molecules22111988

Talbot, G. (2016). The Stability and Shelf Life of Fats and Oils. *The Stability And Shelf Life Of Food*, 461-503. https://doi.org/10.1016/b978-0-08-100435-7.00016-2

Talebi, V., Ghanbarzadeh, B., Hamishehkar, H., Pezeshki, A., & Ostadrahimi, A. (2021). Effects of different stabilizers on colloidal properties and encapsulation efficiency of vitamin D3 loaded nano-niosomes. *Journal Of Drug Delivery Science And Technology*, *61*, 101284. https://doi.org/10.1016/j.jddst.2019.101284

Tamjidi, F., Shahedi, M., Varshosaz, J., & Nasirpour, A. (2013). Nanostructured lipid carriers (NLC): A potential delivery system for bioactive food molecules. *Innovative Food Science &Amp; Emerging Technologies*, *19*, 29-43. https://doi.org/10.1016/j.ifset.2013.03.002

Taylor, D., Francis, T., Guo, Y., Brost, J., Katavic, V., & Mietkiewska, E. et al. (2009). Molecular cloning and characterization of aKCSgene fromCardamine graecaand its heterologous expression inBrassicaoilseeds to engineer high nervonic acid oils for potential medical and industrial use. *Plant Biotechnology Journal*, *7*(9), 925-938. https://doi.org/10.1111/j.1467-7652.2009.00454.x

Taylor, D., Guo, Y., Katavic, V., Mietkiewska, E., Francis, T., & Bettger, W. (2015). New Teichert, S., & Akoh, C. (2011). Characterization of Stearidonic Acid Soybean Oil Enriched with Palmitic Acid Produced by Solvent-free Enzymatic Interesterification. *Journal Of Agricultural And Food Chemistry*, *59*(17), 9588-9595. doi: 10.1021/jf201992k

Temperature and Moisture Content of Stored Rapeseed on the Phytosterol Degradation Rate. *Journal Of The American Oil Chemists' Society*, *89*(9), 1673-1679. https://doi.org/10.1007/s11746-012-2064-4

Tian, Y., Chen, L., & Zhang, W. (2015). Influence of Ionic Surfactants on the Properties of Nanoemulsions Emulsified by Nonionic Surfactants Span 80/Tween 80. *Journal Of Dispersion Science And Technology*, *37*(10), 1511-1517. https://doi.org/10.1080/01932691.2015.1048806

Tikekar, R., & Nitin, N. (2011). Effect of physical state (solid vs. liquid) of lipid core on the rate of transport of oxygen and free radicals in solid lipid nanoparticles and emulsion. *Soft Matter*, *7*(18), 8149. https://doi.org/10.1039/c1sm05031a

Tokle, T., Lesmes, U., Decker, E., & McClements, D. (2012). Impact of dietary fiber coatings on behavior of protein-stabilized lipid droplets under simulated gastrointestinal conditions. *Food Funct.*, *3*(1), 58-66. https://doi.org/10.1039/c1fo10129c

Toorani, M., Farhoosh, R., Golmakani, M., & Sharif, A. (2019). Antioxidant activity and mechanism of action of sesamol in triacylglycerols and fatty acid methyl esters of sesame, olive, and canola oils. *LWT*, *103*, 271-278. doi: 10.1016/j.lwt.2019.01.012

Tura, M., Ansorena, D., Astiasarán, I., Mandrioli, M., & Toschi, T. (2022). Evaluation of Hemp
Seed Oils Stability under Accelerated Storage Test. *Antioxidants*, *11*(3), 490. https://doi.org/10.3390/antiox11030490

Tulevski, G., Franklin, A., & Afzali, A. (2013). High Purity Isolation and Quantification of Semiconducting Carbon Nanotubes via Column Chromatography. *ACS Nano*, *7*(4), 2971-2976. https://doi.org/10.1021/nn400053k

Umemoto, H., Sawada, K., Kurata, A., Hamaguchi, S., Tsukahara, S., Ishiguro, T., & Kishimoto, N. (2014). Fermentative Production of Nervonic Acid by Mortierella capitata RD000969. *Journal Of Oleo Science*, *63*(7), 671-679. https://doi.org/10.5650/jos.ess14029

Uner M. (2006). Preparation, characterization and physico-chemical properties of solid lipid nanoparticles (SLN) and nanostructured lipid carriers (NLC): their benefits as colloidal drug carrier systems. Die Pharmazie, 61(5), 375–386.*Use In Food*, 1-8. https://doi.org/10.1533/9781845691684.1

Utembe, W., Tlotleng, N., & Kamng'ona, A. (2022). A systematic review on the effects of nanomaterials on gut microbiota. Current Research In Microbial Sciences, 3, 100118. https://doi.org/10.1016/j.crmicr.2022.100118

Valero, F. (2012). Heterologous Expression Systems for Lipases: A Review. *Lipases And Phospholipases*, 161-178. https://doi.org/10.1007/978-1-61779-600-5_11

Van Meer, G., Voelker, D., & Feigenson, G. (2008). Membrane lipids: where they are and how
they behave. *Nature Reviews Molecular Cell Biology*, *9*(2), 112-124. https://doi.org/10.1038/nrm2330

Wang, J., Dong, X., Wei, F., Zhong, J., Liu, B., & Yao, M. et al. (2014). Preparation and Characterization of Novel Lipid Carriers Containing Microalgae Oil for Food Applications. *Journal Of Food Science*, *79*(2), E169-E177. https://doi.org/10.1111/1750-3841.12334

Wang, L., Hu, Y., Yin, S., Yang, X., Lai, F., & Wang, S. (2015). Fabrication and Characterization of Antioxidant Pickering Emulsions Stabilized by Zein/Chitosan Complex Particles (ZCPs). *Journal Of Agricultural And Food Chemistry*, *63*(9), 2514-2524. https://doi.org/10.1021/jf505227a

Wang, X., Li, X., Xu, D., Zhu, Y., Cao, Y., Wang, J., & Sun, B. (2019). Comparision of heteroaggregation, layer-by-layer and directly mixing techniques on the physical properties and in vitro digestion of emulsions. *Food Hydrocolloids*, *95*, 228-237. https://doi.org/10.1016/j.foodhyd.2019.04.034

Wang, Y., Xia, L., Xu, X., Xie, L., & Duan, Z. (2012). Lipase-catalyzed acidolysis of canola

oil with caprylic acid to produce medium-, long- and medium-chain-type structured lipids. *Food And Bioproducts Processing*, *90*(4), 707-712. doi: 10.1016/j.fbp.2012.02.003

Waraho, T., McClements, D., & Decker, E. (2011). Impact of free fatty acid concentration and structure on lipid oxidation in oil-in-water emulsions. *Food Chemistry*, *129*(3), 854-859. https://doi.org/10.1016/j.foodchem.2011.05.034

Wason, S., Verma, T., Wei, X., Mauromoustakos, A., & Subbiah, J. (2022). Thermal inactivation kinetics of Salmonella enterica and Enterococcus faecium NRRL B-2354 as a function of temperature and water activity in fine ground black pepper. *Food Research International*, *157*, 111393. https://doi.org/10.1016/j.foodres.2022.111393

Weete, John D., Lai, Oi-Ming., and Akoh, Casimir C.,(2006). In: Akoh, C.C. (Ed.), *Handbook of Functional Lipids*. CRC Press, USA, pp. 767-794.

Wei, W., Bai, F., & Fan, H. (2020). Surfactant-Assisted Cooperative Self-Assembly of Nanoparticles into Active Nanostructures. *Iscience*, *11*, 272-293. https://doi.org/10.1016/j.isci.2018.12.025

Willett, S., & Akoh, C. (2018). Application of Taguchi Method in the Enzymatic Modification of Menhaden Oil to Incorporate Capric Acid. *Journal Of The American Oil Chemists' Society*, *95*(3), 299-311. https://doi.org/10.1002/aocs.12043

Willis, Wendy M., Marangoni, Alejandro G., (2006). Enzymatic Interesterification. In: Akoh, C.C. (Ed.), *Handbook of Functional Lipids*. CRC Press, USA, pp. 808-822

Wu, T., Yan, J., Liu, R., Marcone, M., Aisa, H., & Tsao, R. (2012). Optimization of microwave-assisted extraction of phenolics from potato and its downstream waste using orthogonal array design. *Food Chemistry*, *133*(4), 1292-1298. https://doi.org/10.1016/j.foodchem.2011.08.002

Xu X, Fomuso L, Akoh C. 2000. Modification of menhaden oil by enzymatic acidolysis to produce structured lipids: optimization by response surface design in a packed bed reactor. JAm Oil Chem Soc 77(2):171–6.

Xu, Xuebing (2000a). Enzymatic production of structured lipids process reactions and acyl migration. International News of Fats and Oils and Related Materials, 11, 1121–1129.

Xu, Xuebing (2000b). Production of specific-structured triacylglycerols by lipase-catalyzed reactions: a review. European Journal of Lipid Science & Technology, 102, 287–303.

Yadav S, S.(2014). Development of a Highly Sensitive, Fast and Efficient Screening Technique

for the Detection of 2,3-Butanediol by Thin Layer Chromatography. *Journal Of Chromatography & Separation Techniques*, *05*(06). https://doi.org/10.4172/2157-7064.1000251

Yang, T., Fruekilde, M., & Xu, X. (2003). Applications of immobilized Thermomyces lanuginosa lipase in interesterification. *Journal Of The American Oil Chemists' Society*, *80*(9), 881-887. https://doi.org/10.1007/s11746-003-0789-7

Yang, T.H., Jang, Y., Han, J.J. *et al.* Enzymatic synthesis of low-calorie structured lipids in a solvent-free system. *J Amer Oil Chem Soc* 78, 291–296 (2001). https://doi.org/10.1007/s11746-001-0259-2

Yankah V, Akoh C. 2000. Lipase-catalyzed acidolysis of tristearin with oleic or caprylic acids to produce structured lipids. J Am Oil Chem Soc 77(5):495–500.

Yasuda, S., & Yamamoto, Y. (2020). Highly efficient preparation of 1-lysophosphatidylcholine via high proportion of Novozym® 435 (lipase B from Candida antarctica)-catalyzed ethanolysis. *Biotechnology Reports*, *27*, e00505. https://doi.org/10.1016/j.btre.2020.e00505

Zeb, A., & Ullah, F. (2016). A Simple Spectrophotometric Method for the Determination of Thiobarbituric Acid Reactive Substances in Fried Fast Foods. *Journal Of Analytical Methods In Chemistry*, *2016*, 1-5. https://doi.org/10.1155/2016/9412767

Zelzer, S., Oberreither, R., Bernecker, C., Stelzer, I., Truschnig-Wilders, M., & Fauler, G. (2013). Measurement of total and free malondialdehyde by gas–chromatography mass spectrometry – comparison with high-performance liquid chromatography methology. *Free Radical Research*, *47*(8), 651-656. https://doi.org/10.3109/10715762.2013.812205

Zhang, R., Zhang, Z., Zhang, H., Decker, E., & McClements, D. (2015). Influence of lipid type on gastrointestinal fate of oil-in-water emulsions: In vitro digestion study. *Food Research International*, *75*, 71-78. https://doi.org/10.1016/j.foodres.2015.05.014

Zhang, R., Zhang, Z., Zhang, H., Decker, E., & McClements, D. (2015). Influence of emulsifier type on gastrointestinal fate of oil-in-water emulsions containing anionic dietary fiber (pectin). *Food Hydrocolloids*, *45*, 175-185. https://doi.org/10.1016/j.foodhyd.2014.11.020

Zhao, H., Lu, Z., Bie, X., Lu, F., & Liu, Z. (2007). Lipase catalyzed acidolysis of lard with capric acid in organic solvent. *Journal Of Food Engineering*, *78*(1), 41-46. https://doi.org/10.1016/j.jfoodeng.2005.08.049

Zheng, W., Kollmeyer, J., Symolon, H., Momin, A., Munter, E., & Wang, E. et al. (2006).

Ceramides and other bioactive sphingolipid backbones in health and disease: Lipidomic analysis, metabolism and roles in membrane structure, dynamics, signaling and autophagy. *Biochimica Et Biophysica Acta (BBA) - Biomembranes*, *1758*(12), 1864-1884. https://doi.org/10.1016/j.bbamem.2006.08.009

Zheng, Y., Yu, B., Weecharangsan, W., Piao, L., Darby, M., & Mao, Y. et al. (2010). Transferrin-conjugated lipid-coated PLGA nanoparticles for targeted delivery of aromatase inhibitor 7α-APTADD to breast cancer cells. *International Journal Of Pharmaceutics*, *390*(2), 234-241. https://doi.org/10.1016/j.ijpharm.2010.02.008

Zhou, D., Xu, X., Mu, H., Høy, C., & Adler-Nissen, J. (2001). Synthesis of Structured Triacylglycerols Containing Caproic Acid by Lipase-Catalyzed Acidolysis: Optimization by Response Surface

Zhu, J., Zhuang, P., Luan, L., Sun, Q., & Cao, F. (2015). Preparation and characterization of novel nanocarriers containing krill oil for food application. *Journal Of Functional Foods*, *19*, 902-912. https://doi.org/10.1016/j.jff.2015.06.017

Appendix

Appendix 1. Standard curves for quantitation of the optimized NA-TAG-loaded NLC in encapsulation efficiency.

Appendix 2. Standard curves for quantitation of the lyophilized NLC in encapsulation efficiency.

Appendix 3. Standard curves of Fe(III) for quantitation of peroxide value in lyophilized NLC.

Appendix 4. Standard curves of MDA concentrations for quantitation of TBARs value in lyophilized NLC.

Appendix 5. Orthogonal optimization for the preparation of NLC.

Appendix 1. Standard curves for quantitation of the optimized NA-TAG oil in encapsulation efficiency.

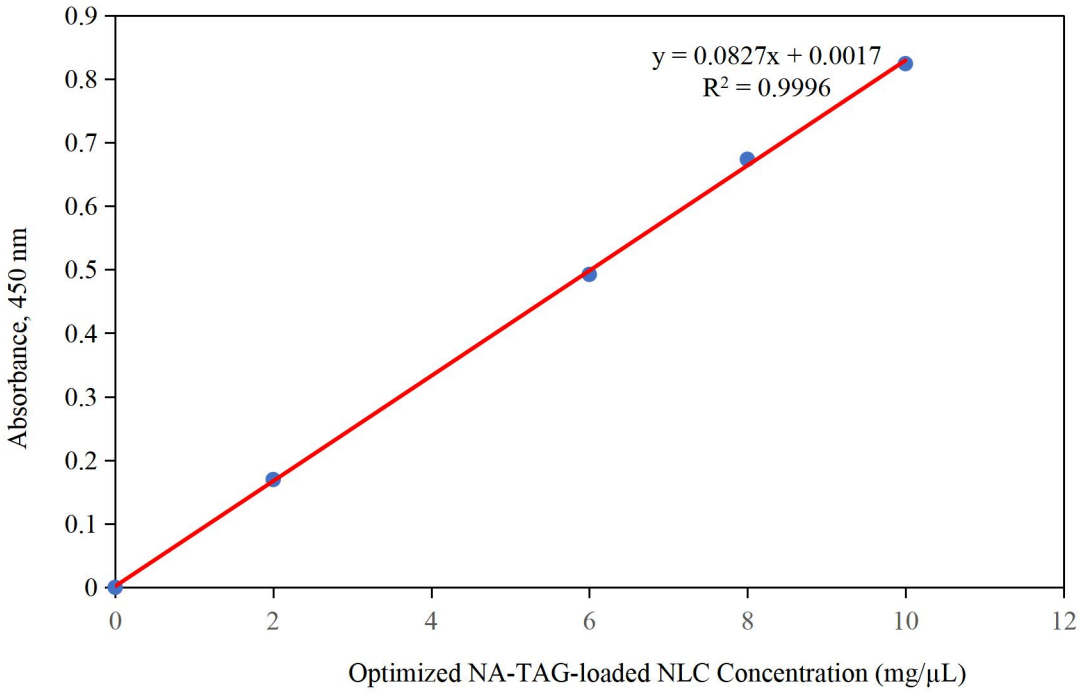

Appendix 2. Standard curves for quantitation of the lyophilized NLC in encapsulation efficiency.

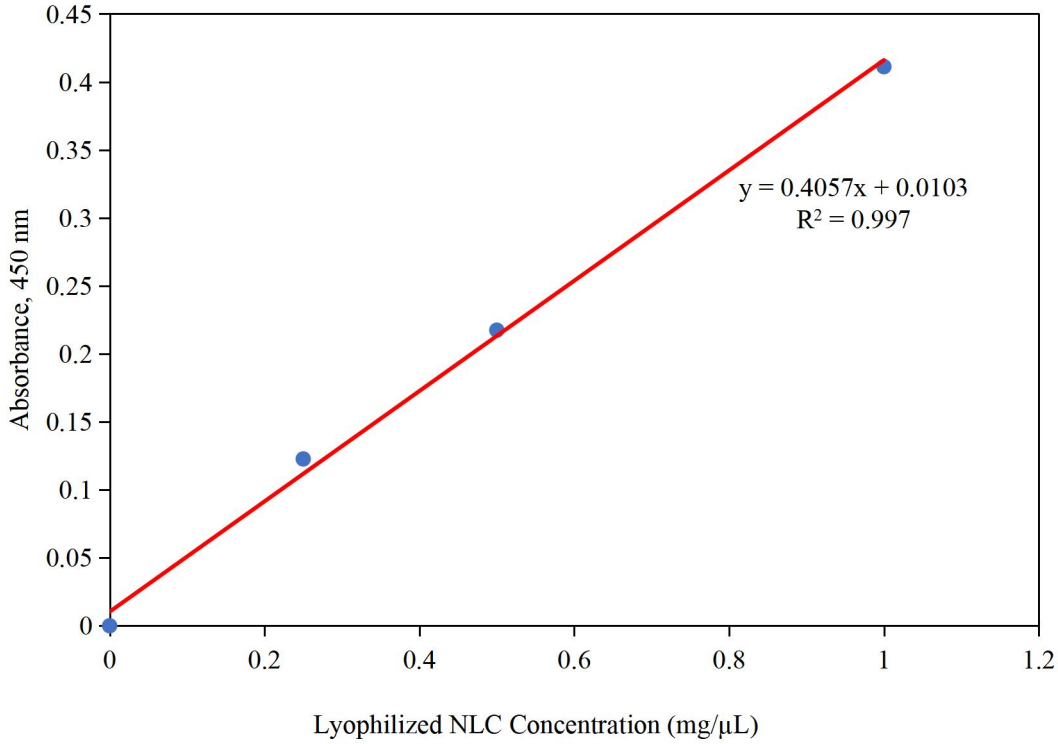

Appendix 3. Standard curves of Fe(III) for quantitation of peroxide value in lyophilized NLC.

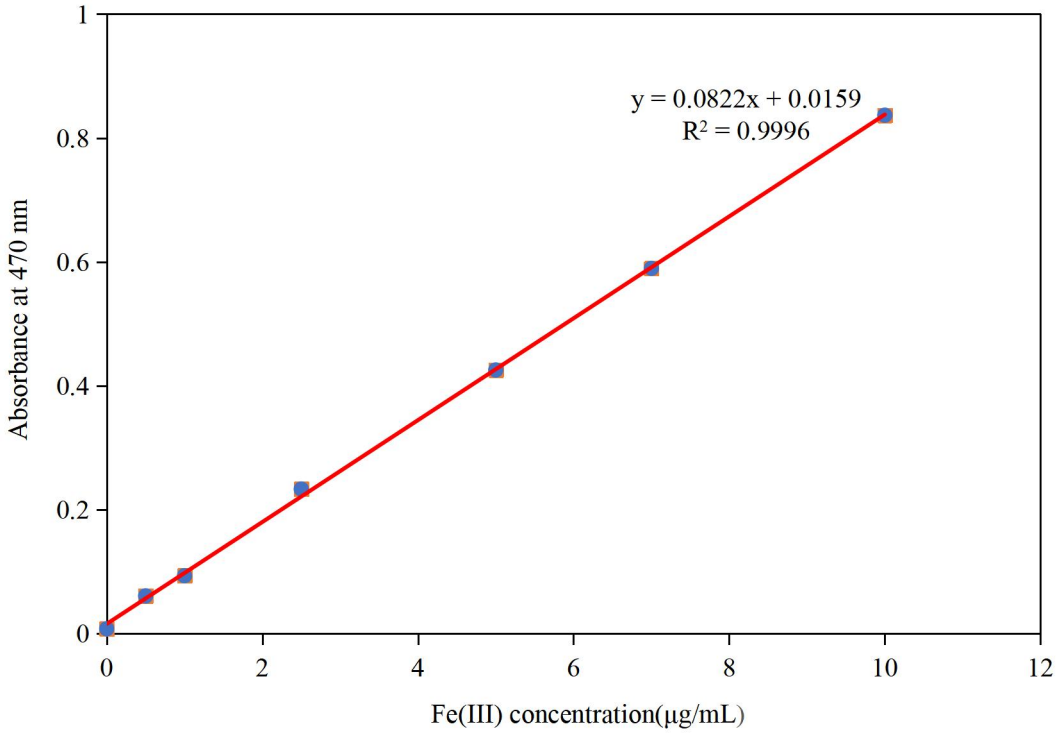

Appendix 4. Standard curves of MDA concentrations for quantitation of TBARs value in lyophilized

NLC.

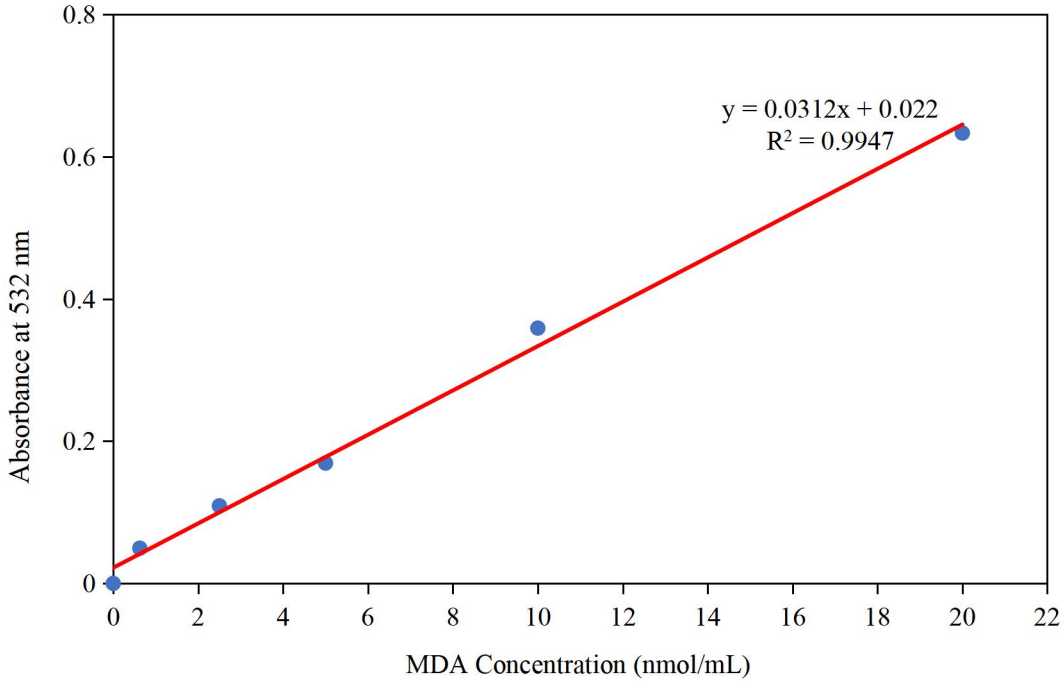
y = 0.0312x + 0.022
R² = 0.9947
Absorbance at 532 nm
MDA Concentration (nmol/mL)
0
0.2
0.4
0.6
0.8
0
2
4
6
8
10
12
14
16
18
20
22

Appendix 5. Orthogonal optimization for the preparation of NLC.

Formulation	Liuqid lipid(soybean oil) (%w/w)	Solid lipid (%w/w)		NA-TAG (%w/w)	Liquid to aqueous phase	Surfactant type (%w/w)			Aqueous Water (%w/w)	Response variables		
		Stearic Acid	GMS			Tween 20	Tween 80	Poloxamer 407		Particle Size (nm)	PDI	Zeta potential (mV)
NLC 6	6		3	1	10 : 90	1	-	-	89	6268 ± 8.485	-	-23.9 ± 0.2
NLC 7	9.33		4.67	1	15 : 85	-	2	-	83	2446 ± 163.9	0.72 ± 0.269	-31.7 ± 0.208
NLC 8	12.67		6.33	1	20 : 80	-	-	3	77	-	-	-
NLC 9	5.67		2.83	1.5	10 : 90	-	-	2	88	-	-	-
NLC 10	9.0		4.5	1.5	15 : 85	3	-	-	82	5913 ± 611.0	-	-25.3 ± 0.917
NLC 11	12.33		6.17	1.5	20 : 80	-	1	-	79	8920 ± 611.0	0.678 ± 0.004	-27.4 ± 0.896
NLC 12	5.333		2.67	2	10 : 90	-	3	-	87	2670 ± 452.8	0.602 ± 0.189	-16.8 ± 0.808
NLC 13	8.67		4.33	2	15 : 85	-	-	1	84	-	-	-
NLC 14	1.2		6.0	2	20: 80	2	-	-	78	6793 ± 667.9	-	-25.7 ± 1.46